Monitoring Phytoremediation of Petroleum Hydrocarbon Contaminated Soils in a Closed and Controlled Environment

A Thesis

Submitted to the College of Graduate Studies and Research

In Partial Fulfillment of the Requirements

For The Degree of

Masters of Science

In the Department of Civil and Geological Engineering

University of Saskatchewan

Saskatoon

By

Alexis McPherson

Permission to Use

In presenting this thesis in partial fulfillment of the requirements for a Postgraduate degree from the University of Saskatchewan, I agree that the Libraries of this University may make it freely available for inspection. I further agree that permission for copying of this thesis in any manner, in whole or in part, for scholarly purposes may be granted by the professor or professors who supervised my thesis work or, in their absence, by the Head of the Department or the Dean of the College in which my thesis work was done. It is understood that any copying or publication or use of this thesis or parts thereof for financial gain shall not be allowed without my written permission. It is also understood that due recognition shall be given to me and to the University of Saskatchewan in any scholarly use which may be made of any material in my thesis.

Requests for permission to copy or to make other use of material in this thesis in whole or part should be addressed to:

Head of the Department of Civil and Geological Engineering
University of Saskatchewan
57 Campus Drive
Saskatoon, Saskatchewan
S7N 5A9

Abstract

Phytoremediation is a relatively new remediation technology that may be useful in removing organic and inorganic pollutants from soils. Much research has focused on this type of remediation in the past few years due to its potential as an efficient and cost effective technology.

The purpose of this project was to extensively monitor phytoremediation of diesel-contaminated field soils in the laboratory under simulated field conditions. The main objectives were: to examine petroleum hydrocarbon (PHC) transfer and degradation processes involved in phytoremediation of contaminated field soils; to compare phytoremediation of contaminated field soils with intrinsic bioremediation; and, to develop a rationally-based model that could be used as a starting point for a quantitative prediction of the rate of PHC removal.

To realize these objectives a series of laboratory scale experiments were designed and carried out. The experiments reproduced pole planting of hybrid poplars into diesel contaminated field soils from a former bulk fuel station. The experiments were conducted in a closed and controlled environment over a 215-230 day period with numerous aspects of the system being monitored including volatilization of PHC from the tree and soil, and microbial activity of the soil.

Monitoring data indicated that microbial degradation of the contaminant was by far the most influential monitored degradation pathway, accounting for 96.3 to 98.7% of the mass removed for soils containing poplars. The monitoring data also indicated a significant difference in the mass of contaminant removed from the soil for soils containing poplars compared to those without. The total estimated mass of contaminant removed varied between 8.3 and 27.7% of the initial mass for soils containing poplars and between 6.0 and 6.1% of the initial mass for soils without poplars. Lastly, using the monitoring data and the below ground biomass of the poplars from each of the

experimental test cells, a rationally-based model was developed to be used as a starting point for quantitative prediction of the rate of PHC removal.

Acknowledgments

I would like to express my sincere gratitude and thanks to Dr. Ian Fleming for his supervision and support during this project. Acknowledgments are extended to the members of my advisory committee, Dr. Richard Farrell and Dr. Malcolm Reeves. Thanks is also due to Dr. John Headley and Kerry Peru of the National Hydrology Research Centre, the staff of the Department of Civil and Geological Engineering, especially Doug Fisher, the staff at Engineering Shops, especially Henry Berg and Keith Palibroda, and to a number of fellow students who have helped along the way including: Kevin Park, Mubashshar Ahmed and Adam Gillespie. Thanks also to Dr. Jim Germida for providing financial support through the Natural Sciences and Engineering Research Council of Canada (NSERC) and to the Department of Civil and Geological Engineering for providing financial support through a two year Departmental Graduate Scholarship and the Graduate Centennial Merit Scholarship.

Special thanks go to Tom, whose help, support and encouragement has been instrumental in the successful completion of this project and to my family who have supported me throughout my education.

Table of Contents

List of Figures

List of Tables

List of Appendices (on CD)

List of Nomenclature

A	Rate constant
A_s	Silica specific surface area
ASTM	American Society for Testing and Materials
ATP	Adenosine triphosphate
B	Intercept
BGB	Below-ground biomass
°C	Degrees Celsius
C	Equilibrium concentration of contaminant in solution
Ca^{2+}	Calcium ion
$CaCl_2$	Calcium chloride
$CaSO_4$	Calcium sulphate
CCME	Canadian Council of Ministers of the Environment
CEC	Cation exchange capacity
CH_4	Methane
cm	Centimetre
CO_2	Carbon dioxide
$CoCl_2$	Cobalt chloride
CS_2	Carbon disulphide
DI	Deionized
E_e	Extraction efficiency
f_{oc}	Mass fraction of organic carbon in the soil
f^*_{oc}	Critical fraction of organic carbon
f_{oi}	Fraction of inorganic matter
f(t)	Function of time
g	Gram
g/cm^3	Grams per cubic centimetre
g/m^2	Grams per square metre
GC-FID	Gas chromatograph flame ionization detector
GC-MS	Gas chromatograph mass spectrometer
H^+	Hydrogen ion

h_b	Height of the voltage response curve at 120s
h_n	Height of the voltage response curve at time step *n*
h_{n+1}	Height of the voltage response curve at time step *n+1*
ID	Inside diameter
K	Kelvin
K	Slope of the normalized cumulative mass of PHC removed over final time interval
K^+	Potassium
K_d	Solid-phase to solution-phase distribution coefficient
K_{oc}	Organic carbon-water partition coefficient
K_{oi}	Inorganic partition coefficient
K_{ow}	Octanol-water partition coefficient
kPa	Kilopascals
l	Litres
lpm	Litres per minute
m	Measured mass
m^3	Cubic metre
m_{actual}	Actual mass
mg	Milligrams
Mg^{2+}	Magnesium ion
min.	Minutes
ml	Millilitre
µl	Microlitre
mmHg	Millimetres of mercury
MSDS	Material Safely Data Sheet
n	Number of moles
N	Nitrogen
Na^+	Sodium ion
nC6	Neat hexane
nC10	Neat decane
nC16	Neat hexadecane

nC34	Neat tetratricontane
NCMR	Cumulative mass PHC removed normalized with respect to mass of contaminated soil
ng	Nanograms
O_2	Oxygen
OD	Outside diameter
OSHA	U.S. Department of Labour Occupational Safety and Health Administration
P	Pressure
P	Phosphorous
Pa	Pascal
PFRA	Prairie Farm Rehabilitation Administration
PHC	Petroleum hydrocarbons
ppm	Parts per million
P(r=0)	Probability that the correlation coefficient is equal to 0
PTFE	Polytetrafluoroethylene or Teflon®
r	Pearson correlation coefficient
R	Universal gas constant
R^2	Coefficient of determination
RF	Response factor
RLU	Relative light units
s	Second
S	Mass of contaminant sorbed to the surface from aqueous solution
SAR	Sodium adsorption ratio
S.E. of r	Standard error of the Pearson correlation coefficient
t	Time
T	Temperature
t_n	Time at time step *n*
t_{n+1}	Time at time step *n+1*
V	Volume
VOC	Volatile organic compound

Chapter 1: Introduction

Contaminated soil and water is a worldwide problem and a major environmental concern. Numerous types of contaminants have been introduced to the environment causing harm to flora and fauna and, in some cases, rendering land unusable.

One common contaminant is diesel, a petroleum hydrocarbon (PHC) which is commonly released into the environment from spills and leaking storage tanks. While a number of technologies are able to remove or contain diesel in the environment, many of these technologies require specialized equipment and extensive monitoring which can be expensive. One potentially efficient and cost-effective remediation technology is phytoremediation, "the use of green plants to remove, contain or render harmless environmental contaminants" (Cunningham and Berti, 1993).

While Cunningham and Berti's (1993) definition appears to be straightforward, in reality a number of processes and complex plant, microbe, soil and contaminant interactions are involved in phytoremediation, both within the plant and within the rhizosphere, "a zone of increased microbial activity and biomass at the root-soil interface that is under the influence of the plant root" (Anderson et al., 1993 from Curl and Truelove, 1986). Phytoremediation processes of plants and their associated microbial populations may

influence each other and may, in turn, influence and be influenced by a number of soil and contaminant properties.

Biologists, microbiologists, chemists, soil scientists, hydrologists, engineers, and scientists from many other disciplines have contributed to a large body of research on phytoremediation. The information that has been gathered has been extremely useful in examining if, how, and with what plant, specific contaminants can be phytoremediated, the processes of phytoremediation, phytoremediation in the field, and other topics. However, most of the experimental research is based on testing carried out under two extremes: first, laboratory studies of phytoremediation that are well monitored but occur under artificially idealized conditions unrepresentative of field conditions; or, second, phytoremediation occurring under field conditions but that is not well monitored, reflecting logistical constraints. There is a lack of documented research between these extremes, namely studying phytoremediation that is both well monitored and occurs under conditions which reasonably mimic those that may be anticipated in the field.

The purpose of this project was to extensively monitor phytoremediation of diesel-contaminated field soils in the laboratory under simulated field conditions. The main objectives were:

1) to examine PHC transfer and degradation processes involved in phytoremediation of contaminated field soils;
2) to compare phytoremediation of PHC contaminated field soils with intrinsic bioremediation, the "use of biological agents to reclaim soil and water contaminated by hazardous substances" (Farrell et al., 2000), by the existing soil

microbial consortia in the absence of the root zone; and,

3) to develop a rationally-based model that could be used as a starting point for a quantitative prediction of the rate of PHC removal.

The first objective, to examine PHC transfer and degradation processes involved in phytoremediation of contaminated field soils, was an attempt to understand contaminant fate in the field and, in doing so, identify the dominant process(es) associated with removal of PHC during phytoremediation.

The aim of identifying and quantifying the various process(es) involved with phytoremediation in PHC contaminated soils also relates to the second objective, to compare phytoremediation of PHC contaminated field soil to intrinsic bioremediation by the existing soil microbial consortia in the absence of the root zone. The intent of determining the dominant process(es) and comparing the masses of PHC removed and rates of PHC removal from the soil was to evaluate the benefit realized by phytoremediation relative to intrinsic bioremediation.

The third and final objective of this project, to develop a rationally-based model that could be used to predict degradation rates in the field, was identified to provide scientists with a predictive model for removal of PHC from contaminated field soils. No work of this type was identified in the course of the detailed literature review carried out regarding this subject.

To realize these objectives, a series of laboratory scale experiments were designed to contain and, to some extent, control and monitor the process(es) involved in the entire phytoremediation system. All inputs to the system and outputs from the system were controlled and monitored, along with numerous aspects of the experimental environment. The mass of PHC volatilized from the soil and the mass of PHC phytovolatilized were each measured. The soil and root respiration also was monitored to evaluate the mass of PHC degraded microbially. In order to simulate field conditions, the experiment modelled "pole planting" of hybrid poplars into diesel-contaminated field soils and the system was exposed to day/night cycles of light and temperature typical of a Canadian summer.

Chapter 2: Literature Review

2.1 Overview

Much of the published literature regarding phytoremediation of petroleum hydrocarbons (PHC) has focused on five general issues:

i) the ability of certain plants to uptake and tolerate specific contaminants (Briggs et al., 1982; Burken and Schnoor, 1996; Burken and Schnoor, 1998; Orchard et al., 2000; Burken et al., 2001; Ramaswami and Rubin, 2001; Ma et al., 2004);

ii) monitoring hydrocarbon degradation in the field (Zynter et al., 2001);

iii) modelling transport and degradation pathways (Chiou et al., 2001; Park et al., 2001; Kim et al., 2004);

iv) investigating bioavailability and aging of the contaminant (Hatzinger and Alexander, 1996; Gunasekara and Xing, 2003; Sharer et al., 2003); and

v) investigating many specific plant-microbe-contaminant-soil interactions that contribute to soil remediation.

In general, this research can be divided into two categories, one dealing with phytoremediation processes and the other dealing with the effects of soil and contaminant properties on phytoremediation.

2.2 Phytoremediation Processes

Before introducing phytoremediation processes it should be acknowledged that the identification and definitions of these processes, as well as other definitions throughout this thesis including that of bioremediation given in Chapter 1, were obtained from *Phytopet*©-A Database of Plants that Play a role in the Phytoremediation of Petroleum Hydrocarbons (Farrell et al., 2000). This database was developed by researchers in the Department of Soil Science at the University of Saskatchewan in cooperation with Environment Canada.

There are four identified processes involved in phytoremediation of PHC: phytodegradation/transformation, phytostabilization, phytovolatilization, and enhanced rhizosphere degradation. Phytodegradation/transformation is "the breakdown of contaminants either internally, through metabolic processes, or externally, through the release of plant-produced enzymes into the soil", phytostabilization is "the use of plants to contain or immobilize contaminants in the soil or groundwater" and phytovolatilization is "the movement of a contaminant out of the soil or groundwater and into, through, and out of a plant into the atmosphere". Lastly, enhanced rhizosphere degradation is "the breakdown of contaminants in the soil as a result of microbial activity that is enhanced in the presence of the rhizosphere". While each these processes may be defined individually they may be interrelated. For example, a compound with a high carbon number may be degraded by microbes in the soil, followed by degradation of the subsequent compounds by root exudates, followed by sorbtion of the subsequent compounds to plant roots.

The rhizosphere is the principal environment for many of these phytoremediation processes. The rhizosphere environment encourages microbial activity through the supply of root exudates which are "low molecular weight metabolites that enter the soil from the roots of plants". Root exudates are an important nutrient source for microorganisms. Also, the roots themselves encourage microbial activity in the rhizosphere by providing a source of organic carbon, increasing surface area for colonization by microbes, and aerating the soil to ensure aerobic degradation near the root zone (Anderson et al., 1993; Schnoor et al., 1995; Burken and Schnoor, 1996). These factors result in a microbial population within the rhizosphere that may be larger by one or several orders of magnitude compared with the microbial population away from the immediate influence of the roots (Anderson et al., 1993; Siciliano and Germida, 1998).

2.2.1 Phytodegradation/transformation

Phytodegradation/transformation, "the breakdown of contaminants either internally, through metabolic processes, or externally, through the release of plant-produced enzymes into the soil", can be divided into two components: first, absorption, translocation and metabolism of contaminants by the plant; and, second, degradation of the contaminant by root exudates.

a. Absorption, Translocation, and Metabolism of Contaminants by the Plant

The first component of phytodegradation/transformation involves the absorption, translocation, and metabolism of contaminants by the plant. Tests of plant-contaminant interactions with hybrid poplars showed that poplars were able to absorb, translocate and

partition numerous volatile organic compounds, VOCs, in hydroponic solution (Burken and Schnoor, 1998). Other experiments also have shown that vegetation can absorb contaminants (Briggs et al., 1982; Orchard et al., 2000; Ramaswami and Rubin, 2001; Ma et al., 2004).

The ability of a plant to absorb, translocate and metabolize contaminants is generally dependent on the solubility of the contaminant, reflected by the octanol-water partition coefficient, K_{ow}, of the contaminant (Cunningham and Berti, 1993; Alkorta and Garbisu, 2001), although other contaminant properties and the type of plant also affect the plant's ability to absorb contaminants (Schnoor et al., 1995). According to Cunningham and Berti (1993), K_{ow} values (typically expressed in log scale) generally fall into three groups defining the ability of a plant to absorb, translocate, and metabolize a specific contaminant, as described below.

Plants are able to absorb, translocate and metabolize contaminants with log $K_{ow} \leq 1$, hydrophilic contaminants. As these contaminants are water-soluble, their absorption is controlled by water influx into the plant and they may pose an additional environmental threat from groundwater contamination. Plants are able to absorb, translocate and may be able to metabolize contaminants with log K_{ow} values between 1 and 4. A study of the uptake of organic compounds by Briggs et al. (1982) indicated that the highest contaminant concentration translocated to the shoots occurred at a log K_{ow} of 1.8 with declining concentrations at higher and lower values of log K_{ow}. Plants are generally not able to absorb, translocate and metobilize contaminants with log K_{ow} values larger than 4, very hydrophobic or lipophylic, because the contaminant adsorbs to lipids on the root

surface (Cunningham and Berti, 1993; Schnoor et al., 1995; Alkorta and Garbisu, 2001). Adsorption of contaminants to lipids on the root surface is considered a phytostabilization process and phytostabilization is discussed in Section 2.2.2.

Once the contaminant has been absorbed by the plant it may be translocated to other parts of the plant where it may be completely or partially degraded, incorporated into the cell structure, or volatilized (Schnoor et al., 1995; Salt et al., 1998). The absorption, translocation and volatilization of the contaminant into the atmosphere is termed phytovolatilization and is discussed in Section 2.2.3.

b. Role of Root Exudates

The second component of phytodegradation/transformation involves degradation of the contaminant by root exudates. Although the definition of phytodegradation refers solely to direct degradation of contaminants by root exudates, root exudates may aid remediation in a number of other ways such as by: increasing the bioavailability of the contaminant, lubricating the soil, and acting as cometabolites with PHC.

Research has found that root exudates were able to degrade some organic contaminants (Salt et al., 1998; Alkorta and Garbisu, 2001). Studies by Schnoor et al. (1995) have shown that specific plant-derived enzymes are able to degrade 2,4,6-trinitrotoluene and trichloroethylene.

Other ways root exudates may aid remediation is by increasing contaminant bioavailability, "the extent to which a contaminant is available to living things" (Farrell

et al., 2000), lubricating the soil, and acting as cometabolites as described below. Organic acids in root exudates may increase the bioavailability of contaminants by competing with the contaminant for sorption sites in the soil. Lipids and sterols, also released by roots, have been found to increase the bioavailability of contaminants by causing organic matter to swell and expose previously non-exposed sorbed contaminants, making them available for microbial degradation. Lipids and sterols also lubricate the soil to facilitate root passage. Lastly, root exudates may act as cometabolites with the contaminant as root exudates and certain PHC are chemically similar (Siciliano and Germida, 1998). Some root exudates and pollutants that are chemically similar can be seen in Figure 2.1.

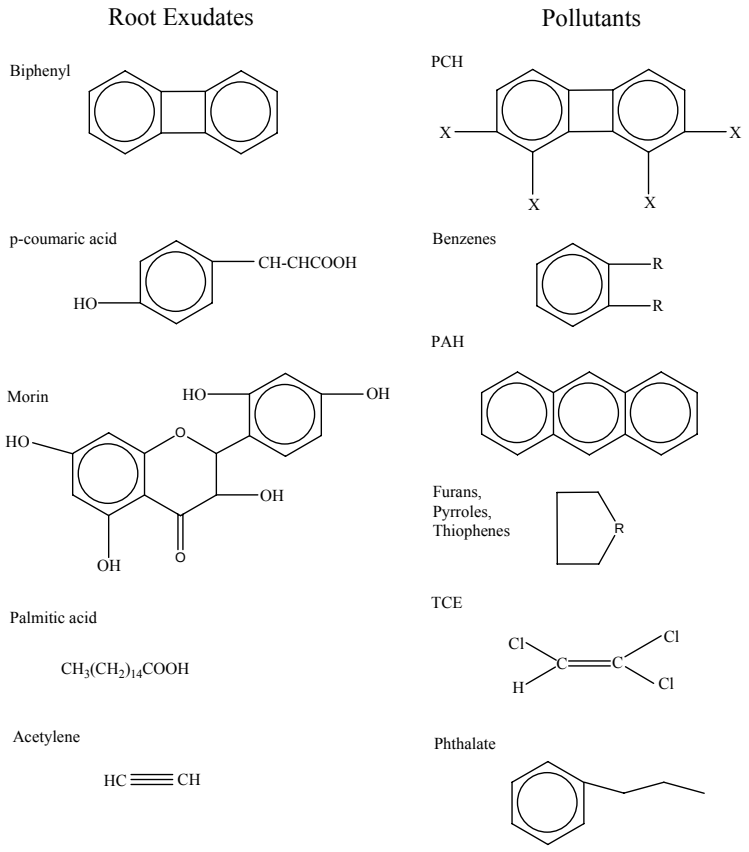

Figure 2.1: Chemical Similarities between Root Exudates and Pollutants (modified from Siciliano and Germida, 1998)

2.2.2 Phytostabilization

As defined by Farrell et al. (2000), phytostabilization is "the use of plants to contain or immobilize contaminants in the soil or groundwater", and can be divided into three mechanisms: "absorption and accumulation by roots, adsorption onto root surfaces, and incorporation into humic materials in the rhizosphere". These three mechanisms are, as with the absorption, translocation and metabolism of contaminants, generally dependent on the value of K_{ow} for each particular contaminant species.

a. Absorption and Accumulation by Roots

Absorption and accumulation results in the contaminant remaining in the roots of the plant. The contaminants are not translocated into the rest of the plant and are therefore not degraded, incorporated into the cell structure, or volatilized. This may occur for contaminants with a log K_{ow} value between 1 and 4 (Cunningham and Berti, 1993).

b. Adsorption to Roots

With this mechanism, contaminants are immobilized by adsorption to lipids on the surface of the roots. This may occur for contaminants with a log K_{ow} value above 4 (Cunningham and Berti, 1993; Schnoor et al., 1995; Alkorta and Garbisu, 2001).

c. Incorporation of PHC onto Organic Components of the Soil

With this mechanism, contaminants are immobilized by adsorption to organic matter within the soil. Sorption of contaminants to organic matter in the soil is discussed in Section 2.3.2a.

2.2.3 Phytovolatilization

Phytovolatilization, "the movement of a contaminant out of the soil or groundwater and into, through, and out of a plant into the atmosphere" (Farrell et al., 2000), occurs when the contaminant is absorbed into the roots, translocated through the plant, and volatilized into the atmosphere.

2.2.4 Enhanced Rhizosphere Degradation

The definition of enhanced rhizosphere degradation, "the breakdown of contaminants in the soil as a result of microbial activity that is enhanced in the presence of the rhizosphere" (Farrell et al., 2000) should include another process in phytoremediation, the removal of contaminants from the soil.

The microbial breakdown and removal of contaminants in the soil occurs through two distinct but interrelated processes, biodegradation and microbial uptake. Biodegradation is the "microbially mediated chemical transformation of organic compounds" (Lyman et al., 1992) while microbial uptake is the direct removal of the contaminant by adsorbing compounds to the membrane surface or absorbing compounds through the membrane. These two processes are interrelated in that the contaminant taken up may be the original contaminant or a biotransformation product.

Enhanced microbial activity in the rhizosphere also may, in some situations, benefit the health of the plant which affects the health of the rhizosphere and the entire phytoremediation system.

a. Biodegradation and Microbial Uptake of PHC

The ability of microbes to degrade and take up contaminants has been well studied and is the conceptual basis for other remediation techniques such as air sparging, land farming, composting, bioreactors, intrinsic remediation, and others (Riser-Roberts, 1998).

While a number of different microorganisms are able to degrade a number of different PHC, the specific catabolic pathway used is dependent on the microbe and contaminant. Although the enzymes used and the oxidation and cleavage locations vary, in general microbes degrade PHC by adsorbing the contaminant to the membrane surface or absorbing the contaminant through the membrane and, using oxygenase enzymes, incorporating oxygen into and cleaving the structure of the hydrocarbon. Continued oxidation of subsequent end products and incorporation into the Krebs cycle may result in the final degradation step, the release of CO_2, H_2O and energy (Chapelle, 1992; Riser-Roberts, 1998), though complete degradation does not always occur. Subsequent end products may be directly taken up by microbes and not degraded further or may be degraded to smaller, simpler, more stable intermediaries and incorporated into the soil as humus or soluble acids, ketones and alcohols (Lyman et al., 1992).

The potential of a particular PHC to be degraded, independent of soil properties, depends on its chemical structure. The main considerations for biodegradation are the size of the contaminant and the types and geometry of its bonds. Some PHC have bonds that microbes have difficulty breaking or are not able to break. Microbes may also find different molecular configurations more difficult to degrade than others. For example,

linear alkanes were found to be more readily biodegradable than branched alkanes (Riser-Roberts, 1998).

The number of different microbes able to degrade a specific contaminant decreases as the contaminant becomes more difficult to degrade. Also, not all microbes are able to directly take up all contaminants. This results in variations of PHC and microbial population composition over time and space with the most readily degradable hydrocarbons and associated microbes being replaced by less degradable hydrocarbons and associated microbes. It should be noted that one type of microorganism is rarely able to fully degrade any specific contaminant. The most effective remediation occurs with a diverse microbial population (Riser-Roberts, 1998).

As with biodegradation, microbial uptake of PHC involves adsorption of contaminants to the membrane surface or absorption of contaminants through the membrane, removing them from the soil. Unlike biodegradation, however, the contaminants may not be further degraded following uptake.

The main factor in direct microbial uptake is the K_{ow} value of the contaminant. Generally, the K_{ow} value of a contaminant increases as the molecular mass of the contaminant increases (Lyman et al., 1992). Similar to the absorption of contaminants into roots, the ability of a contaminant to be absorbed by the microbe decreases with increasing K_{ow}. High molecular mass, high K_{ow} contaminants adsorb to the surface of the microbe while medium molecular mass, intermediate K_{ow} contaminants and low molecular mass, low K_{ow} contaminants can be absorbed by the microbe. However, low

molecular mass, low K_{ow} contaminants are often toxic to microbes because of their inability to control diffusion of the chemical through their cell wall (Riser-Roberts, 1998).

b. Microbial Influence on Rhizosphere

Although microbes are able to completely degrade certain contaminants on their own, the health of the rhizosphere and associated microbial community is dependent on the growth and survival of the vegetation. Microbes have been found to aid plant health by reducing the phytotoxicity of certain contaminants and by providing nutrients. Phytotoxicity of contaminants and limited nutrient availability may retard soil remediation by slowing or preventing plant growth. Microbes have been found to reduce phytotoxicity of contaminants by degrading contaminants to less phytotoxic or non-phytotoxic intermediaries (Siciliano and Germida, 1998) and certain types of bacteria such as nitrogen-fixing bacteria are able to provide plants with needed nutrients.

Although the microbial community in the rhizosphere is enhanced by the plant, the health of the plant is not necessarily enhanced by the microbial community. Decreased phytotoxicity and increased nutrient availability are not always necessary. For example, many contaminants are not phytotoxic and, for those that are, root exudates may degrade these compounds to non-phytotoxic forms, the plant itself may exclude any phytotoxic compounds, or phytotoxic compounds may not be available for plant uptake due to interactions within the soil. Also, in soils with sufficient amounts of nitrogen, nitrogen-fixing bacteria may not be needed.

2.3 Effects of Soil and Contaminant on Phytoremediation

Previous sections have given an overview of plant-microbe-contaminant interactions resulting in the degradation and removal of PHC contaminants. To fully investigate phytoremediation, which includes the entire plant-microbe-contaminant-soil interaction, the effects of the soil and contaminant also must be considered.

2.3.1 Effects of Soil

The soil itself, both chemically and physically, has a large effect on phytoremediation due to its influence on the composition of the microbial population, the type of vegetation that can grow, and the transport and availability of the contaminant. Factors such as: pH; nutrient concentration; cation exchange capacity; soil texture, permeability, and bulk density; temperature; moisture content; and organic matter influence phytoremediation (Donahue et al., 1983; Rendig and Taylor, 1989; Tan, 1994; Tumeo and Guinn, 1997; Eweis et al., 1998; Riser-Roberts, 1998; Siciliano and Germida, 1998; Margesin, 2000; Gibb et al., 2001; Huang et al., 2003; Delille et al., 2004). As an in-situ remediation technology, many of these factors cannot be changed in the field and remediation conditions are often left as they are or a few small amendments are made. Many of these factors are interrelated so amendments to the soil must be carefully planned.

a. pH

Due to pH tolerance and availability of nutrients and contaminants, the soil water pH influences the type of vegetation that can survive and the microbial community. Microbes have an optimum pH of about 7. In more acidic soils bacteria cannot

effectively compete with fungi for nutrients. Nutrient solubility, particularly phosphorous, is sensitive to changes in pH with an optimum of 6.5. Soil pH also affects the amount and species of cation and anion adsorption and will therefore affect the adsorption of certain nutrients and contaminants to clay surfaces (Riser-Roberts, 1998). As pH decreases, more hydrogen, H^+, ions attach to soil particles creating positively charged sites. Nutrients in anionic form, such as nitrogen as NO_3^- and phosphorous as $H_2PO_4^-$ and HPO_4^{2-}, are then bound to the H^+ ions and are less available for uptake. Taking these influences into account an optimum pH for remediation of hydrocarbons was determined to be about 7.8 (Riser-Roberts, 1998 from Dibble and Bartha, 1979). It should also be noted that the pH of the rhizosphere may differ from that of the bulk soil (Rendig and Taylor, 1989). The uptake of anions in excess of cations may cause roots to secrete bicarbonate ions to maintain electric neutrality, raising the pH. Alternately, the uptake of cations in excess of anions may cause roots to secrete hydrogen ions to maintain electric neutrality, lowering the pH (Rendig and Taylor, 1989). Amendments may be made in the field by liming to increase the pH or adding sulphur or other acid-forming agents to decrease the pH (Riser-Roberts, 1998).

b. Nutrient Concentration

Sufficient concentrations of macro-nutrients (nitrogen, phosphorous, organic carbon and potassium) and micro-nutrients (zinc, calcium, manganese, magnesium, iron, sodium and sulphur) must be available to maintain the health of the microbial population and vegetation. In PHC contaminated soils the large amounts of organic carbon available tend to result in rapid depletion of other nutrients, with the limiting nutrients generally being nitrogen and phosphorus. Amendments of depleted nutrients have been found to

enhance remediation (Riser-Roberts, 1998). This being said, it must be realized that competition between vegetation and microbes for nutrients is not fully understood and more research is needed in this area (Siciliano and Germida, 1998).

c. Cation Exchange Capacity

The cation exchange capacity determines the amount of cationic nutrients available, specifically potassium, calcium, magnesium and ammonium. Cation exchange capacity is dependent on pH, the amount of organic matter in the soil, and the amount and type of clay in the soil (Donahue et al., 1983; Tan, 1994).

d. Soil Texture, Permeability, and Bulk Density

Soil texture, permeability, and bulk density influence the transport of water, gases and contaminants through the soil and the ease of root growth. These three factors can be understood as a reflection of the influence of pore size. Smaller pore sizes in finer textured, less permeable, and denser soils reduce the transmission rates of water, gases, and contaminants and may impede root growth whereas larger pores increase the transmission rates of water, gases, and contaminants. The permeability and bulk density of surface soils may be increased and decreased, respectively, through tillage.

e. Temperature

Soil and atmospheric temperature have a large influence on the type of vegetation present, the microbial population, and contaminant availability. It has been proposed that microbial degradation follows an Arrhenius type relationship (Delille et al., 2004 from Leahy and Colwell, 1990) with microbial metabolism doubling for each 10°C

increase from 10-40°C (Delille et al., 2004; Riser-Roberts, 1998 from Bossert et Berta, 1984), although studies by Gibb et al. (2001) and others found that this was not necessarily true. Gibb et al. (2001) found that in laboratory degradation studies with Alberta Sweet Mix crude at 5°C and 21°C the mineralization rate at 5°C was lower than that at 21°C for the lag phase but not for the stationary phase. Also, bioremediation studies in cold climates have shown that cold-adapted indigenous microbes are able to degrade PHC in soils (Tumeo and Guinn, 1997; Margesin, 2000; Delille et al., 2004). Generally, all things being equal, and bearing in mind the importance of adaptation of microbial communities to ambient conditions, degradation of PHC may be slower at lower temperatures due to lower microbial metabolism and a smaller population of cold-adapted microbes able to degrade PHC.

Contaminant bioavailability increases with increased temperature due to decreased adsorption and increased solubility. Although an increase in temperature makes the contaminant more available for degradation, high temperatures may also result in toxicity effects as volatilized hydrocarbons are often toxic to microorganisms. The optimum temperature for degradation was found to be 20°C (Riser-Roberts, 1998 from Dibble and Bertha, 1979), although microbial degradation of hydrocarbons was found to occur between -2 and 70°C (Riser-Roberts, 1998).

Soil temperature varies with soil texture, moisture content, atmospheric temperature and depth. Due to the insulating properties of overlying soil, the deeper the soil the longer it will take for temperature changes from the atmosphere to reach it. Daily temperature

fluctuations do not generally affect soil at depths greater than 30-40 cm and seasonal temperature fluctuations do not generally affect soil at depth greater than 4 m.

f. Moisture Content

Moisture content significantly influences the microbial activity of the soil. An adequate amount of moisture is needed to maintain microbial populations as water is a major component of the bacteria protoplasm and is needed to transport nutrients and contaminants through the system. Alternatively, too much water inhibits gas exchange which can cause anaerobic conditions to develop in the soil (Eweis et al., 1998). Optimal biodegradation by aerobic bacteria was found to occur at moisture contents between 50 and 75% of field capacity. Field capacity being "the amount of water held by soils after excess water has drained by gravity and the downward movement has materially ceased" (Tan, 1994). Field capacity, in turn, is dependent on the soil texture, permeability and density.

g. Organic Matter

The amount and type of soil organic matter significantly affects the microbial population, bioavailability of nutrients, soil moisture content, cation exchange capacity, and contaminant bioavailability.

Soil organic matter is composed of humus, kerogen and black carbon, with humus being the dominant organic component, providing 60-70% of the organic carbon in soil (Donahue et al, 1983). Humus is a combination of plant and animal debris, microbial cells, and products of microbial debris which have undergone transformation so their

parent compounds are unrecognizable (Eweis et al., 1998; Riser-Roberts, 1998). Kerogen, a component of sedimentary rocks, is resistant to weathering and can be incorporated into soil through weathering of sedimentary rocks or through mining, transportation, and combustion of coal. Black carbon is a combustion product from coal, liquid fuel, forest fires, etc. (Huang et al., 2003). Decomposition of plant and animal debris to form humus is performed by microorganisms which absorb nutrients released during decomposition and free nutrients for plants to absorb. The nutrients released during decomposition are mainly carbon with small amounts of oxygen and hydrogen and even smaller amounts of nitrogen, phosphorus, sulphur, boron and molybdenum (Donahue et al., 1983). Humus is also important to the moisture content and permeability of the soil. Humus can absorb large quantities of water (2-3 times its weight) and, through microbial activity, is able to contribute to soil aggregation, creating larger soil pores and better drained soils. The amount of humus also significantly influences the cation exchange capacity as humic substances have large, negatively charged surface areas for ion exchange (Donahue et al., 1983). While these factors are all very important in bioremediation, perhaps the most important is the influence of organic matter on contaminant bioavailability. The effect of organic matter on the bioavailability of the contaminant is presented in Section 2.3.2a.

2.3.2 Effects of Contaminants

The contaminant has a large influence on phytoremediation as seen in Section 2.2 where plant-contaminant and microbe-contaminant interactions were discussed. Although these interactions are extremely important, they cannot occur if the contaminant is not available for uptake or degradation. Bioavailability governs contaminant uptake and

degradation by plants and microbes. Contaminant bioavailability is dependent on the amount of organic matter in the soil, the type and concentration of the contaminant, and the amount of time the contaminant has been in the soil.

a. Sorption of Contaminants to Soil

Contaminant bioavailability is strongly influenced by the K_{ow} value of the contaminant and the amount of organic matter in the soil. Hydrophobic (log K_{ow}>1) organic compounds will sorb to organic matter in the soil, present as solids, thin layers of organic matter surrounding soil particles, or within soil particles (Lyman et al., 1992; Domenico and Schwartz, 1997). Sorption of the contaminant to organic matter in the soil may influence phytoremediation as microbes take up contaminants more readily from the fluid phase than from the sorbed phase (Pignatello and Xing, 1996; Riser-Roberts, 1998).

The amount of contaminant sorbed is dependent on contaminant concentration, the amount of organic carbon in the soil, and the hydrophobicity of the contaminant. This can be shown using the simplest sorption model, the linear Freundlich isotherm, although other sorption models such as the dual mode model (Huang et al., 2003) may more accurately describe sorption for some contaminants. The linear Freudlich isotherm can be expressed as:

$$S = K_d C \qquad [2.1]$$

where

S=mass of contaminant sorbed to the surface from aqueous solution

C=equilibrium concentration of contaminant in solution

K_d= solid-phase to solution-phase distribution coefficient

In turn, the K_d can be expressed as:

$$K_d = K_{oc} f_{oc} \quad [2.2]$$

where

K_{oc}=organic carbon-water partition coefficient

f_{oc}=mass fraction of organic carbon in the soil

K_{oc} can be related to K_{ow}, the octanol-water partition coefficient by the following empirical equations:

$$\log K_{oc} = -0.21 + \log K_{ow} \text{ (Karickhoff et al., 1979)} \quad [2.3]$$

$$\log K_{oc} = 0.49 + 0.72 \log K_{ow} \text{ (Schwarzenbach and Westall, 1981)} \quad [2.4]$$

$$\log K_{oc} = 0.088 + 0.909 \log K_{ow} \text{ (Hasset et al., 1983)} \quad [2.5]$$

These equations give the range of results shown in Figure 2.2.

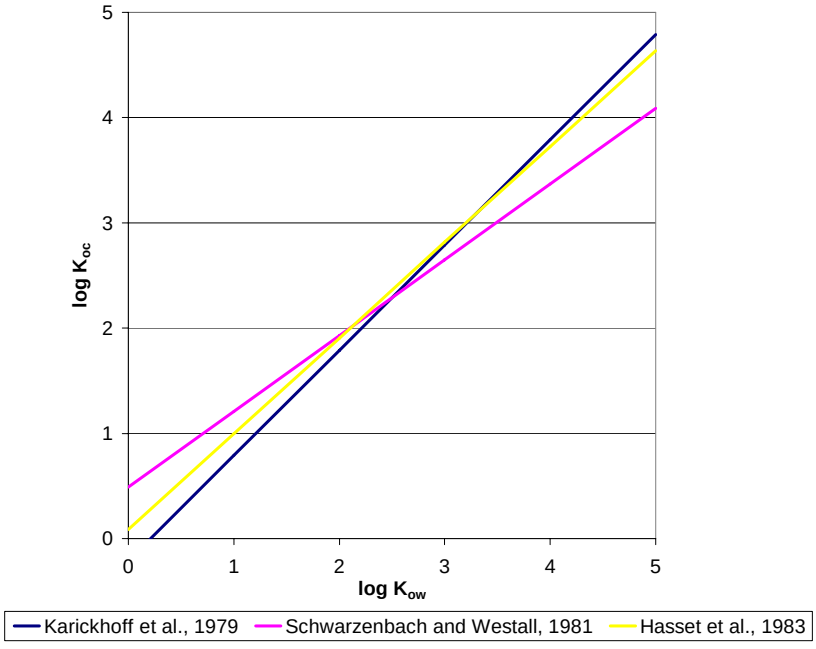

Figure 2.2: Log K_{ow} vs. log K_{oc} for Three Different Studies

Sorption studies have found that organic contaminants will sorb to inorganic matter (i.e. clays) in soils. In general, sorption to inorganic matter is significant for soils with organic carbon contents lower than 0.1%, and the K_{oc}-K_{ow} relationships presented previously are not valid for soils with carbon contents lower than 0.1% (Lyman et al., 1992). A study by McCarty et al. (1981) indicated that the critical fraction of organic carbon (f^*_{oc}) was related to the K_{ow} of the contaminant by the equation:

$$f^*_{oc} = \frac{A_s}{200} * \frac{1}{K_{ow} * 0.84} \qquad [2.6]$$

where

f^*_{oc}=critical fraction of organic carbon

A_s=silica specific surface area

As referenced by Lyman et al. (1992) inorganic sorption can be significant at clay to organic carbon ratios greater than 60. For soils where sorption to inorganic matter is significant the partition coefficient can be determined as follows:

$$K_d = K_{oc} f_{oc} + K_{oi} f_{oi} \qquad [2.7]$$

where

K_{oi}= inorganic partition coefficient

f_{oi}=is the fraction of inorganic matter

b. Aging

A number of studies have found that sorption to and desorption from soil is a kinetic process, with a rapid initial sorption/desorption phase followed by a slow

sorption/desorption phase. In the initial rapid phase a portion of the chemical is sorbed/desorbed within a few minutes or hours, whereas the slow phase may take weeks, months or years to reach equilibrium (Alexander, 1995). To reach sorption sites in water-wet soils, the contaminant travels through the bulk fluid by advection and diffusion, diffuses through the water film surrounding the particle, and sorbs to sites on the particle surface (Lyman et al., 1992). To reach sorption sites in oil-wet soils, soils that were previously completely dry, or where the contaminant displaced the water phase, the contaminant travels through the pores and sorbs directly onto soil particles (Lyman et al., 1992). These are called surface sorption sites and are thought to be sites of rapid sorption/desorption (Alexander, 1995). From surface sorption sites the contaminant diffuses into the pore fluid and the solid particle and sorbs to sites in these locations. The sorption sites within the pores of the particle and within the solid particle are thought to be sites of slow sorption/desorption (Alexander, 1995; Pignatello and Xing, 1996).

Contaminants sorbed to the surface of particles in contact with the aqueous phase are thought to be the most available for degradation since microbial degradation is thought to occur more readily from the aqueous phase. Contaminants sorbed to organic matter within the soil particle are not available for microbial degradation; whereas contaminants sorbed to organic matter on the pore wall may or may not be available, depending on pore size. Contaminants in pores large enough for bacteria to enter (bacteria range in size from 1 to 10 μm) will be available for microbial degradation,

whereas contaminants in pores too small for bacteria to enter or within the soil particle will not be available (Pignatello and Xing, 1996).

For complete contaminant removal desorption must occur. As desorption is driven by diffusion, whenever the concentration of the surface sorbed phase decreases, the contaminant will diffuse out of the pore fluid and the solid particle to maintain equilibrium. Although this process is simply the reverse of sorption, desorption has been found to exhibit hysteresis where desorption occurs slower than adsorption. This may be due to several factors including entrapment of the contaminant within soil organic matter, partial microbial degradation of the contaminant, and experimental conditions (Pignatello and Xing, 1996; Huang et al., 2003).

Many of the soils undergoing or being considered for remediation were contaminated many years ago. The contaminant at these sites has generally been in the soil long enough that slow sorption has occurred and some type of equilibrium has been reached, making these contaminants more difficult to remove from the soil. This aging effect has been found in numerous studies and has distinctive curve as shown in Figure 2.3 (Alexander, 1995).

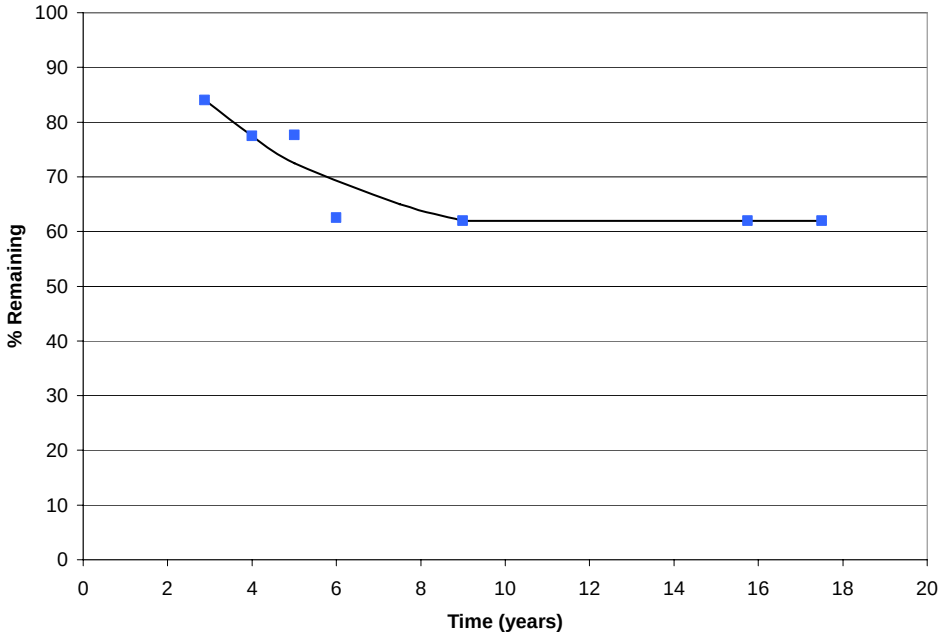

Figure 2.3: Concentration of DDT in Chester Loam Amended with 200 mg of Insecticide per Kilogram of Soil. Replotted from the Data of Nash and Woolson (1967) as reported by Alexander (1995)

A study by Hatzinger and Alexander (1996) examined mineralization of phenanthrene aged for various times in three different sterile soils inoculated with a *Pseudomonas*. Phenanthrene mineralization was found to decrease with increased aging of the contaminant. However, in a loam (pH 7.2, 4.0% organic matter), the mineralization rates converged at about 7 days after inoculation for the contaminant aged for 0, 13, 27 and 84 days. In muck (pH 6.9, 19.3% organic matter), the mineralization rates converged at about 15 days after inoculation for the contaminant aged for 13, 27 and 84 days.

In another experiment from the same study, phenanthrene was aged for 0, 204 and 315 days in muck and the amounts of phenanthrene mineralized were tested at intervals over approximately 33 days. The mineralization rates showed a marked decrease with increased aging but insufficient time was allowed to determine if the mineralization rates would converge. The extraction efficiency of phenathrene decreased from 103.5 ± 3.6% to 91.8 ± 1.8%, 88.2 ± 2.2% and 87.1 ± 3.7% when aged in muck for 13, 27 and 84 days, respectively, and from 105.2 ± 3.1% to 94.4 ± 7.7% and 86.6 ± 3.5% when aged in muck for 204 and 315 days, respectively.

In yet another experiment from the same study, two different amounts of 4-nitrophenol were aged in loam and muck for 40 and 103 days. 4-nitrophenol mineralization was found to decrease with increased aging of the contaminant, particularly at the lower concentration.

The experiments from this study suggest aging influences contaminant bioavailability, although the study did not take into account microbial activity of the contaminant itself as a possible source for decreased recovery. Also, neither this study nor others directly examined the effect of plants on the bioavailability and mineralization of contaminants. As plants have the ability to sequester contaminants and root exudates and surfactants have been found to increase the bioavailability of the contaminant, a reasonable conclusion is that the presence of vegetation may increase the amount and rate of contaminant mineralized.

Reduction in bioavailability of contaminants in soil with time may have implications for soil toxicity. Contaminants tightly sorbed to remote locations (slow sorption) within the soil may not be as toxic to mammals as they would be were they sorbed to the surfaces of particles. Presently toxicity measurements are based on the amount of specific fractions and types of hydrocarbons in the soil as determined by vigorous extraction methods, yet in the environment many of the hydrocarbons extracted by these methods may never be available (Alexander, 1995).

2.4 Summary

Phytoremediation is complex, with numerous interrelated processes and soil and contaminant properties. Much of the research to date has concentrated on very specific relationships within the phytoremediation system with little done in the examination of the system as a whole. While this research has contributed to understanding the processes and influences of phytoremediation, the lack of research involving phytoremediation that is well monitored and occurs under field conditions has limited its adoption as a remediation technology.

Chapter 3: Materials and Methods

3.1 Overview

The purpose of this project was to monitor phytoremediation of diesel contaminated field soils under stimulated field conditions. To perform the experiment, contaminated soil from a field site was placed in a number of gas-tight test cells consisting of upper and lower sealed chambers. Hybrid poplars were planted in four test cells and two test cells were used as blanks, containing only contaminated field soil with no significant growing plants. To enable separate monitoring and quantification of different degradation pathways, the soil and roots were sealed from the stem and leaves and each was sealed from the environment. The bottom chamber of each test cell, containing the soil and roots, was attached to an automated, multi-channel respirometer to provide continuous monitoring of O_2 and CO_2 fluxes in the lower chamber. This data was used to estimate the rate and amount of microbial degradation of petroleum hydrocarbons in the soil. Air sampling tubes were placed upstream of the respirometer to remove hydrocarbons volatilized from the soil for periodic analysis and quantification. The upper chamber of each test cell, containing the stem and leaves, was attached to an air circulation system and air sampling tubes were placed downstream of the upper chamber to remove phytovolatilized hydrocarbons for periodic analysis and quantification.

Numerous index and characteristic tests were performed on the soil before and after the experiment. These tests were performed to enable the observed PHC degradation to be evaluated in the context of clearly defined soil properties determined using standard and commonly-used tests. The index and characteristic tests performed included: grain size distribution; moisture content; cation exchange capacity (CEC); pH; organic carbon; electrical conductivity; calcium (Ca^{2+}), magnesium (Mg^{2+}), sodium (Na^{+}), and potassium (K^{+}); sodium adsorption ratio (SAR); nitrogen (N) and phosphorous (P); and microbial adenosine triphosphate (ATP).

Tests also were performed to quantify PHC concentration before and after the experiment and, upon completion of the experiment, the root length and plant biomass were determined.

3.2 Experimental Design

Experimental test cells were designed to separate the soil and roots from the stem and leaves in order to individually quantify the amount of contaminant volatilized from soil, phytovolatilized and degraded microbially. Each test cell consisted of two chambers, a lower chamber containing the soil and roots and an upper chamber containing the stem and leaves. Lower chambers were constructed using air-tight PVC containers and upper chambers were constructed using air-tight acrylic containers. The test cells were manufactured in the Engineering Shops at the University of Saskatchewan. A photo of three of the experimental test cells can be seen in Figure 3.1 and drawings of the experimental test cells are presented in Appendix A. The lower chambers were attached to a respirometer to measure soil and root respiration and obtain estimated values of the

amounts of contaminant degraded microbially. Air sampling tubes were placed downstream of the lower and upper chambers to measure the amount of PHC volatilized from the soil and phytovolatilized, respectively.

Figure 3.1: Experimental Test Cells

During the experiment the following environmental conditions were controlled: temperature and light conditions; the phreatic surface; and air circulation in the upper chamber. Also, soil and air temperatures were monitored throughout the experiment.

3.2.1 Lower Chamber

A schematic and photos of the lower chamber can be seen in Figures 3.2 to 3.4. Each lower chamber consisted of a 46 cm (18") section of 30 cm (12") ID PVC pipe with 1.9 cm (3/4") thick walls sealed on each end by a 38 cm (15") diameter, 2.5 cm (1") thick PVC plates. A cylindrical section was removed from the centre of the top plate and a groove was cut into the PVC plate where the cylindrical section had been removed. An o-ring was placed in this groove to create a seal between the lower and the upper chamber. A plastic fuel spout was positioned through the hole in the top PVC plate and sealed to the bottom of the top plate. Upon setup of the experiment, a hybrid poplar stem was threaded through the fuel spout and sealed with Panasil® Contact Plus (Kettenbach Dental, Eschenburg, Germany), a low viscosity, polyvinyl siloxane dental impression material (Figure 3.4). Along the length of each pipe segment two 1.3 cm (1/2") diameter holes were drilled at a distance of 1.1 cm (7/16") from each end. Attached to these two holes was an assembly used to maintain a constant phreatic surface in each lower chamber (Figure 3.3).

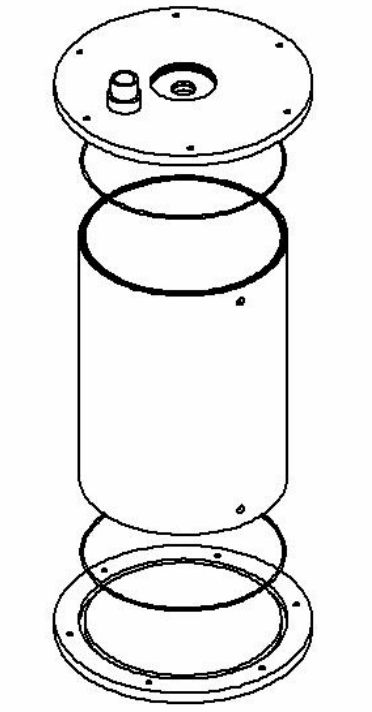

Figure 3.2: Schematic of the Lower Chamber

Figure 3.3: Lower Chamber

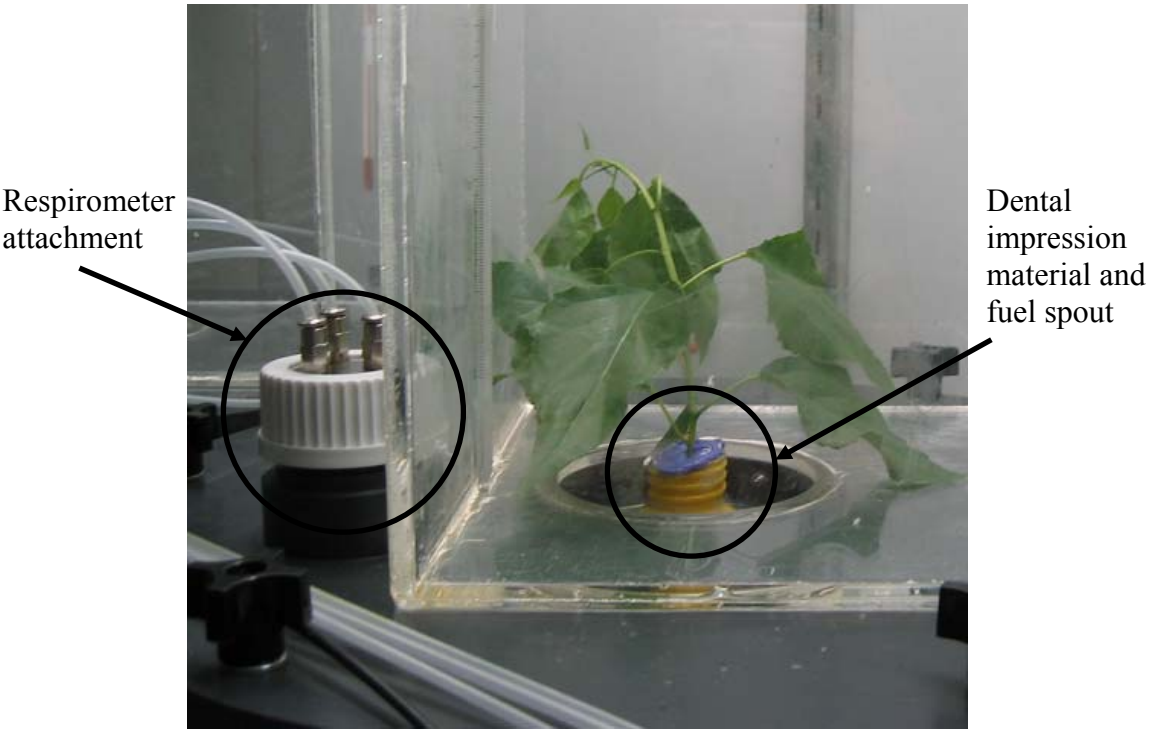

Figure 3.4: Lower and Upper Chamber Connection

Prior to assembly of the experiment, each lower chamber was tested for leaks by placing a handheld data logging pressure transducer (YSI 556 MPS, YSI Incorporated, Yellow Springs, Ohio, USA) into the chamber, sealing the chamber, blocking off the plastic fuel spout and the respirometer attachment, and pressurizing the chamber. The transducer was left in the chamber for approximately 1 hour, removed, and the pressure data was examined for any indication of leaks.

3.2.2 Upper Chamber

A schematic and photo of the upper chamber can be seen in Figures 3.5 and 3.6. The upper chambers consisted of gas-tight acrylic containers that sealed to each lower chamber as described in Section 3.2.1 and as can be seen in Figures 3.1, 3.3, 3.4 and 3.6.

The chambers were made of 0.5 cm (3/16”) thick acrylic, cut and glued together to form parallelepiped, with the exception of the upper chamber of test cell 2 which was made of a 0.6 cm (1/4”) thick, 20.3 cm (8”) ID acrylic pipe. Each rectangular side measured 56 cm (22”) by 22.5 cm (8.9”). The upper chambers sealed to the lid of the lower chambers at one of the square sides through 0.6 cm (1/4”) thick, 8.9 cm (3½”) ID acrylic pipes that were glued into a hole in one of the square sides.

Two holes were drilled into the rectangular side of each upper chamber, one near the top and one near the bottom. Plastic tubing fittings were placed in these holes and pieces of Tygon® tubing were attached to the fittings. These were used to create an air circulation system in each of the upper chambers. The air circulation system was designed so air flowed at a known rate into the upper chambers from the top holes and out through the bottom holes. Air sampling tubes were placed downstream of the upper chambers to collect phytovolatilized PHC.

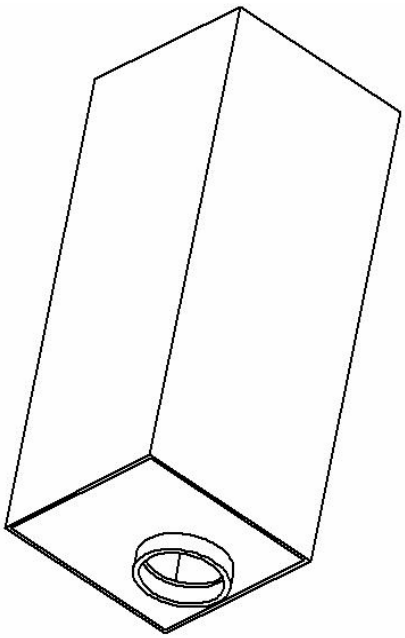

Figure 3.5: Schematic of the Upper Chamber

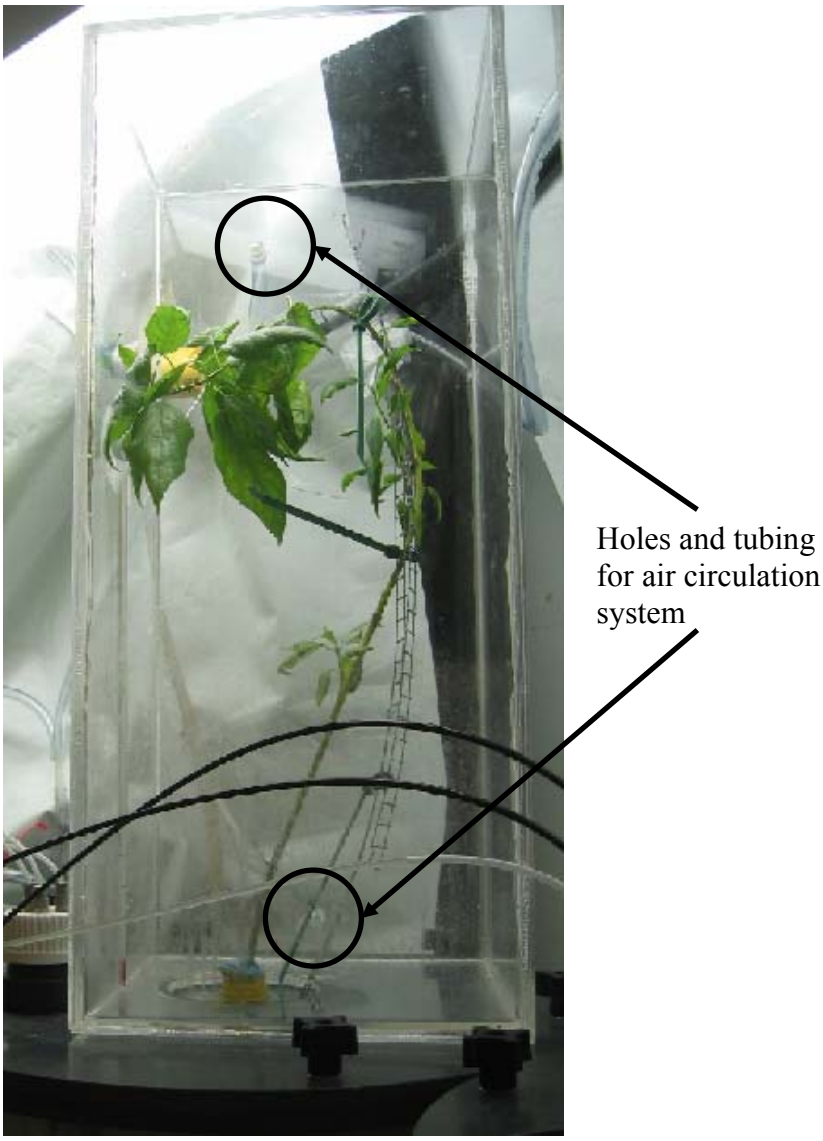

Figure 3.6: Upper Chamber

Prior to assembly of the experiment each upper chamber and the seal between the upper and lower chamber was tested for leaks by blocking off the plastic fuel spout, sealing the upper chamber to the lid of the lower chamber, and running air at a known flowrate through the chambers. The flowrate was measured at the chamber inlet and outlet. If the flowrate was found to be equal at the inlet and outlet, the upper chamber and the seal between the upper and lower chamber was deemed leak-free.

3.2.3 Contaminated Soil

The soil used in this experiment was collected from a former bulk fuel station in eastern Saskatchewan. The soil was taken from a depth of ~1 m using a mini-excavator. The soil was placed in buckets, transported to the University of Saskatchewan and kept in cold storage until it was placed in the lower chambers of the experimental test cells two days after it had been collected.

Placement of the contaminated soil was accomplished by positioning coils of copper tubing, a layer of gravel, and a 420 g/m^2 geotextile inside each lower chamber followed by the contaminated soil in the proper configuration.

Coils of copper tubing were positioned flush against the inside walls of the lower chambers. Tubing entered the first lower chamber through a hole drilled in the bottom of the chamber and exited through the top. From the top of the first lower chamber the tubing went to the bottom of the second lower chamber, continuing through all six chambers. The copper tubing was sealed with rubber stoppers and silicone sealant at the locations where the tubing entered and exited the lower chambers to ensure an air-tight seal. A water bath set at 2°C pumped an antifreeze and water mixture through the copper tubing in an attempt to keep the soil at a lower temperature than the temperature of the environmental chamber.

After the copper tubing was in position, gravel was placed in each of the lower chambers to allow good drainage for the water level indicator. Before placement the gravel was autoclaved to ensure no bacteria were added to the system. A nonwoven geotextile was

then positioned on top of the gravel for separation between the gravel and contaminated soil. Enough gravel was placed in the lower chamber that the top of the geotextile was 10 cm from the top of the lower PVC plate.

Four sections of soil with different ratios of contaminated soil to potting soil were placed at several intervals to create a soil configuration that increased in concentration radially from the tree. Potting soil without any contaminated soil was located immediately surrounding the tree, at a diameter of 5 cm extending radially from the centre. The next section consisted of a homogenized mixture of 1/3 contaminated soil and 2/3 potting soil was placed between the 5 cm diameter core out to a diameter of 9 cm followed by a section containing a homogenized mixture of 2/3 contaminated soil and 1/3 potting soil between the 9 cm diameter soil out to a diameter of 13 cm. The final section consisted of contaminated soil only between the 13 cm diameter out to the edges of the lower chamber. With this configuration the soil goes from potting soil only at the centre, to 1/3 contaminated soil and 2/3 potting soil, to 2/3 contaminated soil and 1/3 potting soil, and contaminated soil at the edges only. The soil configuration can be seen in Figure 3.7.

To place the soil in the configuration described above a bottom portion of contaminated soil was placed above the geotextile. A container with a diameter of 13 cm was then placed on the initial bottom portion of contaminated soil and the space surrounding the container was filled with contaminated soil to a known height. The target density for this portion of soil was 1.2 g/cm^3, and the actual average density was between 1.07 and 1.66 g/cm^3 with the density of five of the six containers between 1.07 and 1.15 g/cm^3.

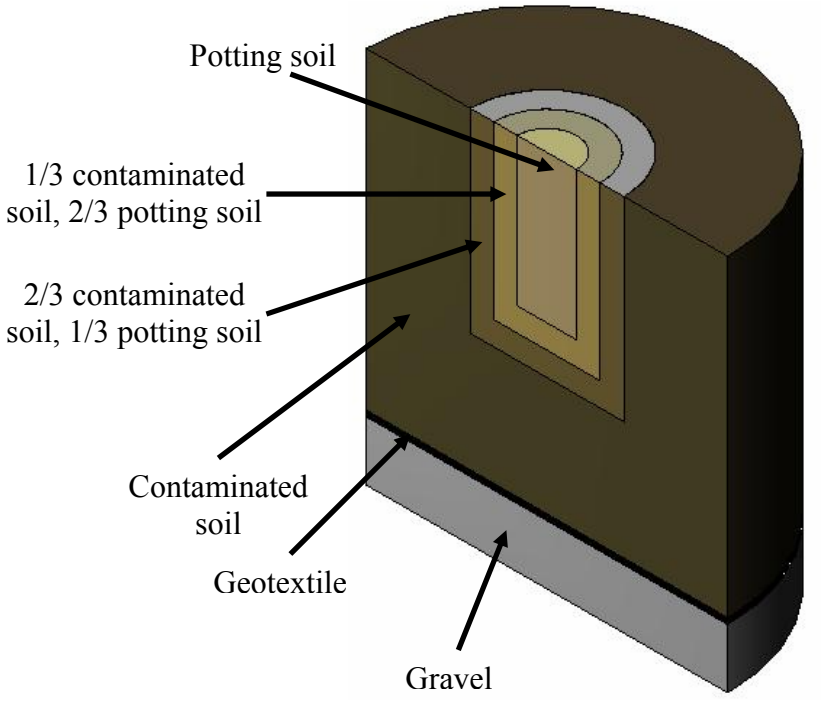

Figure 3.7: Soil, Geotextile, and Gravel Configuration

Next the 13 cm diameter container was removed and the bottom portion of the 2/3 contaminated soil, 1/3 potting soil section was put into place. A container with a diameter of 9 cm was then placed on that bottom portion of 2/3 contaminated soil, 1/3 potting soil and the space surrounding the container was filled with that soil to the same height as the contaminated soil. This soil had an average density between 0.85 and 0.89 g/cm^3.

The 9 cm diameter container was removed and the bottom portion of the 1/3 contaminated soil, 2/3 potting soil was put into place. A thin-walled piece of PVC pipe with a diameter of 5 cm was placed on that bottom portion of 1/3 contaminated soil, 2/3 potting soil and the space surrounding the container was filled with that soil to the same height as the two previous soils. This soil had an average density between 0.70 and 0.75

g/cm^3. Some potting soil was then placed into the PVC pipe followed by the poplar tree and more potting soil.

Between each of the sections a small amount of white rock flour was sprinkled onto the soil to aid in the identification of the section boundaries upon dismantling of the experimental test cells.

This soil placement was followed for each lower chamber, although the soil configuration of the second lower chamber was later modified. The tree in the second chamber was replaced on August 18, 2005, 6 days after the experiment began. When the tree was replaced the soil configuration was disturbed. As a result there were no definite boundaries between the different soils. The tree in the third chamber was replaced on August 31, 2005, 19 days after the experiment began, although the soil configuration of this chamber was maintained.

3.2.4 Walker Poplars

Walker Poplars were chosen for this experiment because they are demonstrated phytoremediators by phytovolatilization (Burken and Schnoor, 1998) and suspected phytoremediators by enhanced rhizosphere degradation (Jordahl et al., 1997), they grow quickly, cuttings were easily obtained, and they are native to Saskatchewan. Walker Poplars were cloned from seedlings of *Poplar deltoides* at the Prairie Farm Rehabilitation Administration (PFRA) Shelterbelt Centre in Indian Head, Saskatchewan. PFRA supplied a number of Walker Poplar cuttings which were planted in potting soil and grown for about three months until they were transplanted into contaminated soil.

During this initial three month period the trees were exposed to the same temperature and light conditions used during the experiment. These conditions are described in Section 3.2.8.

3.2.5 Sealing and Leakage Control

After placing the soil in the proper configuration and planting the trees, the experimental chambers were sealed in four locations.

First, the top plate of the lower chamber was attached. This was done by threading the tree though the fuel spout attached to the top plate, placing the edges of the lower chamber into grooves on the underside of the top plate, and then tightening the thumb screws.

Second, a seal was placed around the tree between the tree stem and the fuel spout. This was done by placing a small circular piece of foam around the tree stem and injecting Panasil® Contact Plus, a low viscosity, polyvinyl siloxane dental impression material, onto the foam around the tree stem. Panasil® Contact Plus was used to allow the tree stem to grow a small amount radially while maintaining a seal and to prevent damage to the tree itself. Other materials with the same desired properties as Panasil® Contact Plus, produce acids as they dry which can damage the tree.

Third, thermometers were attached, using clear tape, to the inside of each upper chamber and the upper chambers were placed over the trees and sealed to the top plates of the lower chambers. Last, the respirometer was attached to each lower chamber.

3.2.6 Respirometer

Soil and root respiration were measured using a Micro-Oxymax automated, multi-channel respirometer (Columbus Instruments, Columbus, OH). This instrument measures headspace gas concentration using a 0-10% carbon dioxide (CO_2) sensor, a 0-10% methane (CH_4) sensor, and an oxygen (O_2) sensor. The CO_2 and CH_4 sensors are single-beam infrared sensors and the O_2 sensor is a paramagnetic oxygen sensor.

The Micro-Oxymax is a closed system respirometer, meaning the air is pumped from the test chamber, through the gas sensors, and returned to the test chamber without being exposed to the environment. There is one exception to this, however, which is called 'refresh'. Continued production and consumption of gases, in this case CO_2 and O_2, results in changes in concentration of these gases which may inhibit the respiration being monitored. To solve this problem, channels are 'refreshed', meaning the headspace gas is replaced with fresh gas at specified measurement intervals or gas concentration changes.

The instrument is recalibrated after each set of measurements using a reference chamber with a reference air supply. This results in measurements that are independent of changes in ambient conditions (Columbus Instruments, 2002).

In this experiment, the headspace gas concentration of O_2, CO_2 and CH_4 was measured periodically in each lower chamber and changes in gas concentrations were used to compute O_2 consumption and CO_2 production. CH_4 concentrations were monitored to ensure aerobic microbial degradation. The software provided O_2 consumption and CO_2

production in μL. The amount of O_2 consumed and CO_2 produced was converted to moles using the gas law as seen below.

$$n = \frac{PV}{RT} \qquad [3.1]$$

where

P=pressure (Pa)

V=volume (m^3)

n=moles

R=universal gas constant, 8.3145 J/mole*K

T=temperature (K)

As the software automatically normalizes consumption and production information to standard temperature and pressure, the temperature used was 0°C (273.15 K) and the pressure used was 760 mmHg (101325 Pa).

The contribution of root respiration was removed by assuming 48.5% of O_2 consumed was from root respiration (Hanson et al., 2000). O_2 readings were used because the paramagnetic oxygen sensor is more sensitive than the single beam infrared CO_2 sensor. The cumulative moles of O_2 consumed from soil respiration (51.5% of the total) were then converted to mg of PHC using two stoichiometric equations for the microbial degradation of diesel (equations 3.2 and 3.3) found in literature. The stoichiometric equations used were:

$C_{16}H_{34}+24.5O_2 \rightarrow 17H_2O+16CO_2$ (after Zynter et al., 2001) [3.2]

3.5 mg $O_2 \rightarrow$ 1 mg diesel (Hinchee and Ong, 1992; Dupont, 1993; Downey, 1995; Bregnard, 1996; Davis, 1998) [3.3]

The final estimated amount of diesel degraded microbially was determined using the average amount of diesel degraded from the two stoichiometric equations.

During the course of the experiment the respirometer programme was periodically restarted to replant trees, terminate the measurement of certain channels (initially the respiration was also being measured from the upper chambers), and fix leaks. When leaks were detected in the test cells and tubing, attempts were made to fix the leaks while the instrument was running but it was often necessary for the experiment to be restarted. Both restarting the respirometer programme and fixing leaks without restarting the respirometer programme resulted in erroneous readings of cumulative O_2 consumption and CO_2 production. To solve this problem the cumulative O_2 consumption and CO_2 production was extrapolated using a number of values from the previous data set or, when leaks were fixed without restarting the respirometer programme, using a number of values previous to any detected leaks.

Additional details regarding the Micro-Oxymax respirometer hardware, software, set-up, diagnostics, measurement, calibration, initialization and calculations are presented in Appendix B.

3.2.7 Air Sampling Tubes

Two types of air sampling tubes were placed downstream of the soil and plant to collect vapour phase PHC: ORBO™32L and ORBO™402. Both tubes were manufactured by Supelco®, Inc., Bellefonte, Pennsylvania, USA. They were glass, 100 mm long with an 8 mm OD, contained two adsorbent beds and three retaining plugs and were sealed at

both ends. A generalized diagram of the air sampling tubes is shown in Figure 3.8 and the contents of the tubes are given in Table 3.1.

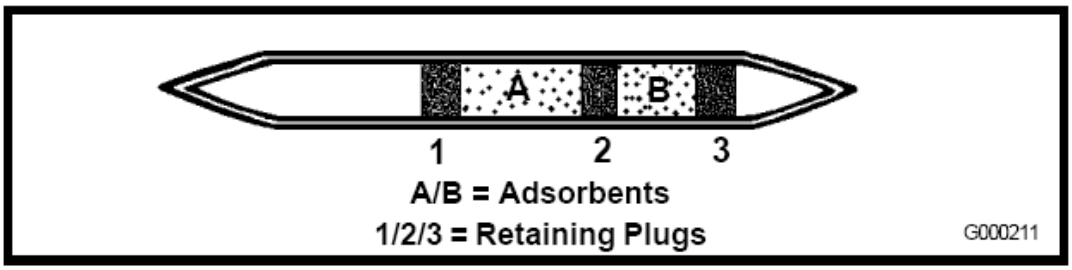

Figure 3.8: Schematic of ORBO™32L and ORBO™402 Air Sampling Tubes

Table 3.1: Contents of ORBO™32L and ORBO™402 Air Sampling Tubes

Air Sampling Tube	Bed	Adsorbent Bed Material	Adsorbent Bed Mass (mg)	Particle Size (mesh)	Retaining Plug Material		
					1	2	3
ORBO™32L	A	activated coconut charcoal	400	20-40	glass wool	polyurethane	polyurethane
	B	activated coconut charcoal	200	20-40			
ORBO™402	A	Tenax® TA	100	35-60	glass wool	polyurethane	polyurethane
	B	Tenax® TA	50	35-60			

3.2.8 Control of Environmental Conditions

The experimental test cells were placed in an environmental chamber located in the Engineering building at the University of Saskatchewan. In the environmental chamber a number of environmental conditions were controlled including day and night cycles of

light and temperature. The light and temperature conditions were set for 16 hour days and 8 hour nights. The day temperature was 22 ± 0.5°C and the night temperature was 15 ± 0.5°C. Temperatures were controlled using a servo motor attached to the manual temperature control dial outside the chamber. The servo motor was controlled using a simple Visual Basic programme. Lights were mounted on two ballasts and positioned directly above the test cells, within ~2 cm to the top of the upper chamber. The lights were Sylvania, 60 W, high output, wide spectrum fluorescent lights (Osram Sylvania Limited, Danvers, Massachusetts, USA). The lighting ballasts and experimental test cells were enveloped in black and white poly, with the white side towards the trees, to reflect light back to the trees.

As described in Section 3.2.3, an attempt was made to keep the soil at a lower temperature than the temperature of the environmental chamber.

Soil and air temperatures were monitored throughout the course of the experiment. The soil temperature was monitored at a constant location in each test cell. Holes were drilled through the wall of the lower chamber just below the soil level. Thermometers were passed through rubber stoppers, the rubber stoppers were inserted into the holes, and silicone sealant was applied around the thermometers and rubber stoppers to ensure an air-tight seal. Thermometers taped to the inside of the upper chambers were used to monitor air temperature in the chambers.

The phreatic surface was kept constant for each test cell by using the Tygon® tubing assembly.

An air circulation system was set up for the upper chamber. The air circulation system consisted of high pressure air from a line in the lab flowing through a regulator, then through a flowmeter. From the flowmeter the line was divided into four lines which ran to the plastic tubing fittings at the top of each upper chamber. The flowrate through each of the top sections was ~0.75 l/min. Tubing was attached to fittings near the bottom of the upper chambers. The air stream was dehumidified prior to flow through the air sampling tubes by using, as a condenser, a digestion flask immersed in a 2°C water bath.

3.3 Analytical Methods

Numerous tests were performed in the course of this research. The tests can be divided into two groups: index and characteristic testing of soil and chromatographic methods for quantification of PHC in soil and vapour phase.

3.3.1 Index and Characteristic Soil Tests

Numerous index and characteristic tests were performed on the soil before and after the experiment to characterize the soil and monitor changes that may have occurred during the course of the experiment. The tests performed included: grain size analysis; moisture content; cation exchange capacity (CEC); pH; organic carbon (%); calcium (Ca^{2+}), magnesium (Mg^{2+}), sodium (Na^{+}), and potassium (K^{+}); sodium adsorption ratio (SAR); nitrogen (N) and phosphorous (P); and ATP assays.

a. Grain Size Analysis

Grain size analysis was performed on a number of soil samples before the experiment began and after the experiment was disassembled. The American Society for Testing and Materials (ASTM) test procedure D422-63 (2002) was followed.

b. Moisture Content

Moisture content of a number of soil samples were measured before the experiment began after and the experiment was disassembled. The moisture content was determined using method 2.411 in the Manual on Soil Sampling and Methods of Analysis (McKeague, 1976).

c. Cation Exchange Capacity

The cation exchange capacity of a number of soil samples was measured before the experiment started and after the experiment was disassembled. The cation exchange capacity was measured using the barium chloride compulsive exchange method. This method was taken from an online document called Recommended Methods for Determining Soil Cation Exchange Capacity (Ross, 1995), based on the method of Gillman and Sumpter (1986) (see Appendix C).

d. pH

The pH of a number of soil samples was measured before the experiment began and after the experiment was disassembled. The pH was determined using method 3.11, "pH in 0.01 M calcium chloride, $CaCl_2$", in the Manual on Soil Sampling and Methods of Analysis (McKeague, 1976).

e. Organic Carbon

The fraction of organic carbon was determined using a modified Walkley-Black method (Allison, 1965) obtained from the Geotechnical Research Centre at the University of Western Ontario. This method can be seen in Appendix C.

f. Soluble Salts: Calcium, Magnesium, Sodium, and Potassium

The amount of calcium (Ca^{2+}), magnesium (Mg^{2+}), sodium (Na^{+}), and potassium (K^{+}) in a number of soil samples was measured before the experiment began and after the experiment was disassembled. The concentration of Ca^{2+}, Mg^{2+}, Na^{+}, and K^{+} was determined using method 3.22, soluble salts in a 1:1 soil:water mixture, from the Manual on Soil Sampling and Methods of Analysis (McKeague, 1976). This method can be seen in Appendix C. The extract was analyzed with a flame photometer to determine the amount of sodium and potassium and with an EDTA complexometric method to determine the amount of calcium and magnesium.

g. Sodium Adsorption Ratio

The sodium adsorption ratio, *SAR*, was determined using the concentrations of Na^{+}, Ca^{2+} and Mg^{2+} as described in Equation 3.4 (McKeague, 1976).

$$SAR = \frac{Na^{+}}{\sqrt{\frac{\left(Ca^{++} + Mg^{++}\right)}{2}}} \qquad [3.4]$$

h. Nitrogen and Phosphorous

The concentration of nitrogen (N) and phosphorous (P) in a number of soil samples was measured before the experiment began and after the experiment was disassembled. The method used was a persulphate digestion method followed by a semi-micro Kjeldahl method to determine the concentration of N and a stannous chloride spectophotometric method to determine the concentration of P. These methods described in methods 4500-N_{org} C and 4500-P D in Standard Methods for the Examination of Water and Wastewater, 18th Edition (Greenburg et al., 1992).

i. ATP Assay

ATP assays were carried out to estimate the initial and final microbial population of the contaminated soil. The ATP assays were performed using a luciferin/luciferase method with a Lumat LB 9507 luminometer from Berthold Technologies, Bad Wildbad, Germany, the EnLiten® ATP Assay System (Promega Corperation, Madison, Wisconson, USA) and an ATP releasing reagent with Phosphate (Biochemical Diagnostics Incorperated, Edgewood, New York, USA). The method used was modified from a procedure developed by Celsis (formerly Lumac, Landgraaf, the Netherlands) and obtained from Dr. Leila Hrapovic at Queen's University in Kingston, Ontario, Canada (Hrapovic and Rowe, 2002). The modified procedure can be seen in Appendix C.

3.3.2 Gas Chromatography for PHC

Gas chromatography was used to analyze extracts from soil samples and air sampling tubes. All gas chromatography was performed at the National Hydrology Research Institute (Saskatoon, Saskatchewan, Canada). Extraction efficiencies, E_Es, for soil and

tube extracts were determined using a gas chromatograph mass spectrometer (GC-MS) and PHC concentrations of soil and tube extracts were determined using a gas chromatograph flame ionization detector (GC-FID). Detailed descriptions and specifications of the GC-MS and GC-FID can be found in Appendix D.

Hydrocarbon standards were used to determine the concentration of each fraction from samples run on the GC. Standard solutions of n-hexane (nC6), n-decane (nC10), n-hexadecane (nC16) and n-tetratricontane (nC34) at concentrations of 0, 25, 50, 75 and 100 ppm, were run prior to and following each batch of samples, as well as intermittently with larger sample sets. These standards were chosen because they are markers between different hydrocarbon fractions; fraction 1 (F1) is nC6-nC10, fraction 2 (F2) is nC10-nC16 and fraction 3 (F3) is nC16-nC34 (Canadian Council of Ministers of the Environment (CCME), 2001). The instrument responses of these standard solutions were used to determine the concentration of each fraction for samples from the same set. The areas under the curves, area counts, from each of the standards were divided by the concentration resulting in a 'response factor' (RF) for each fraction of the standard. For example, the RF for F1, from the beginning of nC6 to the highest nC10 voltage peak, using a 50 ppm standard would be the area count of fraction 1 divided by 75 ppm. A higher concentration was used for F1 than was used for F2 and F3 because F1 includes the entire nC6 peak (50 ppm) and half the nC10 (50 ppm/2) peak, resulting in an actual concentration of 75 ppm. For F2 and F3 the area counts are taken from peak to peak resulting in actual concentrations of 50 ppm. For all fractions at each standard concentration, the average and error of the RF were determined and the resultant RF

along with the sample volume and E_Es were used to calculate the mass and mass error of each fraction. These calculations can be found in Appendix D.

3.3.3 Sample Preparation

The soil samples and air sampling tubes were analyzed using a GC by desorbing the PHC into an appropriate solvent. Following desorption of PHC into a solvent the total solvent volume was reduced to increase the concentration of PHC and the resulting response from the GC.

a. Soils

PHC were extracted from contaminated soils using a modification of the method of Schwab et al. (1999). This method was modified for the specific purpose of this project by increasing the mass of soil used to prepare the extracts and changing the extracting solvent. The mass of soil was increased in an attempt to reduce the effect of textural variation on the PHC concentration. For the extracting solvent carbon disulphide, CS_2, was used in place of methanol or a 50-50 hexane-acetone solution. This modification to the method was made because hexane is within the carbon number range of interest for F1. Methanol was not used because it deteriorates the coating of the GC column.

The modified method consisted of placing a known mass of soil in a 125 ml soil sampling jar. A specific amount of CS_2 was added to the soil sampling jar. The jars were then sealed and shaken with a Burrell wrist action shaker (Model 75, Burrell Corporation, Pittsburg, Pennsylvania, USA) at the maximum setting for 30 minutes. The CS_2 was decanted using a pasture pipette, placed in an evaporating flask, and sealed.

The entire procedure was repeated twice (three times total) with the decanted solvent being added to the same evaporating flask each time. The CS_2 was then evaporated down to ~2 ml with a roto-evaporator and water bath. The vacuum pressure on the roto-evaporator was set to a maximum of ~35 kPa and the water bath temperature was set to 35^{o}C. The final volume of solvent was measured and the remaining extract was placed in a 2 ml PTFE lined vial and run on a GC-MS and GC-FID.

Under certain circumstances there were two small variations in the extraction method described above. The first variation was that "spiked" soils (see Section 3.4.2) and field soils under initial conditions were extracted at a soil to solvent ratio of approximately 1:1, whereas field soils under final conditions were extracted at soil to solvent ratios between 0.12:1 and 0.64:1. The second variation was that ~5 g of sodium sulphate was added to field soils extracted under initial conditions and ~2.5 g of sodium sulphate was added to field soils extracted under final conditions. Variation in soil to solvent ratios for soil extracted under initial and final condition was a result of the mass of soil available under each condition. Under initial conditions soil for analysis was abundant, whereas under final conditions the mass of soil available for analysis was limited. Variation in the amount of sodium sulphate used was a result of the decreased mass of soil extracted under final conditions. Sodium sulphate was added as a dispersing agent because field soils were forming small balls during shaking. This was attributed to the moisture content of the field soils (>10%) and the highly hydrophobic properties of CS_2. Sodium sulphate was not added to the spiked soils because they were basically dry. In the samples where sodium sulphate was added the soils still formed balls during shaking so the balls were broken up manually after the soils were shaken. The balls were broken

up so the soil particles were in contact with CS_2, allowing the PHC adsorbed to the soil to diffuse into the CS_2. Failure to do this would have created a longer diffusion pathway resulting in lower amounts of hydrocarbons extracted and subsequently measured.

b. Air Sampling Tubes

The extraction method used for the air sampling tubes was based on the U.S. Department of Labor Occupational Safety and Health Administration (OSHA) Method 07. This is a generalized method designed for the collection of organic vapours on charcoal, extraction with an organic solvent and analysis with a GC-FID. This method is presented in Appendix D.

Both air sampling tubes were extracted using the same method but with different extracting solvents. Adsorbent beds from the ORBO™32L tubes were extracted with CS_2 and the adsorbent beds from the ORBO™402 tubes were extracted with toluene. Each adsorbent bed was removed and placed in separate 4 ml vials with PTFE lined lids. 3 ml of the extracting solvent was slowly added to the vials and the lids replaced. The CS_2 had to be added slowly because heat was generated when CS_2 came in contact with the activated coconut charcoal. The vials were then sonicated in ice water for 30 minutes. It was necessary for the vials containing activated coconut charcoal and CS_2 to be sonicated in ice water because at the elevated temperatures resulting from sonication CS_2 becomes volatile, possibly causing the lids to blow off the vials. After sonicating, the extracting solvent was decanted using a pasture pipette, placed in an evaporating flask, and sealed. The entire procedure was repeated twice (three times total) with the decanted solvent being added to the same evaporating flask each time. The extracting

solvent was then evaporated down with a roto-evaporator and water bath to a final volume of ~2 ml. The vacuum pressure on the roto-evaporator was set to a maximum of ~35 kPa and the water bath temperature was set to 35°C for the CS_2 and a maximum of ~70 kPa and 60°C for the toluene. The final volume of solvent was measured, placed in a 2 ml PTFE lined GC vial and run on a GC.

3.3.4 Processing of Chromatographic Data

Processing of the chromatographic data was necessary to interpret the GC output and obtain PHC concentrations for each soil sample and air sampling tube. After the samples were run, raw data files were created for each sample. These raw data files, containing only the voltage response at each measured time interval, were analyzed using Matlab® scripts, one for samples in toluene and one for samples in CS_2. These Matlab® scripts were written to numerically integrate the area under the curve of the response at specific time intervals and can be found in Appendix D. The time intervals between which the area under the curve was integrated were determined using average times from the standards run on the GC-FID. Only fractions 2 and 3 were quantified for samples in toluene due to interference from the toluene (C7) whereas fractions 1, 2 and 3 were quantified for samples in CS_2. The start and peak times were determined manually from the raw data files of the standards.

The Matlab® scripts applied the trapezoidal rule to determine the area count for each fraction. An explanation of the manner in which the trapezoidal rule was applied follows and can be seen graphically in Figure 3.7. The Matlab® scripts first identified the voltage response at t=120 second, h_b, and set this as a baseline value. Next, the area

count for each fraction were determined by taking the sum of the midpoint of the two voltages in each time step minus the baseline multiplied by the time step for the each time step between the times that specify each fraction. This can be expressed by the equation:

$$\Sigma = \left(\left(\frac{h_n + h_{n+1}}{2} \right) - h_b \right) * \left(t_{n+1} - t_n \right) \quad [3.5]$$

where

h_n=height of the voltage response curve at time step n

h_{n+1}=height of the voltage response curve at time step $n+1$

h_b=height of the voltage response curve at 120s

t_n=time at time step n

t_{n+1}= time at time step $n+1$

To determine the mass of each fraction in milligrams (mg) on the soils and air sampling tubes, the concentration in ppm (after the RF had been applied) was multiplied by the extract sample volume in ml and was divided by 1000. Then, to determine the actual mass of each fraction, the E_E, found from the GC-MS analysis of the soils and air sampling tubes, was applied to the mass. This was done by multiplying the mass by 100 divided by the E_E as seen in Equation 3.6 below.

$$m_{actual} = m * \frac{100}{E_E} \quad [3.6]$$

where

m_{actual}=actual mass

m=measured mass

E_E=extraction efficiency

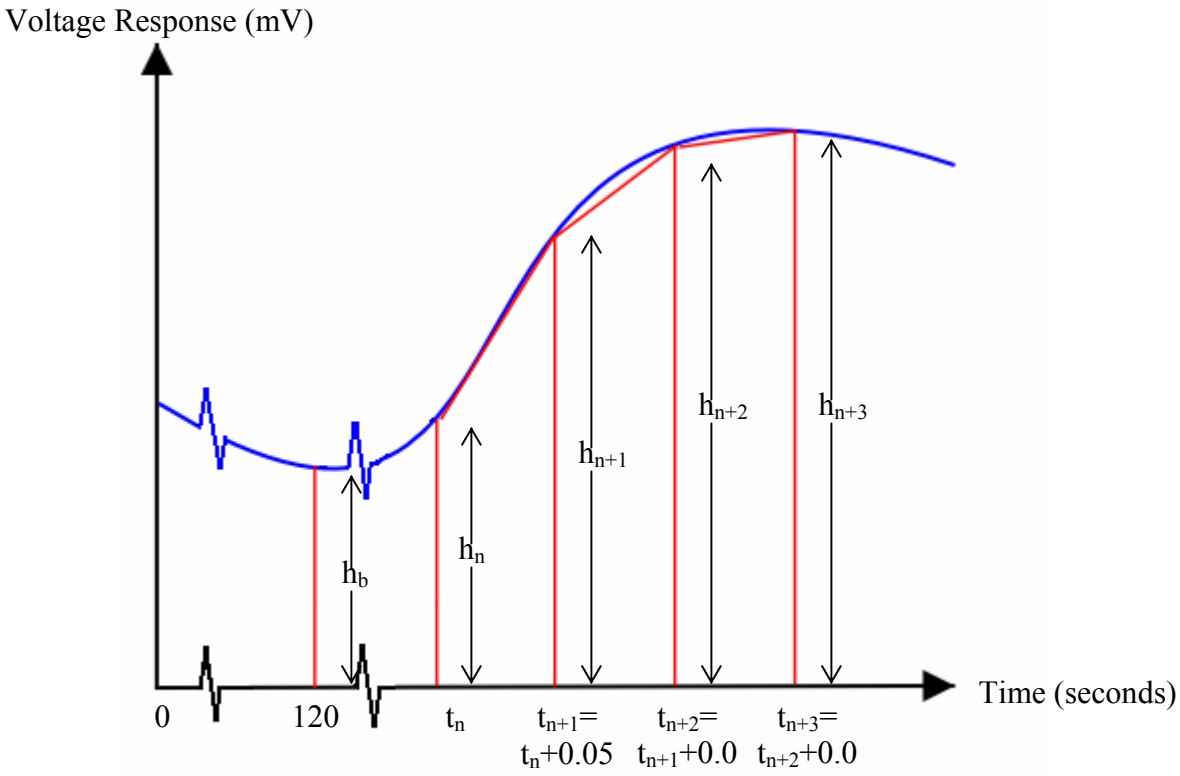

Figure 3.9: Graphical Explanation of Trapezoidal Rule Used to Integrate the Area Below the Voltage Response Curve

3.4 Quality Assurance/Quality Control Programme

A quality assurance/quality control programme was included to ensure that the results obtained were reproducible and defendable. The main areas of interest to the quality

assurance/quality control programme for this project was the use of high purity standards and solvents and the use of internal standards to determine E_Es.

3.4.1 Standards and Solvents

All standards were purchased from Supelco®, Inc., Bellefonte, Pennsylvania, USA. The CS_2 and toluene were high purity solvents, both 99.9% pure by GC analysis, manufactured for use in spectrophotometry and chromotography by EMD Chemicals, Inc., Norwood, Ohio, USA.

The standard solutions of nC6, nC10, nC16 and nC34 in various concentrations, 25, 50, 75 and 100 ppm, were made by adding specific volumes of n-hexane, n-decane and n-hexadecane and a specific mass of n-tetratricontane to the extracting solvents. The concentrations of all standards were expressed in ppm as mass per volume (i.e. mg/L). Specific gravities of 0.66, 0.73 and 0.77 (from material safety data sheets (MSDS) provided with the chemicals), respectively, were used to convert volume to mass for the liquid samples.

3.4.2 Internal Standards

Internal standards were used to determine the E_Es of the soil and the adsorbent beds in the air sampling tubes. "Blanks", soil samples, and adsorbent beds with only solvent applied, also were used to ensure no hydrocarbons were being released from the clean soil samples and adsorbent beds.

Internal standards of cleaned soil were prepared by "spiking" samples of cleaned soil with known concentrations of hydrocarbon standards. The standards used were nC6, nC10, nC16 and nC34 in CS_2. The standards were added to cleaned, hydrocarbon-free samples of the soil used in the experiment. The soil samples were cleaned using a Soxlet extractor. Soils were "spiked" using a protocol (slightly modified as described below) published by Reid et al. (1998). Modifications to the protocol included the type of standards added to the soil, the volume of standards added, the total mass of soil used, and the addition of the extracting solvent to prevent volatilization of the standards. Using the modified protocol, ~1/5 of the soil was mixed with the total amount of the contaminant to be added to the soil using a metal spatula for ~3 minutes. The remaining clean soil and the newly contaminated soil were divided into quarters. The quarters of the clean soil were individually mixed with the quarters of the newly contaminated soil for ~20 seconds. Each of the quarters were then mixed together, placed in one jar, and left overnight before being extracted. During the spiking procedure extra CS_2 was added to ensure that the soil remained moist with CS_2 so a minimal amount of the standards were volatilized.

Internal standards of the adsorbent beds in the air sampling tubes were prepared by "spiking" clean adsorbent beds with known concentrations of hydrocarbon standards and subsequently extracted. The standards applied to the ORBO™32L air sampling tubes were nC6, nC10, nC16 and nC34 in CS_2 and the standards applied to the ORBO™402 air sampling tubes were nC10, nC16 and nC34 in toluene. The air sampling tubes were "spiked" by removing the glass tip closest to adsorbent bed A, removing the retaining

plug at that end, and injecting the standard directly onto adsorbent bed A. The glass tubes were then resealed with a plastic cap and left for one day before being extracted.

Additional testing was performed to ensure the hydrocarbon standards (nC6, nC10, nC16 and nC34) remained sorbed to the ORBO™32L air sampling tubes after air was blown through the tube. For a few of the "spiked" ORBO™32L air sampling tubes, air was blown through at the same flowrate that air circulated through the upper chamber prior to extraction. E_Es of ORBO™32L air sampling tubes with air blown through was compared to E_Es of ORBO™32L air sampling tubes without air blown through to determine if the hydrocarbon standards remained sorbed after air was blown through.

Internal standards of the soil and adsorbent beds in the air sampling tubes were used to determine the E_Es. The "spiked" soils and adsorbent beds were extracted using identical equipment and procedures as were used for the samples obtained during the course of the experiment. The extracts were run on the GC-MS and the chromatograms were analyzed to determine the concentration of each fraction extracted. The resultant concentration was divided by the known concentration and multiplied by 100% to determine E_Es for each fraction (Equation 3.7). The average and error E_E for each fraction with the soil and both types of adsorbent beds were determined. These E_Es were used to calculate the concentration and concentration error of soil samples and air sampling tubes.

$$E_E = \frac{concentration_{measured}}{concentration_{known}} * 100\% \qquad [3.7]$$

3.5 Disassembly of Experiment

Upon completion of the experiment the test cells were disassembled one at a time. This was completed in a number of steps including shutting down the respirometer and the air circulation system, removing and storing the air sampling tubes, draining the soil water, removing the above-ground portion of the tree, and removing a section of the soil for sampling and analysis.

Immediately after the experiment was disassembled, a number of samples were taken and analyzed. These included: soil samples for grain size analysis, moisture content, ATP assays, etc. as described in Section 3.3.5; removal of roots for analysis of root length; and processing plant samples to determine above- and below-ground biomass. All time-sensitive testing was completed immediately, before the next test cell was disassembled.

3.5.1 General Disassembly

The respirometer was shut down manually and the respirometer attachments were removed from the bottom portion of the experimental test cell. The air sampling tubes were removed, capped, and placed in cold storage until they were extracted. The air circulation system was then sealed off with a tube clamp and the tubing to the top section removed. The entire upper chamber was then removed and the tree cut off just above the fuel spout, put in a plastic bag, and sealed. The seal around the tree at the fuel spout was removed and the water drained from the lower chamber by detaching the Tygon® tubing of the assembly used to observe and maintain the phreatic surface and using it to drain the soil water. The soil water was drained into glass sampling jars, with

PTFE lined caps, which had been washed and rinsed with acetone. These sampling jars were then capped and placed in cold storage. Next the PVC lid of the bottom section of the experimental test cell was removed. The tree was cut off at the soil, put in the same bag as the rest of the tree, sealed, and placed in cold storage. The copper tubing was then removed from the bottom section, taking care to minimize soil disturbance.

At this point only the soil and roots (for 4 of the 6 test cells), geotextile and gravel remained in the lower chamber. Two 38 cm * 24 cm, 0.5 cm thick steel plates with one sharpened edge were inserted, sharp side down, into the soil on either side of the tree. The lower chamber was then placed on its side and positioned so the steel plates were parallel to the ground. The steel plates were then pushed into the soil until they were in contact with the geotextile. Next the top steel plate was removed, with all the soil on top, and placed in a section of 30 cm (12") ID PVC pipe (the same pipe that was used to manufacture the lower chambers). This soil was set aside. Next the bottom steel plate was removed, with the section of soil from between the plates on top, and set aside. Finally the top plate was placed onto the remaining soil. The bottom portion of the experimental test cell was then rolled over 180°, the plate was removed with all the soil on top, placed in another section of 30 cm (12") ID PVC pipe, and set aside.

3.5.2 Soil Sampling

All the soil for analysis was sampled from the section of soil between the two plates. The soil sampling for moisture content, PHC extractions and ATP assays was done as quickly as possible to reduce exposure of the soil to the environment so that the final soil sampling conditions were as close as possible to in-situ conditions.

The first step of the final soil sampling was to identify the section boundaries, the boundaries of contaminated soil of different concentrations. These were measured radially, measuring from the centre of the lower chamber according to the dimensions used during initial placement of the soil. Visual identification of the rock flour that had been sprinkled between each section aided in the identification of the different boundaries.

After the boundaries were identified, sampling locations were identified using the soil surface as vertical reference. Soil sampling locations were the same for all test cells. Samples for moisture content were taken first, followed by samples for PHC analysis, samples for the ATP assay, samples for nutrient and cation analysis, and lastly samples for grain size analysis. Sampling locations can be seen in Appendix E.

After all the soil sampling and the soil testing for moisture content, the PHC extractions and the ATP assays were complete, the roots were removed from the soil. This was done manually, by picking the roots out of the three sections of soil with tweezers. As the roots were removed from the soil they were rinsed and placed on moist paper towel. When as many of the roots as possible were removed they were put in a plastic bag, sealed, and placed in cold storage.

3.5.3 Root Length

The roots collected from each test cell were separated into two groups, roots>1 mm in diameter and roots<1 mm in diameter. The root lengths were determined using a scanner and NIH Image, a public domain imaging and analysis programme for

MacIntosh computers. Before the root lengths were determined three standards were scanned and analyzed. These standards were sheets of paper with lines of known length drawn on them to simulate roots. After the analyzed length of the standards were determined and compared to the actual length, each group of roots were placed onto a piece, or pieces, or cellophane, scanned and analyzed. Each piece of cellophane was scanned and analyzed five times with the average being used as the final root length.

3.5.4 Plant Samples

Plant samples were divided into three groups: roots (already separated from the rest of the plant); leaves; cuttings; and stems. All plant samples were dried at ~60°C for at least 48 hours and weighed individually to determine plant biomass. The plant biomass was then further divided into two groups, below-ground biomass and above-ground biomass. The below-ground biomass consisted of the dry mass of roots and the tree cutting and the above-ground biomass consisted of the dry mass of leaves and stems.

Chapter 4: Experimental Results

4.1 Overview

The experimental results are divided into five sections: index and characteristic tests of soils and biological measurements; quantification of PHC in the soil; plant biomass measurements; experimental monitoring; and mass balance.

4.2 Soil Tests and Biological Measurements

Numerous index and characteristic tests were performed on the soil before and after the experiment to characterize the soil and monitor changes that may have occurred during the course of the experiment.

Also, a number of biological measurements were made on the hybrid poplar upon disassembly of the experiment to yield a size index for the plant in each cell. Using the results of ATP assays, the final and initial microbial biomass in the soil was calculated. The biological measurements performed on the hybrid poplars were used in an attempt to relate the measurements of the hybrid poplar biomass and root length to the mass of PHC degraded in each of the experimental test cells (see Chapter 5). The initial and final microbial biomass in the soil was calculated to monitor the change in microbial biomass during the course of the experiment.

4.2.1 Index and Characteristic Tests of Soils

Initial tests were performed on samples of homogenized soil prior to placement in the experimental test cells and final tests were performed on samples taken from discrete sampling locations during disassembly of the experimental test cells. The final sampling locations from each test cell and the calculations used to determine the mass of soil corresponding to each of the sampling locations can be found in Appendix D. With the exception of moisture content samples and ATP assay samples, samples were taken vertically at a constant distance from the central axis. All raw data for the index and characteristic testing of soils can be found in Appendix C. Initial and final results from these index and characteristic tests can be seen in Table 4.1.

Table 4.1: Initial and Final Results from Index and Characteristic Soil Tests

Index and Characteristic Tests	Initial Results (all)	Final Results						
		Test Cell #*						
		1	2	3	4	5	6	Average
D_{60} (mm)	2.0	1.6	1.9	2.1	1.5	4.1	2.2	2.2
D_{30} (mm)	0.40	0.32	0.43	0.38	0.28	0.50	0.42	0.39
D_{10} (mm)	0.006	0.006	0.009	0.006	0.003	0.01	0.009	0.007
Moisture content (%)	9.7	7.1-63.3	9.2-31.9	9.9-67.3	8.7-70.8	9.1-43.6	10.5-60.6	28.9
CEC (meq/100g_{soil})	3.01	2.57	2.89	2.92	3.05	3.22	3.25	2.98
pH	7.8	7.5	7.5	7.6	7.8	7.8	7.8	7.7
Organic Carbon (%)	0.3	0.3	0.3	0.5	0.3	0.3	0.4	0.4
Electrical Conductivity (μS/cm)	324	743	625	681	502	-**	567	624
Ca^{2+} (mg_{Ca2+}/g_{soil})	0.14	0.29	0.25	0.30	0.23	-**	0.25	0.26
Mg^{2+} (mg_{Mg2+}/g_{soil})	0.03	0.07	0.05	0.03	0.06	-**	0.07	0.06
Na^{+} (mg_{Na+}/g_{soil})	0.07	0.07	0.08	0.09	0.06	0.12	0.06	0.08
K^{+}(mg_{K+}/g_{soil})	0.05	0.16	0.13	0.12	0.11	0.18	0.11	0.14
SAR (meq)	0.80	0.55	0.69	0.72	0.53	-**	0.50	0.60
Total N (mg_N/g_{soil})	1.86	0.69	1.12	1.68	1.25	1.85	2.25	1.53
Total P (mg_P/g_{soil})	0.012	0.019	0.021	0.031	0.022	0.009	0.012	0.019
ATP (mg)	2.6	4.4	3.7	1.9	2.5	2.2	1.7	2.7

*Test cells 1-4 were planted with Walker poplars; test cells 5 and 6 were unplanted
**Insufficient soil for analysis

4.2.2 Biological Measurements

Biological measurements of hybrid poplars and results of calculations of microbial biomass in the soil can be seen in Table 4.2. Biological measurements of the hybrid poplars included the dry stem, leaf, cutting and root mass and the root lengths. The "above-ground plant biomass" refers to the sum of the dry stem and leaf mass, "below-ground plant biomass" refers to the sum of the dry cutting and root mass, the "total plant biomass" refers to the sum of the dry stem, leaf, cutting and root mass, and the "total biomass" refers to the sum of the total plant biomass and the microbial biomass.

Table 4.2: Biological Measurements

Biological Measurements	**Initial Results**	**Final Results**					
		Test Cell #*					
		1	**2**	**3**	**4**	**5**	**6**
Dry Stem Mass (g)	0.00	6.38	5.02	4.42	2.10	0.00	0.00
Dry Leaf Mass (g)	0.00	3.68	1.02	1.50	0.41	0.00	0.00
Dry Cutting Mass (g)	0.00	8.91	15.24	14.17	6.24	0.00	0.00
Dry Root Mass (g)	0.00	0.50	1.21	0.24	0.20	0.00	0.00
Root Length (cm)	0	1585	4390	1526	1057	0.00	0.00
Above-Ground Plant Biomass (g)	0.00	10.06	6.03	5.92	2.51	0.00	0.00
Below-Ground Plant Biomass (g)	0.00	9.41	16.45	14.40	6.43	0.00	0.00
Microbial Biomass (g)	0.35-0.59	0.67-0.90	0.55-0.74	0.29-0.39	0.38-0.51	0.33-0.44	0.26-0.36
Total Plant Biomass (g)	0.00	19.47	22.48	20.32	8.94	0.00	0.00
Total Biomass (g)	0.35-0.59	20.14-20.38	23.03-23.22	20.61-20.72	9.32-9.45	0.33-0.44	0.26-0.36

*Test cells 1-4 were planted with Walker poplars; test cells 5 and 6 were unplanted

4.3 Quantification of PHC in the Soil

The initial and final mass of PHC in each of the experimental test cells was quantified by preparing and analyzing soil extracts. The PHC concentration of each soil extract was determined through GC analysis and a quality assurance/quality control programme

which involved the use of internal and external standards, details of which are presented in Section 4.3.3. The data presented in Section 4.3.3 will demonstrate the basis upon which the quantification of PHC concentration in soil extracts were made.

4.3.1 Initial Conditions

The initial PHC concentration of the soil was determined by extracting 10 soil samples taken after the soil had been homogenized and before the soil was placed in the experimental test cells. The results from these samples can be seen in Table 4.3 and the raw data and analysis can be seen in Appendix D.

Table 4.3: Initial PHC Concentrations

Sample #	F1 (mg_{PHC}/kg_{soil})	F2 (mg_{PHC}/kg_{soil})	F3 (mg_{PHC}/kg_{soil})	Total (mg_{PHC}/kg_{soil})*
1	55	103	1041	1200
2	288	604	4157	5048
3	184	440	2738	3361
4	164	455	3217	3836
5	117	442	3431	3990
6	96	403	3083	3582
7	32	132	1697	1860
8	75	152	1700	1928
9	13	49	949	1010
10	17	49	896	970
Average	104 ± 15	283 ± 44	2291 ± 475	2678 ± 477

*Due to rounding errors, there may be some differences between the total PHC concentrations and the summation of the F1, F2, and F3 concentrations

The mass of PHC in each test cell was determined from the average initial PHC concentration and the total mass of contaminated soil placed in each experimental test cell (Table 4.4). Variation of the mass of contaminated soil in each test cell resulted from attempting to place the soil in the proper configuration. The initial and final mass of PHC in each test cell is given in Table 4.5.

Table 4.4: Masses of Contaminated Soil

Test Cell #	Mass of Contaminated Soil (kg)
1	30.6
2	30.9
3	26.5
4	26.5
5	27.6
6	24.5

4.3.2 Final Conditions

The mass of PHC remaining in each experimental test cell upon completion of the experiment was determined from soil samples taken from between 8 and 11 discrete sampling locations during disassembly of the experimental test cells. The sampling locations from each test cell and the calculations used to determine the mass of soil corresponding to each of the sampling locations can be found in Appendix E. The concentration of PHC in the soil samples and the mass of soil corresponding to each sampling location were used to calculate the total mass of contaminant remaining in each test cell (Table 4.5).

Table 4.5: Initial and Final Mass of PHC

Test Cell #	Initial Mass of PHC (mg)*				Final Mass of PHC (mg)**				% Removed
	F1	F2	F3	Total	F1	F2	F3	Total	Total
1	3186 ± 460	8648 ± 1351	70062 ± 14522	81895 ± 14592	989 ± 181	1533 ± 372	2327 ± 533	4849 ± 675	94
2	3219 ± 465	8737 ± 1365	70787 ± 14672	82743 ± 14743	3846 ± 706	4758 ± 1155	5443 ± 1246	14047 ± 1840	83
3	2760 ± 399	7493 ± 1171	60707 ± 12583	70961 ± 12644	6168 ± 1290	4118 ± 669	5623 ± 1216	15909 ± 1895	78
4	2760 ± 399	7493 ± 1171	60707 ± 12583	70961 ± 12644	1133 ± 237	1018 ± 116	2173 ± 470	4325 ± 552	94
5	2873 ± 415	7799 ± 1219	63189 ± 13097	73862 ± 13160	461 ± 85	789 ± 192	1653 ± 378	2903 ± 433	96
6	2552 ± 369	6928 ± 1082	56126 ± 11633	65605 ± 11689	862 ± 180	721 ± 117	1958 ± 423	3540 ± 475	95

*n=10 for all test cells

**n=8 for test cell #1, n=9 for test cell #2, and n=11 for test cells # 3-6

A shift in the fractionation of PHC from initial to final conditions occurred. This shift can be seen in Table 4.6 where the percent of each fraction is given under initial and final conditions. The lower and upper value for each fraction at the end of the experiment reveals the overall range of values obtained from the test cells.

Table 4.6: Initial and Final Fractionation of PHC

Initial Conditions			**Final Conditions**		
F1 (%)	**F2 (%)**	**F3 (%)**	**F1 (%)**	**F2 (%)**	**F3 (%)**
6	10	84	16-39	20-34	35-57

Table 4.6 shows a shift in fractionation of PHC towards the lighter (F1) fraction. This shift was expected and can be attributed to partial degradation of heavier fractions into lighter fractions with accumulation of partial degradation products. This shift in fractionation notwithstanding, the amount of PHC removed from the soil during the experiment was quite large. Indeed, as can be seen in Section 4.5, Table 4.24 the percentage of the total mass of PHC removed, based on initial and final soil conditions, is much larger than the percentage of total mass of PHC removed through the measurement of volatilization from soil, phytovolatilization, and microbial degradation. That a larger than anticipated mass of PHC was removed from the soil can be attributed to several sources of error inherent in the assembly and disassembly procedure and the calculations used to determine the mass of PHC remaining in the experimental test cells. First, as the test cells were filled and later disassembled, the soil was exposed to the atmosphere. During this time an unknown mass of PHC would have volatilized into the air and would therefore not have been included in the mass of PHC obtained from soil extractions. Second, soil sampling to determine the final mass of PHC remaining

consisted of using between 8 and 11 discrete sampling locations in each test cell. Spatial variability could have contributed to the larger than anticipated mass of PHC removed from the soil, particularly considering the large amount of variability of PHC concentration that occurred under initial conditions in homogenized soil (Table 4.3). Third, the soil extraction efficiencies used to determine the mass of PHC present in the soil under initial conditions were used to determine the mass of PHC present in the soil under final conditions. As the extraction efficiencies for contaminated soil mixed with potting soil is expected to be less than the extraction efficiencies for solely contaminated soil, the use of the same extraction efficiencies could have resulted in a greater mass of PHC remaining in the soil than was calculated.

4.3.3 Quality Assurance/Quality Control for Quantification of PHC in Soil

The quality assurance/quality control programme used to quantify the mass of PHC in soil extracts involved using internal and external standards. Internal standards were used to determine the soil extraction efficiencies, E_E, for each fraction (Table 4.7). External standards were used to determine the GC response factors. External standards and the soil samples to which they correlate are presented in Appendix D.

Table 4.7: Soil Extraction Efficiencies

Extraction Efficiencies, E_Es		
F1 (%)	**F2 (%)**	**F3 (%)**
86 ± 22	102 ± 14	82 ± 13

4.4 Monitoring of PHC Removal

Monitoring data collected over the duration of the experiment determined the mass of PHC removed or, in the case of the respiration data, the mass of PHC estimated to have been removed, for all monitored degradation pathways. The three monitored degradation pathways were volatilization from soil, phytovolatilization and microbial degradation.

The mass of PHC volatilized from soil and phytovolatilized was determined by extracting air sampling tubes placed downstream of the bottom and top chambers. The masses of PHC volatilized from soil and phytovolatilized were quantified by GC analysis of the tube extracts and a quality assurance/quality control programme which, as with the quantification of PHC in soil, involved the use of internal and external standards. Details of the quality assurance/quality control programme are presented in Section 4.4.2.

The final monitored degradation pathway, the mass of PHC degraded by microbes, was determined by measuring the O_2 consumption and CO_2 production from the soil. This data was then used to obtain an estimated mass of PHC degraded by microbes.

Last, by combining the results from the three monitored degradation pathways an estimated total mass of PHC removed from each experimental test cell was determined.

4.4.1 Volatilization Monitoring

The total mass of each PHC fraction extracted from the air sampling tubes can be seen in Table 4.8.

Table 4.8: Mass of PHC Extracted from Air Sampling Tubes

Test Cell #*	Chamber	Mass of PHC Fraction (mg)			
		F1	F2	F3	Total
1	Upper	53 ± 4	14 ± 2	5 ± 1	72 ± 5
	Lower	130 ± 9	66 ± 6	5 ± 1	201 ± 11
2	Upper	72 ± 6	9 ± 1	2 ± 0.5	82 ± 6
	Lower	148 ± 10	60 ± 5	1 ± 0.2	210 ± 12
3	Upper	125 ± 10	42 ± 6	1 ± 0.3	168 ± 12
	Lower	176 ± 12	46 ± 4	3 ± 0.5	225 ± 13
4	Upper	53 ± 4	15 ± 2	2 ± 0.5	69 ± 5
	Lower	100 ± 7	45 ± 4	9 ± 1	149 ± 8
5	Lower	10 ± 0.7	7 ± 0.8	1 ± 0.2	19 ± 1
6	Lower	3 ± 0.3	2 ± 0.3	0.5 ± 0.1	6 ± 0.4

*Test cells 1-4 were planted with Walker poplars; test cells 5 and 6 were unplanted

Using the mass of PHC extracted from the air sampling tubes and the tube installation and removal dates for the lower chamber (Table 4.9), the cumulative mass of PHC volatilized over time was determined. The cumulative mass of PHC volatilized over time also was normalized with respect to the mass of contaminated soil in each test cell to facilitate comparisons between different test cells. Graphs of the cumulative mass of PHC and the normalized cumulative mass of PHC volatilized over time are shown in Figures 4.1 and 4.2, respectively. The error bars for these, and all other plots, using the cumulative mass of PHC and the normalized cumulative mass of PHC volatilized are from RFs and E_Es.

Table 4.9: Air Sampling Tube Installation and Removal Dates to Monitor PHC Volatilized from Soil

Time Interval	Date Installed	Date Removed	Elapsed Time (days)
1	August 12, 2005	September 8, 2005	27
2	September 8, 2005	October 19, 2005	41
3	October 19, 2005	December 1, 2005	43
4	December 1, 2005	January 16, 2006	46
5	January 16, 2006	March 15-30, 2006	58-73

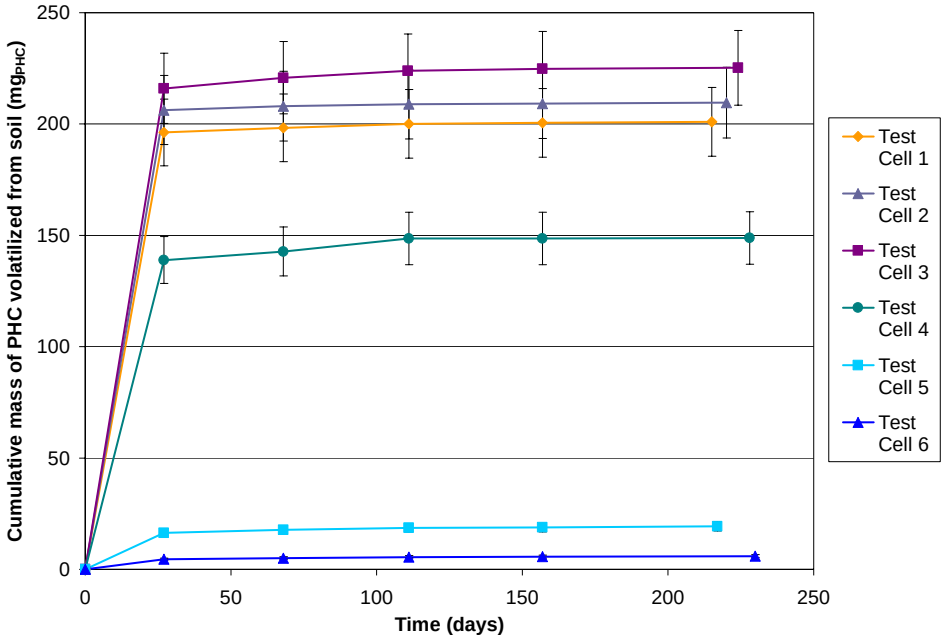

Figure 4.1: Cumulative Mass of PHC Volatilized From Soil

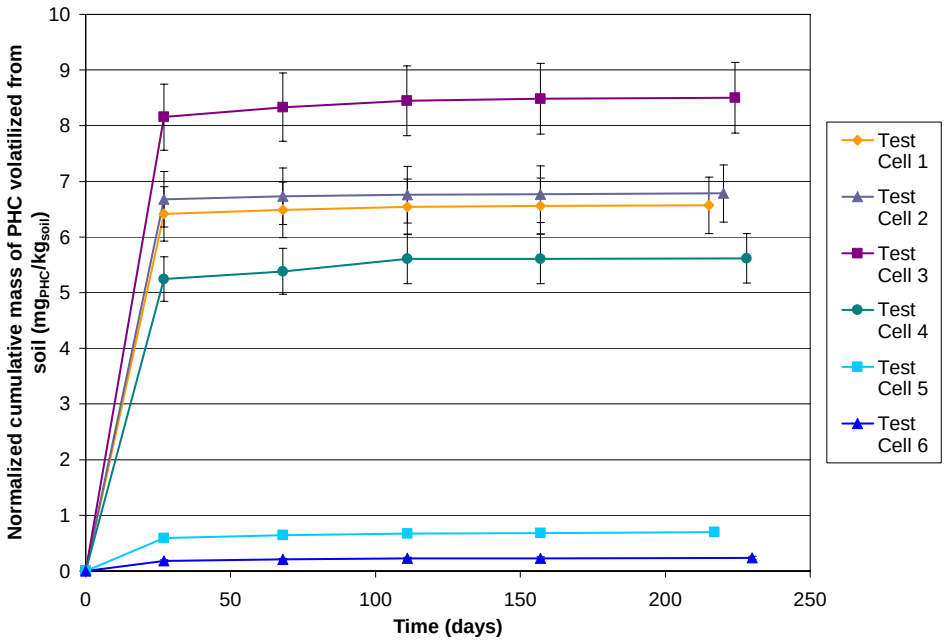

Figure 4.2: Cumulative Mass of PHC Volatilized from Soil Normalized with Respect to Mass of Contaminated Soil

There was a much greater mass of PHC volatilized over the first 27 days than over the remaining experiment (188-203 days). This may be attributed to a combination of placement effects and rapid degradation of easily degradable compounds in the soil. Placement effects may include homogenization of the soil prior to placement, soil placement, initialization of the respirometer prior to commencement of measurements, and settlement of the soil. Homogenization, soil placement, and initialization of the respirometer may have aerated the soil, adding oxygen that could result in a high initial release of PHC from the soil and settlement of the soil would have forced some of the soil gas, containing volatilized PHC, into the headspace. The data also indicates that volatilization and normalized volatilization rates from soil generally decrease with increasing time. This may be attributed to decreasing degradability of compounds in the soil and stabilization of the entire system, specifically the microbial population present in the soil.

Table 4.10: Volatilization Rates from Soil (mg_{PHC}/day)

Test Cell #*	**Time Interval**				
	1	**2**	**3**	**4**	**5**
1	7.26 ± 0.56**	0.05 ± 0.005	0.04 ± 0.004	0.010 ± 0.002	0.007 ± 0.001
2	7.64 ± 0.57	0.04 ± 0.004	0.02 ± 0.002	0.006 ± 0.002	0.006 ± 0.001
3	8.00 ± 0.59	0.11 ± 0.009	0.07 ± 0.01	0.020 ±0.003	0.006 ± 0.001
4	5.15 ± 0.39	0.09 ± 0.01	0.14 ± 0.02	0.001 ± 0.0008	0.003 ± 0.0004
5	0.60 ± 0.05	0.04 ± 0.01	0.02 ± 0.002	0.003 ± 0.001	0.008 ± 0.001
6	0.17 ± 0.02	0.01 ± 0.002	0.01 ± 0.001	0.003 ± 0.001	0.003 ± 0.0004

*Test cells 1-4 were planted with Walker poplars; test cells 5 and 6 were unplanted
**The calculated error was derived from the extraction efficiencies and response factors

Table 4.11: Normalized Volatilization Rates from Soil [$\mu g_{PHC}/(kg_{soil}*day)$]

Test Cell #*	Time Interval				
	1	2	3	4	5
1	237.55 ± 18.15**	1.75 ± 0.17	1.33 ± 0.12	0.35 ± 0.06	0.22 ± 0.04
2	247.31 ± 18.53	1.37 ± 0.12	0.67 ± 0.05	0.20 ± 0.05	0.19 ± 0.03
3	302.00 ± 22.12	4.32 ± 0.35	2.79 ± 0.38	0.79 ± 0.13	0.22 ± 0.04
4	194.16 ± 14.78	3.49 ± 0.41	5.15 ± 0.65	0.05 ± 0.03	0.12 ± 0.02
5	21.79 ± 1.78	1.32 ± 0.39	0.77 ± 0.08	0.10 ± 0.04	0.29 ± 0.04
6	6.80 ± 0.69	0.57 ± 0.07	0.41 ± 0.06	0.11 ± 0.05	0.11 ± 0.01

*Test cells 1-4 were planted with Walker poplars; test cells 5 and 6 were unplanted
**The calculated error was derived from the extraction efficiencies and response factors

The volatilization data also indicates significant differences in the mass of PHC volatilized from different experimental test cells. The soils planted with trees (test cells 1-4) volatilized a greater mass of PHC than the soils without trees and the volatilization rates and the normalized volatilization rates from soil are generally greater for soil planted with trees compared to the controls.

The cumulative mass of PHC phytovolatilized over time (Figure 4.3) also was normalized with respect to the mass of contaminated soil in each test cell (Figure 4.4) to facilitate comparisons. The error bars for these, and all other plots, using the cumulative mass of PHC and the normalized cumulative mass of PHC phytovolatilized are from RFs and E_Es.

Table 4.12: Air Sampling Tube Installation and Removal Dates to Monitor PHC Phytovolatilized

Time Interval	Date Installed	Date Removed	Elapsed Time (days)
1	August 12, 2005	October 11, 2005	60
2	October 11, 2005	December 1, 2005	51
3	December 1, 2005	January 16, 2006	46
4	January 16, 2006	March 15-30, 2006	63

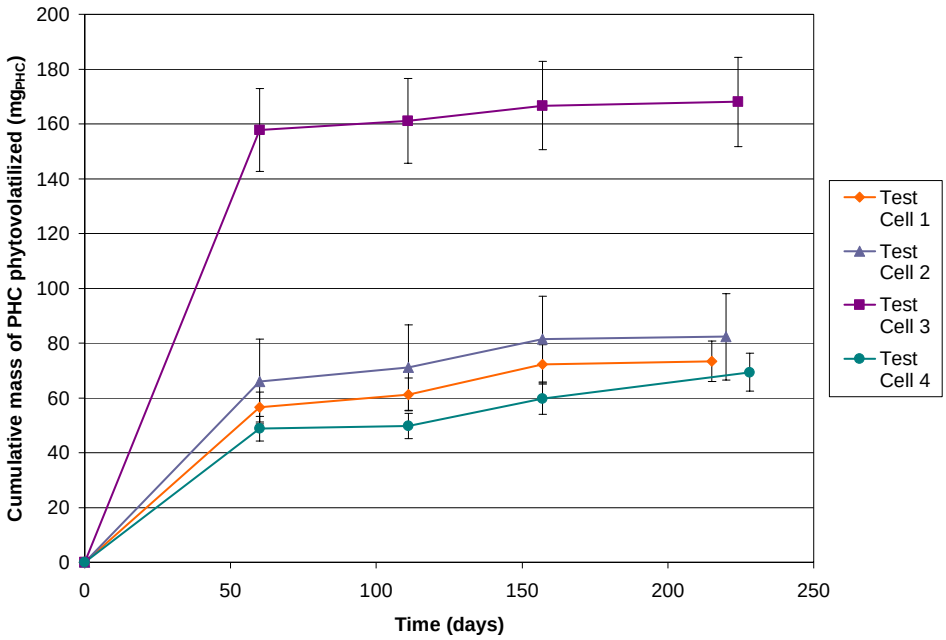

Figure 4.3: Cumulative Mass of PHC Phytovolatilized

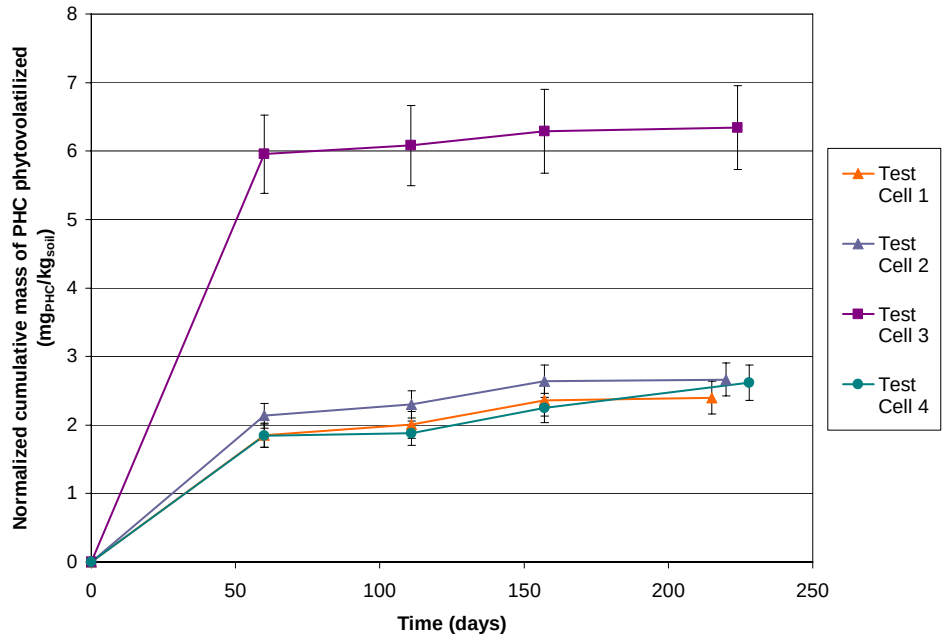

Figure 4.4: Cumulative Mass of PHC Phytovolatilized Normalized with Respect to Mass of Contaminated Soil

As with the mass of PHC volatilized from soil, the cumulative mass of PHC phytovolatilized (and the normalized cumulative masses of PHC phytovolatilized) was removed quickly at the start of the experiment and slowed dramatically as time increased. All test cells have a high phytovolatilization rate over the first 60 days followed by much lower rates over the next 51 days. The phytovolatilization rate increased during the period from day 111 to day 157 but then decreased over the last 63 days (Tables 4.13 and 4.14). The high initial rate of phytovolatilization may be attributed to rapid uptake and release of compounds that are easily phytovolatilized and, to a lesser extent, the release of PHC from the dental impression material used to form a seal around the tree stem. The generally decreasing rate of phytovolatilization with increasing time may be attributed to decreasing degradability of compounds by phytovolatilization and increasing amounts of PHC that are not readily phytovolatilized sorbed to the roots of the tree.

Table 4.13: Phytovolatilization Rates (mg_{PHC}/day)

Test Cell #	Time Interval			
	1	2	3	4
1	0.94 ± 0.09**	0.09 ± 0.01	0.24 ± 0.03	0.02 ± 0.002
2	1.10 ± 0.09	0.10 ± 0.01	0.23 ± 0.03	0.01 ± 0.002
3	2.63 ± 0.25	0.06 ± 0.01	0.12 ± 0.01	0.02 ± 0.002
4	0.81 ± 0.07	0.02 ± 0.002	0.21 ± 0.02	0.14 ± 0.02

**The calculated error was derived from the extraction efficiencies and response factors

Table 4.14: Normalized Phytovolatilization Rates [$\mu g_{PHC}/(kg_{soil}*day)$]

Test Cell #	Time Interval			
	1	2	3	4
1	30.87 ± 2.97**	2.98 ± 0.32	7.79 ± 0.86	0.63 ± 0.08
2	35.61 ± 3.01	3.20 ± 0.34	7.32 ± 0.82	0.43 ± 0.05
3	99.26 ± 9.53	2.44 ± 0.27	4.56 ± 0.52	0.76 ± 0.09
4	30.68 ± 2.83	0.76 ± 0.09	8.08 ± 0.88	5.15 ± 0.63

**The calculated error was derived from the extraction efficiencies and response factors

4.4.2 Quality Assurance/Quality Control for Quantification of Volatilized PHC

The quality assurance/quality control programme used to quantify the mass of PHC extracted from the air sampling tubes involved using internal and external standards. Internal standards were used to determine the extraction efficiencies, E_Es, of the air sampling tubes for each fraction and external standards were used to determine the GC response factor.

Upon initial setup, the configuration of the air sampling tubes consisted of an ORBO™402 tube followed by an ORBO™32L tube. After replacing the third set of tubes collecting volatilized PHC from soil and the second set of tubes collecting phytovolatilized PHC on December 1, 2006, the configuration was changed to consist of an ORBO™32L tube only. This new configuration remained for all subsequent tubes. This configuration was implemented as, upon additional testing of the tubes after the experiment was setup and before December 1, 2006, it was discovered that, contrary to the manufacturers specifications, the ORBO™32L tubes adsorbed the full range of hydrocarbon standards used in this experiment. The E_Es from the tubes to which hydrocarbon standards were applied and which had air blown through them were found to be within the error range for the E_Es from the tubes to which hydrocarbon standards were applied and which did not have air blown through them (4.15).

Table 4.15: Extraction Efficiencies of ORBO™32L Air Sampling Tubes to which Hydrocarbon Standards had been Applied With and Without Air Blown Through

Air Sampling Tubes	Extraction Efficiencies, E_Es		
	F1 (%)	F2 (%)	F3 (%)
ORBO™32L: Air sampling tubes without air blown through (n=3)	58 ± 17	103 ± 22	102 ± 34
ORBO™32L: Air sampling tubes with air blown through (n=3)	62 ± 11	114 ± 9	88 ± 37

The E_Es for the ORBO™402 tubes (Table 4.16) were the averages of three tubes to which hydrocarbon standards were applied and which did not have air blown through them.

Table 4.16: Extraction Efficiencies of ORBO™32L and ORBO™402 Air Sampling Tubes

Air Sampling Tubes	Extraction Efficiencies, E_Es		
	F1 (%)	F2 (%)	F3 (%)
ORBO™32L* (n=6)	60 ± 15	108 ± 16	95 ± 35
ORBO™402 (n=3)	n/a	92 ± 11	105 ± 6

*Overall averages for tubes with and without air blown through (from Table 4.15)

4.4.3 Degradation Monitoring Using Automated Respirometry

The lower chambers of the experimental containers were attached to a respirometer which measured O_2 consumption (Figure 4.5) and CO_2 production (Figure 4.6) from the soil and roots during the course of the experiment. This data was then used to infer the mass of PHC degraded by microbes in the soil.

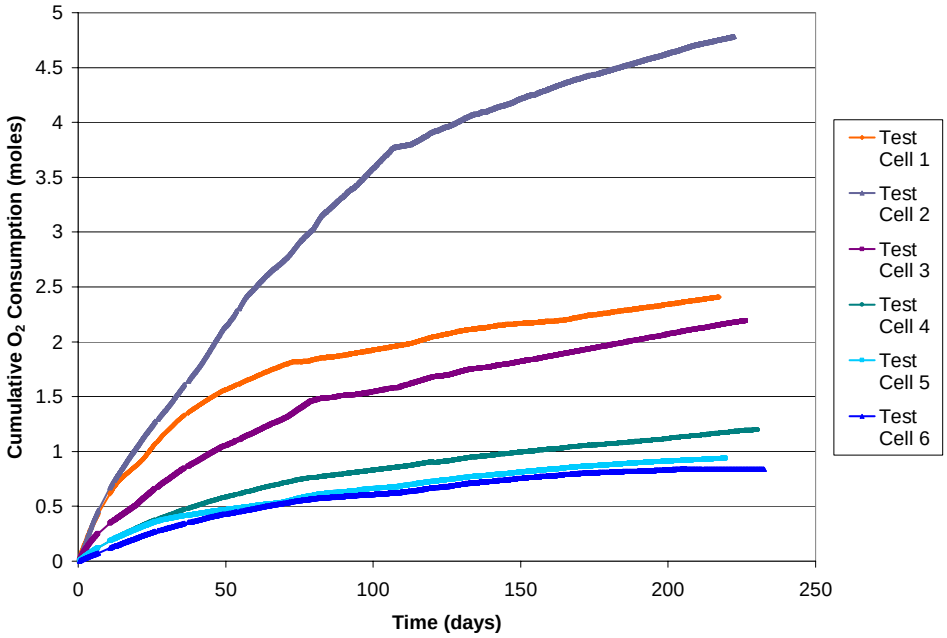

Figure 4.5: Cumulative O_2 Consumption

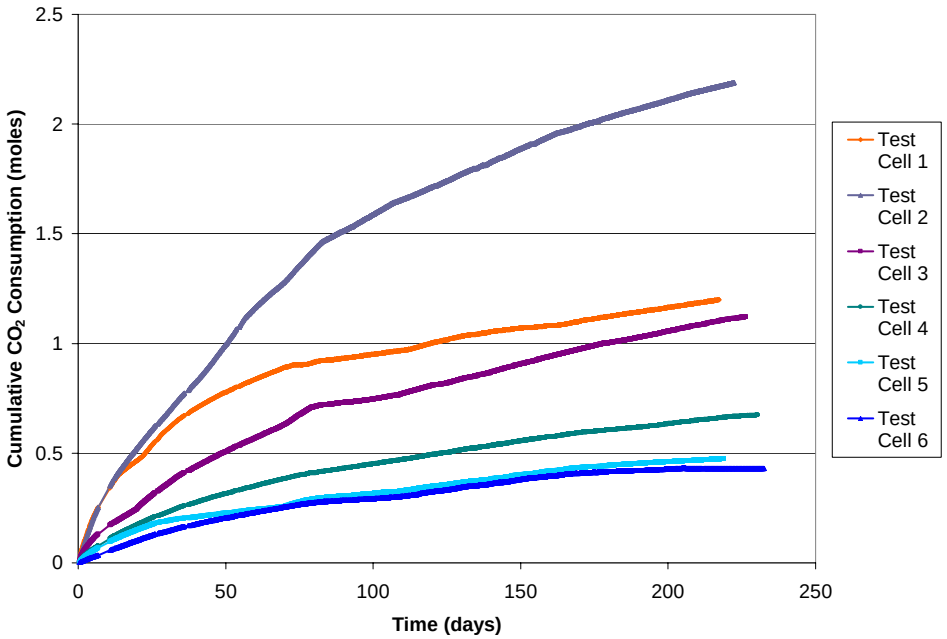

Figure 4.6: Cumulative CO_2 Production

To calculate the mass of PHC degraded by microbes O_2 consumption attributed to soil respiration (51.5% of the total), in moles, was converted to mg of PHC using equations 3.2 and 3.3 (Section 2.3.6). Because of the strong correlation between the two equations, the two were averaged to yield the mass of PHC degraded by microbes (4.17).

Table 4.17: Estimated Masses of PHC Degraded by Microbes

	Estimated Mass of PHC Degraded using O_2 Consumption (mg)		
Test Cell #*	**Equation 3.2**	**Equation 3.3**	**Average**
1	11464	11340	11402
2	22769	22523	22646
3	10436	10324	10380
4	5707	5645	5676
5	4467	4419	4443
6	3992	3948	3970

*Test cells 1-4 were planted with Walker poplars; test cells 5 and 6 were unplanted

The estimated cumulative mass of PHC degraded by microbes was calculated at time intervals to correspond with removal of air sampling tubes measuring the amount of PHC volatilized from the soil and through the plant. As with volatilized PHC, the cumulative mass of PHC degraded (Figure 4.7) was normalized with respect to the mass of contaminated soil in each container (Figure 4.8).

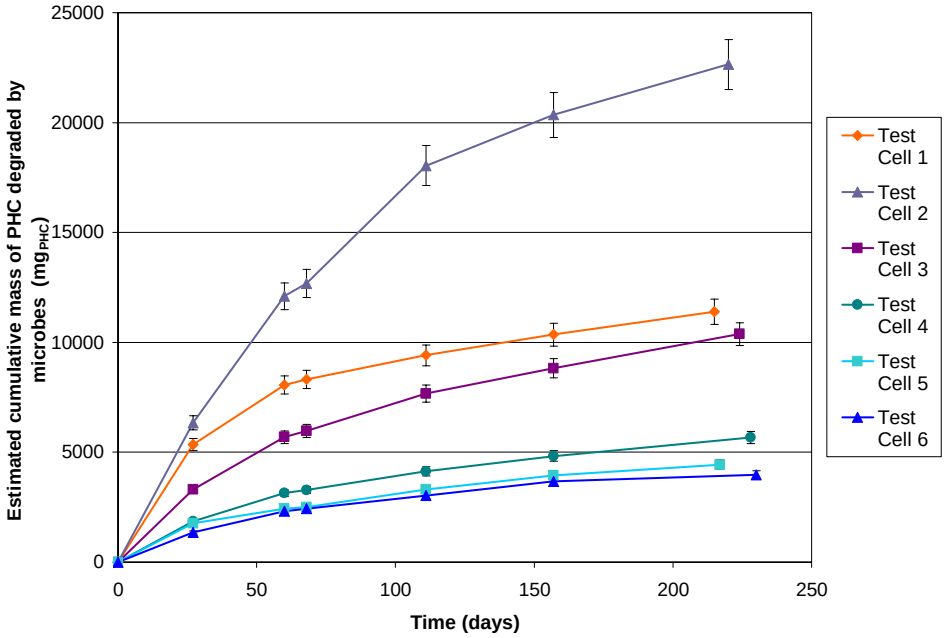

Figure 4.7: Estimated Cumulative Mass of PHC Degraded by Microbes

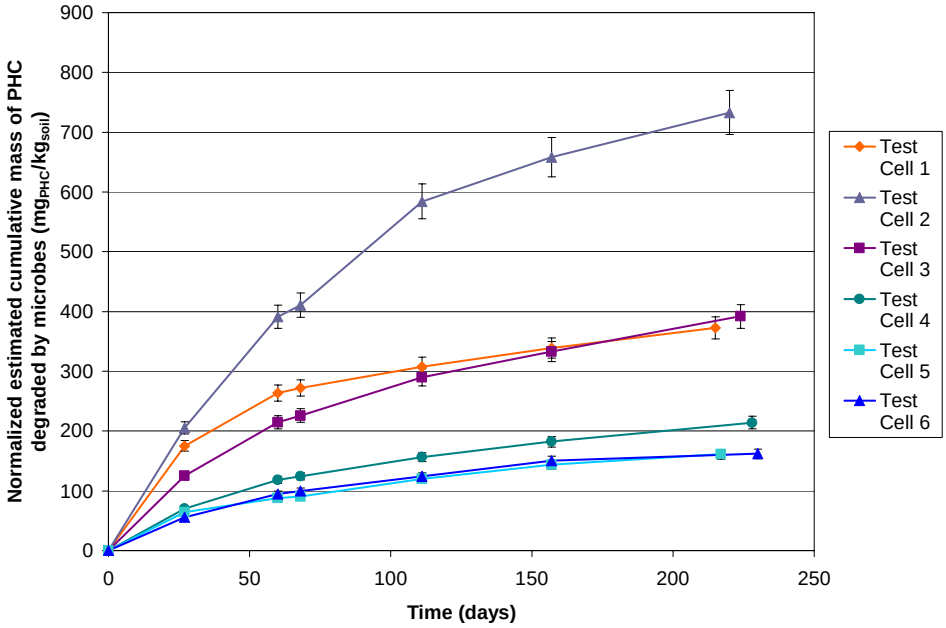

Figure 4.8: Estimated Cumulative Mass of PHC Degraded by Microbes Normalized with Respect to Mass of Contaminated Soil

In all cases, there is a greater mass of PHC degraded over the first 27 days with degradation rate generally decreasing over subsequent time intervals (Tables 4.18 and 4.19). As with volatilization of PHC from soil, this may be attributed to a combination of placement effects and rapid degradation of easily degradable compounds in the soil

Table 4.18: Estimated Microbial Degradation Rates (mg_{PHC}/day)

Test Cell #*	Time Interval					
	1	2	3	4	5	6
1	198.3 ± 9.9	82.1 ± 4.1	32.4 ± 1.6	25.4 ± 1.3	20.5 ± 1.0	18.0 ± 0.9
2	234.7 ± 11.7	174.6 ± 8.7	73.4 ± 3.7	124.7 ± 6.2	50.1 ± 2.5	36.4 ± 1.8
3	122.7 ± 6.1	72.0 ± 3.6	36.9 ± 1.8	39.4 ± 2.0	25.0 ± 1.2	23.2 ± 1.2
4	68.9 ± 3.4	38.7 ± 1.9	19.0 ± 1.0	19.7 ± 1.0	15.0 ± 0.8	11.9 ± 0.6
5	65.6 ± 3.3	19.8 ± 1.0	9.8 ± 0.5	18.7 ± 0.9	14.0 ± 0.7	8.2 ± 0.4
6	50.2 ± 2.5	29.3 ± 1.5	14.2 ± 0.7	14.0 ± 0.7	14.0 ± 0.7	3.9 ± 0.2

*Test cells 1-4 were planted with Walker poplars; test cells 5 and 6 were unplanted

Table 4.19: Estimated Microbial Degradation Rates Normalized with Respect to Mass of Contaminated Soil [$\mu g_{PHC}/(kg_{soil}*day)$]

Test Cell #*	Time Interval					
	1	2	3	4	5	6
1	6485 ±324	4395 ± 134	4003 ± 53	2774 ± 42	2158 ± 34	1734 ± 29
2	7596 ± 380	5650 ± 282	2377 ± 119	4035 ± 202	1620 ± 81	1179 ± 59
3	4631 ± 232	2717 ± 136	1392 ± 70	1486 ± 74	942 ± 47	875 ± 44
4	2601 ± 130	1460 ± 73	719 ± 36	745 ± 37	567 ± 28	449 ± 22
5	2380 ± 119	718 ± 36	355 ± 18	677 ± 34	508 ± 25	297 ± 15
6	2051 ± 103	1198 ± 60	581 ± 29	571 ± 29	573 ± 29	159 ± 8

*Test cells 1-4 were planted with Walker poplars; test cells 5 and 6 were unplanted

While an attempt has been made to remove the contribution of root respiration from the respiration data, there are a number of other processes that would influence the measured respiration. The potential influence of these processes is fully acknowledged, however, it would have been impossible to further separate different sources of respiration.

A number of processes would have contributed to the measured values of respiration resulting in an overestimation of the mass of diesel degraded by microbes. The processes that could result in an overestimation are: cometabolism of root exudates and PHC by microbes, degradation of root exudates by microbes, degradation of organic matter (ie. humic substances) by microbes, incomplete degradation of PHC, and root respiration.

There also were a number of processes that would have resulted in an underestimation of the mass of diesel degraded by microbes. These processes include: degradation of PHC by root exudates, storage and transformation of contaminant within the plant, sorbtion to roots and other organic matter in the soil, conversion to new biomass and humus, and perhaps small amounts of PHC degradation by anaerobic bacteria.

Due to the assumption that 51.5% of O_2 consumption is solely the result of microbial degradation of diesel, the mass of diesel degraded by microbes and the microbial degradation rates have previously been referred to as estimated masses and rates. From this point onwards the mass of diesel degraded microbially will be understood to include all processes that could result in an overestimation or underestimation of the mass of diesel degraded mentioned in the previous two paragraphs.

4.4.4 Combined Monitoring Data for PHC Removal

The monitoring data from the degradation pathways presented in Sections 4.4.1 and 4.4.3 were combined to obtain a total mass of PHC removed from each experimental container. As some of the air sampling tube dates varied the sampling times and the

corresponding cumulative masses were averaged to fit with the sampling times from all the tubes. The dates used for the combined monitoring data can be seen in Table 4.20.

Table 4.20: Air Sampling Tube Installation and Removal Dates for the Cumulative Mass of PHC Removed

Time Interval	Date Installed	Date Removed	Elapsed Time (days)
1	August 12, 2005	October 15, 2005*	64
2	October 15, 2005*	December 1, 2005	111
3	December 1, 2005	January 16, 2006	157
4	January 16, 2006	March 15-30, 2006	215-239

*October 19, 2005 (elapsed time of 68 days) was used for containers 5 and 6

The cumulative mass and normalized cumulative mass of PHC removed from the soil through volatilization from soil, phytovolatilization and degradation by microbes is presented in Figures 4.9 and 4.10. The degradation rates and normalized degradation rates are summarized in Tables 4.21 and 4.22.

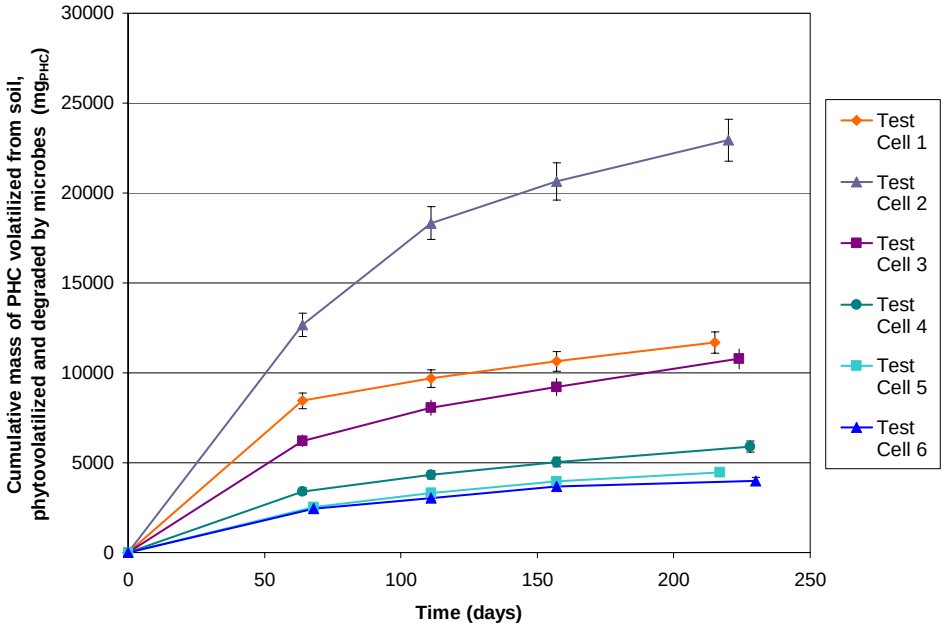

Figure 4.9: Cumulative Mass of PHC Removed

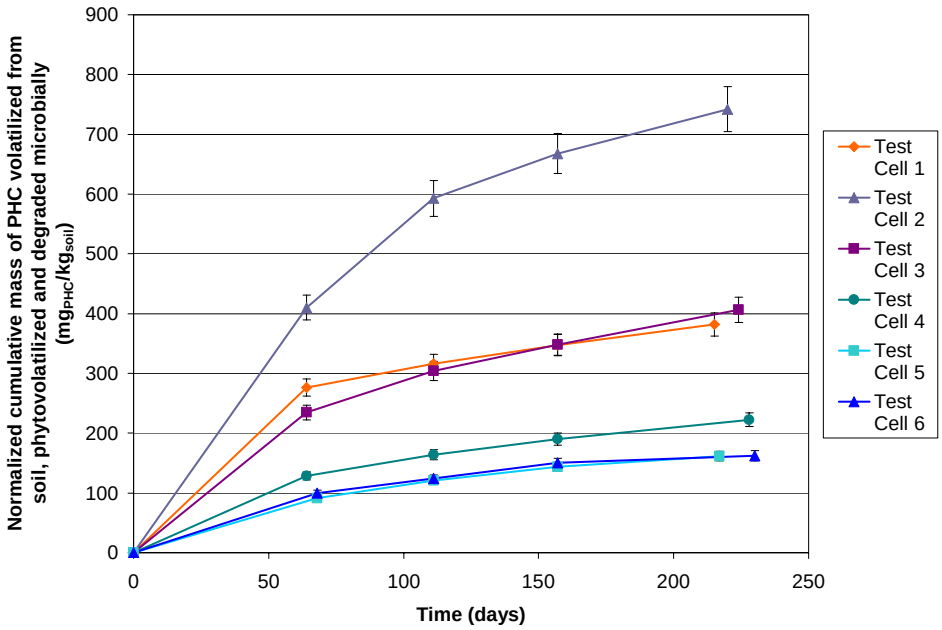

Figure 4.10: Cumulative Mass of PHC Removed Normalized with Respect Mass of Contaminated Soil

Table 4.21: Removal Rates from Volatilization from Soil, Phytovolatilization, and Degradation by Microbes (mg$_{PHC}$/day)

Test Cell #*	**Time Interval**			
	1	**2**	**3**	**4**
1	132 ± 7	26 ± 1	21 ± 1	18 ± 1
2	198 ± 10	120 ± 6	50 ± 3	36 ± 3
3	97 ± 5	39 ± 2	25 ± 1	23 ± 1
4	53 ± 3	20 ± 1	15 ± 1	12 ± 1
5	37 ± 2	19 ± 1	14 ± 1	8 ± 0
6	36 ± 2	14 ± 1	14 ± 1	4 ± 0

*Test cells 1-4 were planted with Walker poplars; test cells 5 and 6 were unplanted

Table 4.22: Normalized Removal Rates from Volatilization from Soil, Phytovolatilization, and Degradation by Microbes [$\mu g_{PHC}/(kg_{soil}*day)$]

Test Cell #*	Time Interval			
	1	2	3	4
1	4317 ± 220	854 ± 43	680 ± 34	588 ± 29
2	6405 ± 324	3898 ± 195	1628 ± 82	1180 ± 59
3	3665 ± 191	1483 ± 75	648 ± 48	876 ± 44
4	2008 ± 104	748 ± 38	575 ± 29	455 ± 23
5	1345 ± 71	678 ± 33	508 ± 25	297 ± 15
6	1467 ± 76	571 ± 29	573 ± 29	159 ± 8

*Test cells 1-4 were planted with Walker poplars; test cells 5 and 6 were unplanted

The influence of each degradation pathway on the total estimated mass of PHC removed is summarized in Table 4.23.

Table 4.23: Percentage Contribution of Each Degradation Pathway to the Total Mass Removed

Test Cell #*	% Volatilized from Soil	% Phytovolatilized	% Degraded by Microbes
1	1.7	0.6	97.7
2	0.9	0.4	98.7
3	2.1	1.6	96.3
4	2.5	1.2	96.3
5	0.4	0.0	99.6
6	0.1	0.0	99.9

*Test cells 1-4 were planted with Walker poplars; test cells 5 and 6 were unplanted

The estimated mass of PHC degraded by microbes had the greatest influence on the total estimated mass of PHC removed.

4.5 Evaluation of Mass Balance

A mass balance did not occur for any of the test cells (Table 4.24).

Table 4.24: % PHC Removed

Test Cell #*	$\Delta PHC_{measured}$ (%)**	$\Delta PHC_{estimated}$ (%)†	$\left(1-\frac{\Delta PHC_{estimated}}{\Delta PHC_{measured}}\right)\times 100$ ‡	
1	94	14	85	
2	83	28	66	84 ± 8
3	78	15	81	
4	94	8	91	
5	96	6	94	94 ± 0
6	95	6	94	

*Test cells 1-4 were planted with Walker poplars; test cells 5 and 6 were unplanted
**Measured change in PHC concentration based on GC analysis of soils under initial and final conditions
†Estimated change in PHC concentration based on monitoring data (Note: initial soil concentration based on GC analysis)
‡Percentage of PHC unaccounted for by the monitoring data

The absence of mass balance was not unforeseen due to a number of expected and unavoidable errors inherent in the experimental design. These errors were: volatilization of PHC from the soil during initial placement of the soil in the test cells and later upon disassembly and final soil sampling; the use of between 8 and 11 discrete sampling locations per experimental test cell to determine the final mass of PHC in the containers; and the sources of error identified in Section 4.4.3 concerning the use of O_2 consumption to determine the mass of diesel degraded in the soil.

Volatilization of PHC from the soil during placement and upon disassembly and final soil sampling likely resulted in an overestimation of the mass of PHC removed during the experiment. For example, as the containers were disassembled, the soil was exposed to the atmosphere while the section boundaries were identified and soil samples were collected. During this period any PHC volatilized from the soil would have been unaccounted for in the analysis. Similar losses would have occurred during assembly of the experimental test cells.

Also, the use of between 8 and 11 discrete sampling locations per experimental test cell to determine the total mass of contaminant remaining in each container may not have resulted in a representative mass of PHC remaining.

Due to the unknown magnitude of volatilization from the soil, the variation in volatilization between containers, and the potential errors inherent in determining the final PHC concentration in the soil from a limited number of discrete samples, the mass of PHC removed from the soil ($\Delta PHC_{measured}$) was not reliable. The author proposes that the mass of PHC removed from the soil based on the monitoring data, although having a few identified flaws, is the more credible method of measurement.

Chapter 5: Development of a Rationally-Based Model for Prediction of Phytoremediation

5.1 Overview

The results presented in Chapter 4, specifically the mass of PHC removed from the soil and the biological measurements, were used to develop a rationally-based model for predicting the rate of removal of PHC from soil during the course of a phytoremediation project. First, the normalized mass of PHC removed was compared to a number of biological measurements to obtain a preliminary correlation of results. Next, two numerical methods were used to determine a rate constant for each test cell. The resultant rate constants were then plotted against three biological measurements, selected based on the preliminary correlation. From these three plots one was selected to be used as the final model. This simple model may be used to predict the mass of weathered diesel removed in the course of phytoremediation.

5.2 Correlations between the Mass of PHC Removed and Biological Measurements

The total mass of PHC removed, normalized with respect to the mass of contaminated soil, was compared to root length, root mass, below-ground plant biomass, above-ground plant biomass, total plant biomass, and total biomass (Figures 5.1 to 5.6).

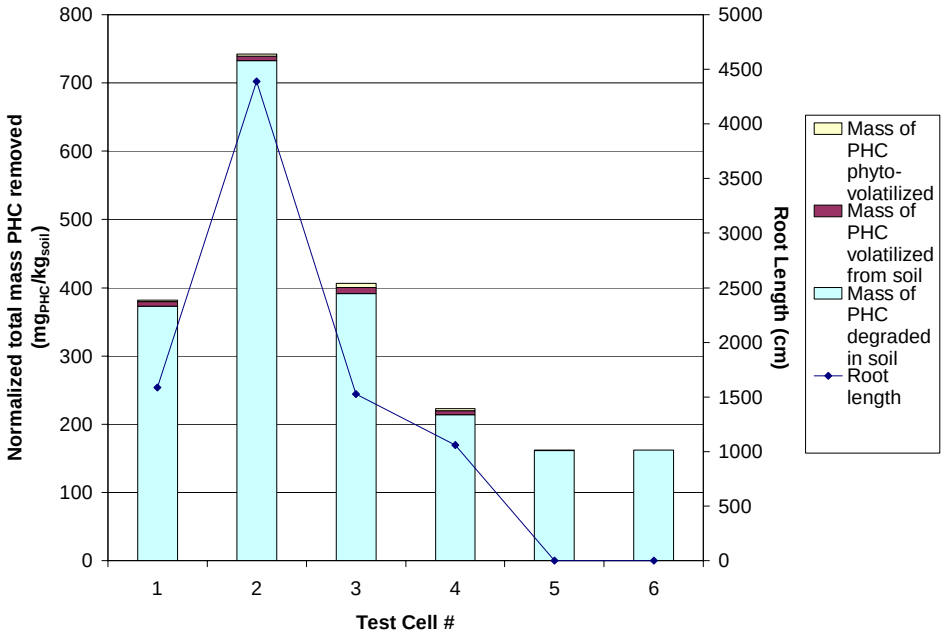

Figure 5.1: Total Mass of PHC Removed Normalized with Respect to Mass of Contaminated Soil and Root Length

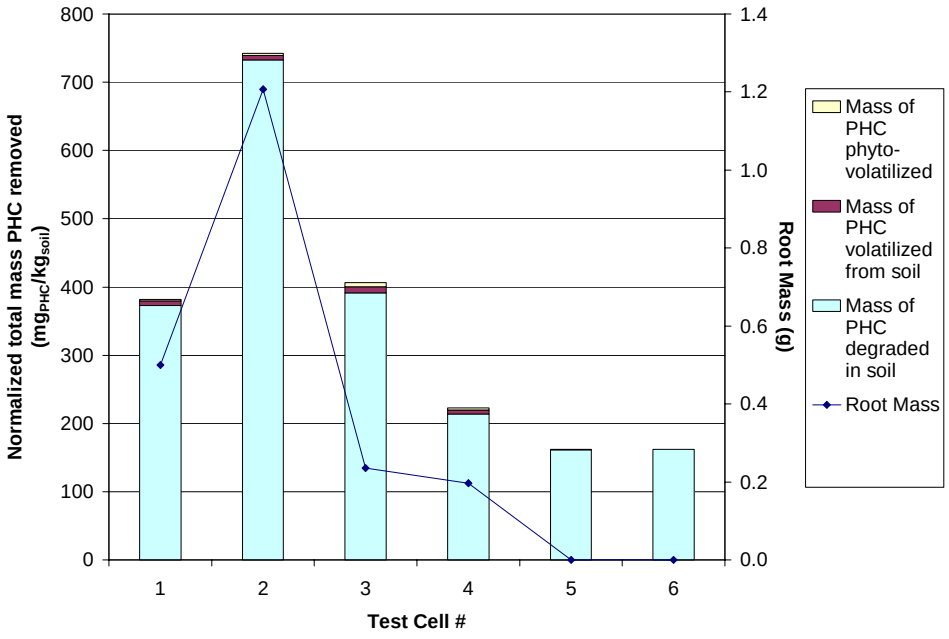

Figure 5.2: Total Mass of PHC Removed Normalized with Respect to Mass of Contaminated Soil and Root Mass

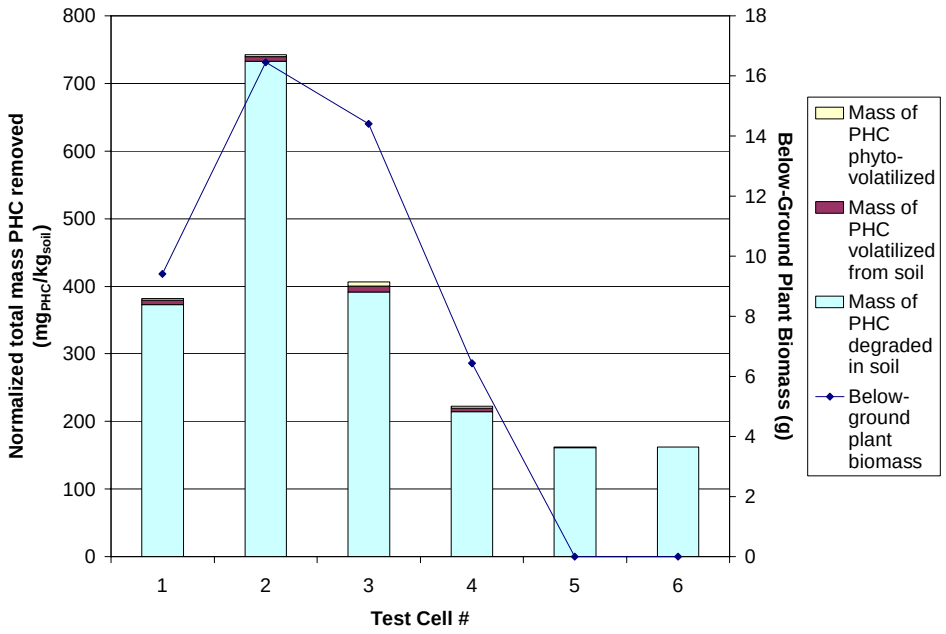

Figure 5.3: Total Mass of PHC Removed Normalized with Respect to Mass of Contaminated Soil and Below-Ground Plant Biomass

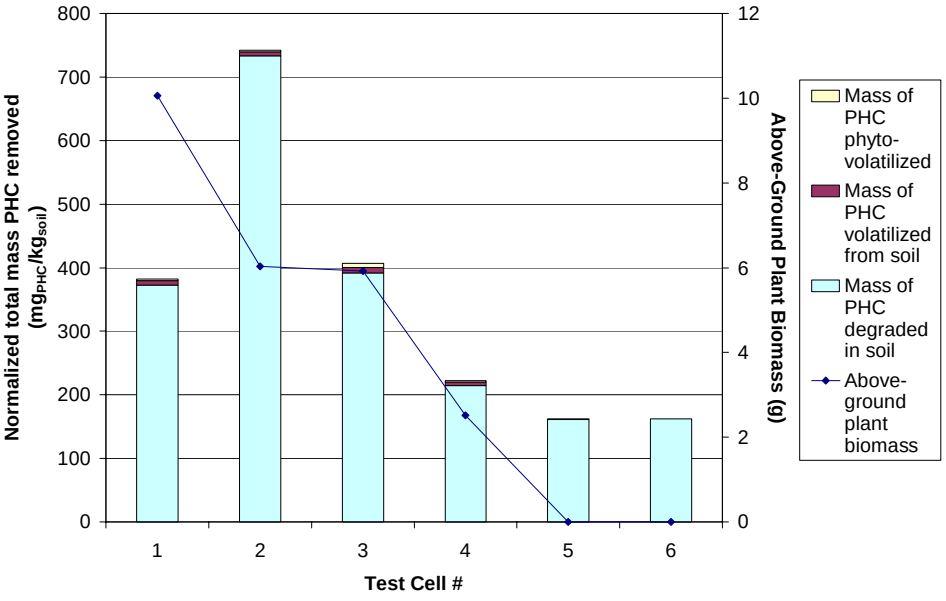

Figure 5.4: Total Mass of PHC Removed Normalized with Respect to Mass of Contaminated Soil and Above-Ground Plant Biomass

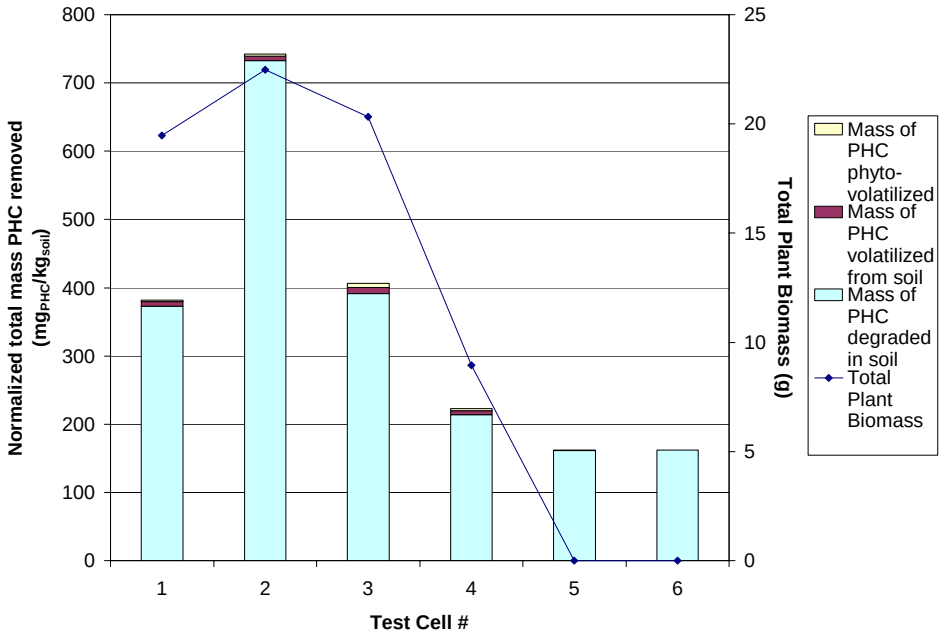

Figure 5.5: Total Mass of PHC Removed Normalized with Respect to Mass of Contaminated Soil and Total Plant Biomass

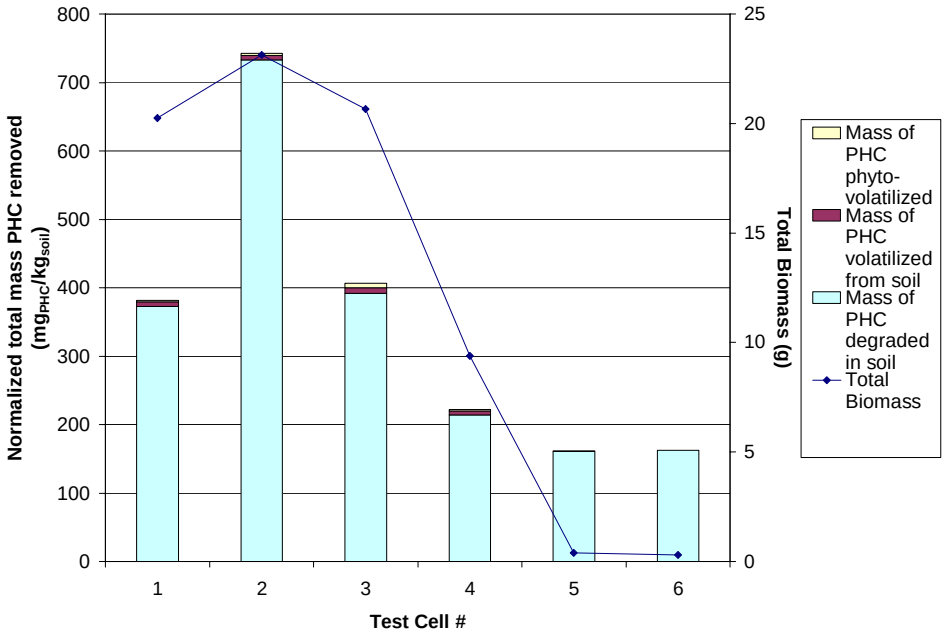

Figure 5.6: Total Mass of PHC Removed Normalized with Respect to Mass of Contaminated Soil and Total Biomass

The correlation coefficient (r), standard error of the correlation coefficient (S.E. of r), and probability that the correlation coefficient is equal to 0 [P(r=0)] were determined for the data plotted in Figures 5.1 to 5.6 (Table 5.1).

Table 5.1: Correlations of the Total Mass of PHC Removed Normalized with Respect to the Mass of Contaminated Soil with Root Length, Root Mass, Below-Ground Plant Biomass, Above-Ground Plant Biomass, Total Plant Biomass, and Total Biomass

Data (n=6)	r	S.E. of r	P(r=0)
Figure 5.1: Total mass of PHC removed normalized with respect to mass of contaminated soil and root length	0.983	0.090	0.0004
Figure 5.2: Total mass of PHC removed normalized with respect to mass of contaminated soil and root mass	0.865	0.251	0.0260
Figure 5.3: Total mass of PHC removed normalized with respect to mass of contaminated soil and below-ground plant biomass	0.895	0.223	0.0161
Figure 5.4: Total mass of PHC removed normalized with respect to mass of contaminated soil and above-ground plant biomass	0.636	0.386	0.1745
Figure 5.5: Total mass of PHC removed normalized with respect to mass of contaminated soil and total plant biomass	0.851	0.262	0.0316
Figure 5.6: Total mass of PHC removed normalized with respect to mass of contaminated soil and total biomass	0.852	0.262	0.0313

The total mass of PHC removed normalized with respect to the mass of contaminated soil showed significant correlation [$P(r=0) \leq 0.05$] with, in decreasing order of correlation: root length, below-ground biomass, root mass, total biomass and total plant biomass. Correlation with above-ground biomass was not significant. It was expected that the root length, root mass and below-ground biomass would correlate well as the amount of root surface area affects number of microbes in the soil, the amount of contaminant absorbed by the roots, the amount of contaminant sorbed to the roots, and the amount of root exudates released, all of which affect the amount of contaminant removed from the soil.

5.3 Determination of Rate Constants

Rate constants were determined for each test cell using two different methods. The first method fit a number of mathematical models to the normalized cumulative mass of PHC removed over time for each container and identified the rate constant from the best fit model. The second method identified the "equilibrium" normalized rates of removal of PHC for each test cell. These "equilibrium" rates were calculated using the last monitoring interval of the normalized cumulative mass of PHC removed over time. The rate constants obtained using each method were then plotted against the three most significant biological measurements: root length, root mass, and below-ground biomass.

5.3.1 Method 1: Determination of Rate Constants using Mathematical Models over the Entire Experiment

A number of mathematical models were fit to the normalized cumulative mass of PHC removed over time for each test cell. The general forms of these mathematical models were:

$$NCMR = At + B \quad [5.1]$$

$$NCMR = A\ln(t) + B \quad [5.2]$$

$$NCMR = Bt^{A} \quad [5.3]$$

$$NCMR = Be^{At} \quad [5.4]$$

where

NCMR=cumulative mass PHC removed normalized with respect to mass of contaminated soil (mg_{PHC}/kg_{soil})

A=rate constant

t=time (days)

B=constant

To determine an appropriate mathematical model, a number of different models were fit to the data, excluding the initial data point (0,0). The initial data point was excluded due to the large initial mass of PHC removed over the first time interval, partially attributed to soil placement effects, and the limit to the number of models that can be used with a data point at (0,0). The best fit model was identified based on the coefficient of determination (R^2) where the mathematical model with an average R^2 value closest to 1 was selected. The data were fit to linear, natural logarithmic, exponential and power models (Figure 5.7) and the R^2 values for each model are summarized in Table 5.2.

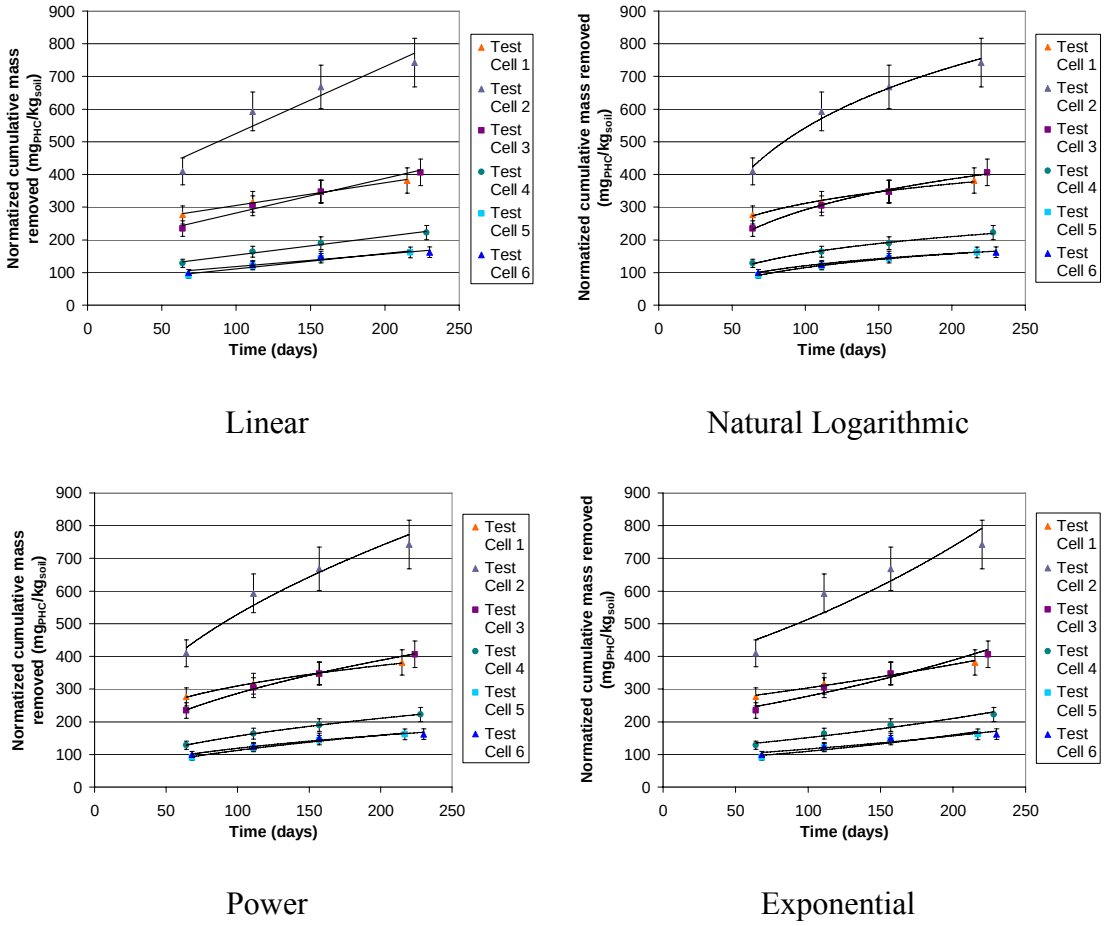

Figure 5.7: Cumulative Mass of PHC Removed Normalized with Respect to Mass of Contaminated Soil Over Time with Various Models

Table 5.2: R^2 Values for Various Mathematical Models

Model	Test Cell #*						
	1	2	3	4	5	6	Average
Linear	0.992	0.913	0.983	0.986	0.966	0.920	0.960
Natural Logarithmic	0.991	0.986	0.996	0.995	0.999	0.980	0.991
Power	0.998	0.962	0.998	1.000	0.992	0.973	0.987
Exponential	0.981	0.863	0.953	0.959	0.932	0.892	0.930

*Test cells 1-4 were planted with Walker poplars; test cells 5 and 6 were unplanted

The best fit model based on R^2 values was a natural logarithmic model (Figure 5.8). This model has the general form:

$$NCMR = A\ln(t) + B \qquad [5.2]$$

The rate constants, *A*, intercepts, *B*, R^2 values and, root mean squared error, RMSE, from this model can be seen in Table 5.3.

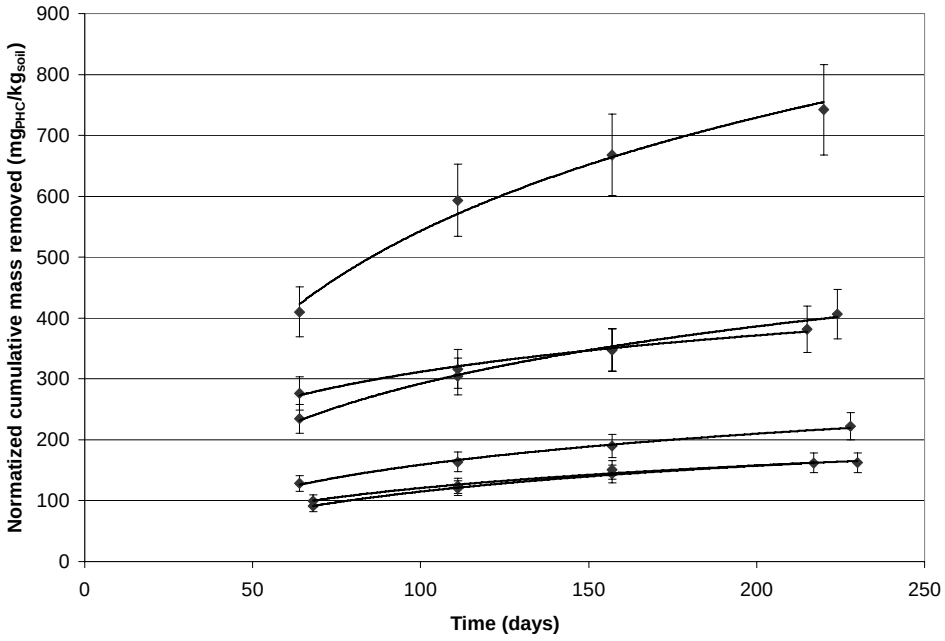

Figure 5.8: Cumulative Mass of PHC Removed over Time Normalized with Respect to the Mass of Contaminated Soil with Natural Logarithmic Model

Table 5.3: Rate Constants, *A*, Intercepts, *B*, R^2, and RMSE of the Cumulative Mass of PHC Removed over Time Normalized with Respect to the Mass of Contaminated with Natural Logarithmic Model

Test Cell #*	Rate Constant (mg_{PHC}/kg_{soil}*day)	Intercept (mg_{PHC}/kg_{soil})	R^2	RMSE (mg)
1	86	-86	0.991	4
2	269	-694	0.986	14
3	136	-332	0.996	4
4	74	-180	0.995	3
5	61	-167	0.999	1
6	53	-125	0.980	3

*Test cells 1-4 were planted with Walker poplars; test cells 5 and 6 were unplanted

This model also corresponds to a logical progression of the mass of PHC removed over time. The rate of removal of PHC was expected to decrease with time, taking into account factors such as the decreasing effect of soil placement, removal of easily degradable PHC and sorption of PHC to root surfaces.

5.3.2 Method 2: Determination of Rate Constants Using "Equilibrium" Conditions

Linear trend lines were fit to the normalized cumulative mass of PHC removed over time for each test cell under "equilibrium" conditions to determine rate constants for each test cell (Figure 5.8). "Equilibrium" conditions were considered to occur during the final time interval (157 days to between 215 days and 230 days). Although the data is obviously not linear over the entire experiment (see Figure 4.10), the slope of the normalized cumulative mass of PHC removed is decreasing over each time interval for all test cells as can be seen in Table 5.4.

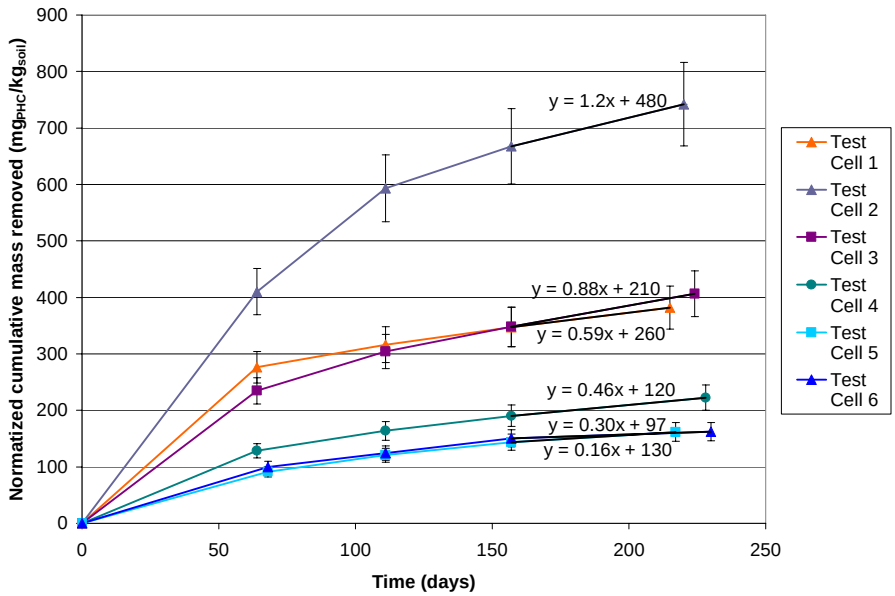

Figure 5.9: Cumulative Mass of PHC Removed over Time Normalized with Respect to the Mass of Contaminated Soil with Linear Trend Lines under "Equilibrium" Conditions

Table 5.4: Slopes of the Normalized Cumulative Mass of PHC Removed over Time Normalized with Respect to the Mass of Contaminated Soil over Each Time Interval

Test Cell #*	Time Interval (days)			
	0-64 or 0-68**	64-111 or 68-111**	111-157	157-(215-230)
1	4.32	0.85	0.68	0.59
2	6.40	3.90	1.63	1.18
3	3.66	1.48	0.95	0.88
4	2.01	0.75	0.58	0.45
5	1.52	0.57	0.51	0.30
6	1.66	0.48	0.57	0.16

*Test cells 1-4 were planted with Walker poplars; test cells 5 and 6 were unplanted
**64 days for test cells 1 to 4 and 68 days for test cells 5 and 6

5.4 Variation of Rate Constants with Plant Size Index

Rate constants determined using both methods were plotted against root length, root mass and below-ground plant biomass. Based on these plots, the best method of determining rate constants was selected to be used in the final model. Plots of rate constants determined using equation 5.2, a natural logarithmic model fit to the

normalized cumulative mass of PHC removed over the entire experiment, can be seen in Figures 5.10 to 5.12. Plots of the "equilibrium" rate constants are presented in Figures 5.13 to 5.15.

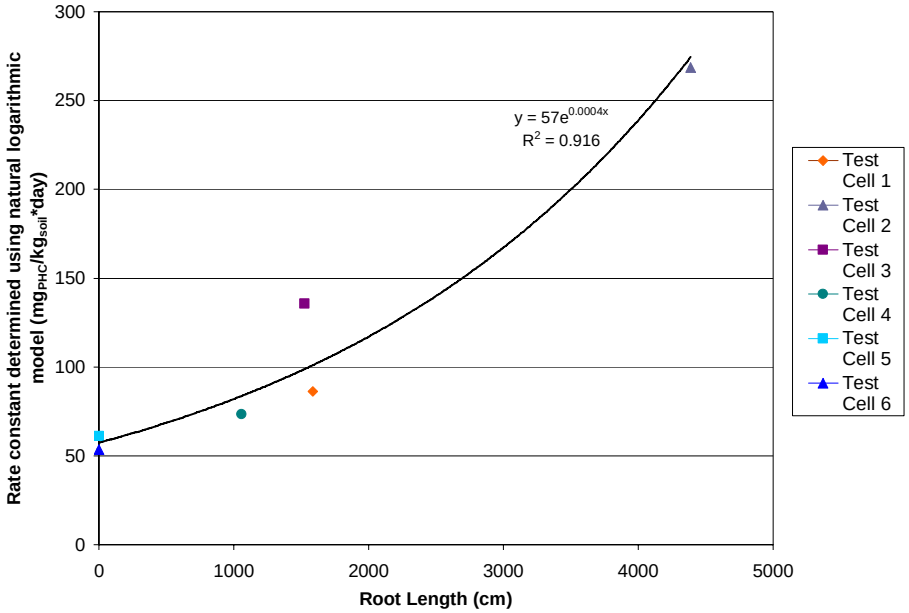

Figure 5.10: Rate Constants (Normalized with Respect to Mass of Contaminated Soil) Determined using the Natural Logarithmic Model and Root Length

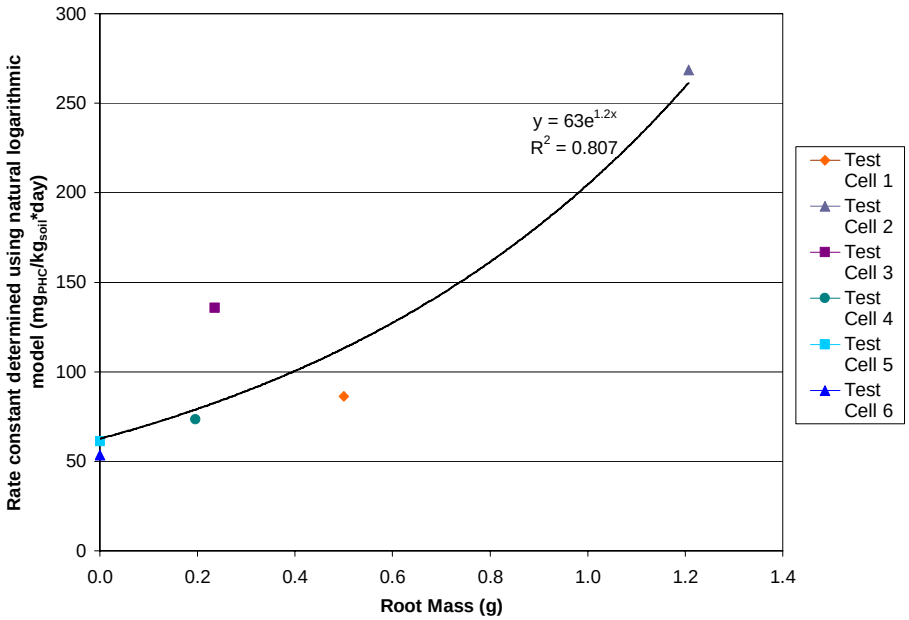

Figure 5.11: Rate Constants (Normalized with Respect to Mass of Contaminated Soil) Determined using the Natural Logarithmic Model and Root Mass

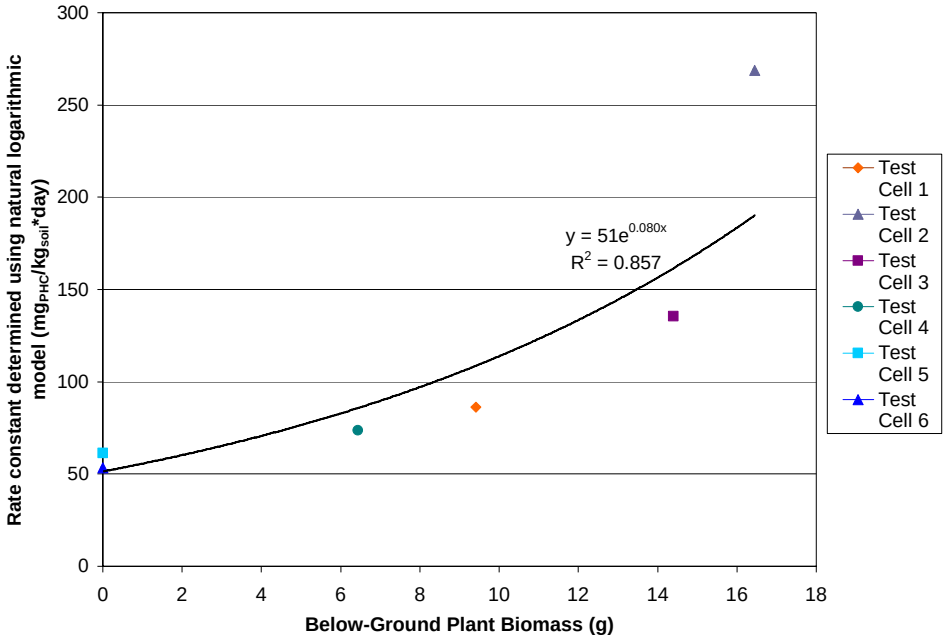

Figure 5.12: Rate Constants (Normalized with Respect to Mass of Contaminated Soil) Determined using the Natural Logarithmic Model and Below-Ground Plant Biomass

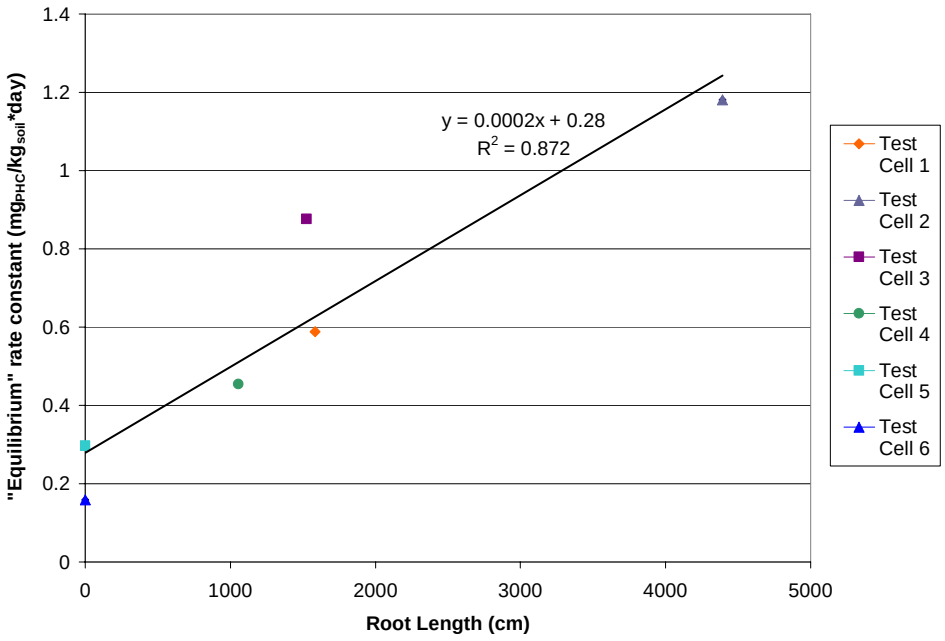

Figure 5.13: Rate Constants (Normalized with Respect to Mass of Contaminated Soil) Determined using "Equilibrium" Conditions and Root Length

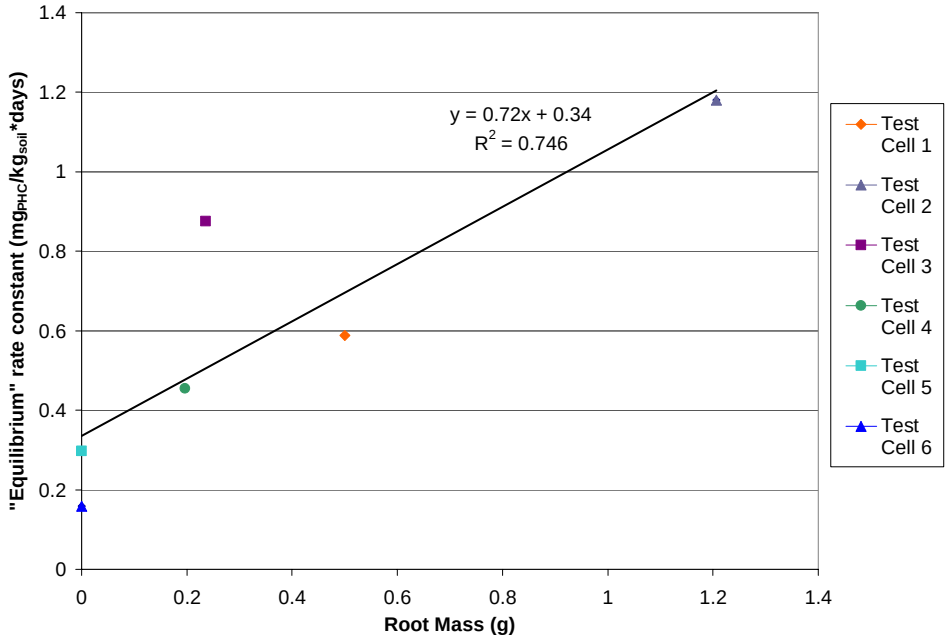

Figure 5.14: Rate Constants (Normalized with Respect to Mass of Contaminated Soil)

Determined using "Equilibrium" Conditions and Root Mass

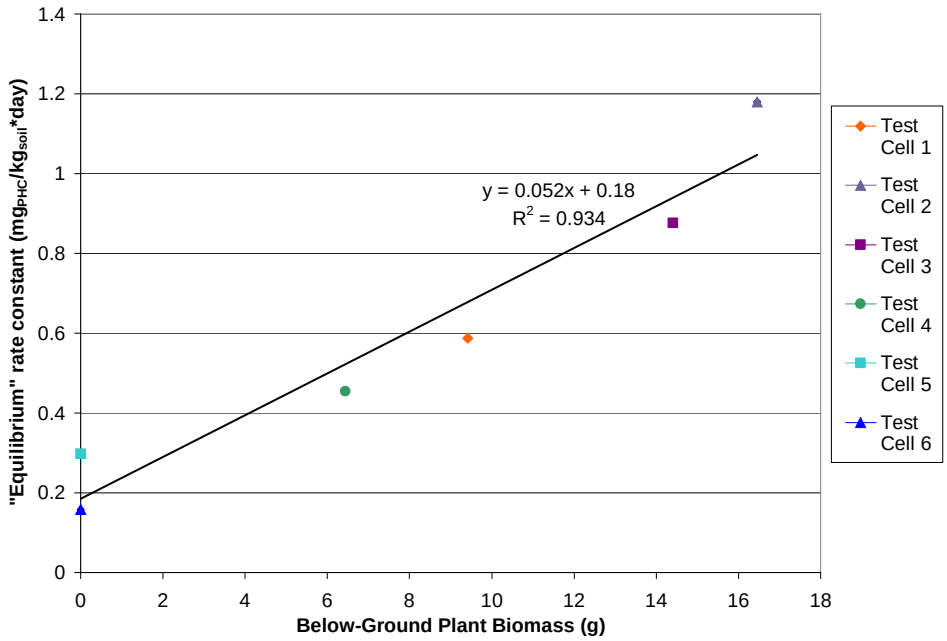

Figure 5.15: Rate Constants (Normalized with Respect to Mass of Contaminated Soil)

Determined using "Equilibrium" Conditions and Below-Ground Plant Biomass

The normalized rate constants determined using the natural logarithmic model plotted against root length, root mass, and below-ground biomass and fit with the best fit equations show that the normalized rate constant increases at an increasing rate with increasing root length, root mass, below-ground biomass and above-ground biomass. This indicates that as biomass increases the normalized rate of removal of PHC increases much more quickly. This does not correspond with the original data of normalized cumulative mass of PHC removed over time presented in Figure 4.10. Looking at Figure 4.10 and referring to the data presented in Table 5.4, the normalized rate of removal of PHC is decreasing over time and since, as time increases so do the values of the biological measurements, the normalized rate of removal of PHC should decrease with increasing values of biological measurement. Thus, the natural logarithmic model (Equation 5.2) was considered unsuitable for use in the final model.

The normalized "equilibrium" rate constants plotted against root length, root mass, and below-ground biomass and fit with the best fit equations show that the normalized "equilibrium" rate constant increases linearly with increasing root length, root mass, and below-ground biomass. This agrees with the original data of normalized cumulative mass of PHC removed over time presented in Figure 4.10 and therefore this method of determining rate constants was selected to be used in the final model. The below-ground biomass best correlates with the initial data of normalized cumulative mass of PHC degraded (Table 5.1) and with the normalized "equilibrium" rate constants (Figure 5.15). Thus, below-ground biomass was selected to be the plant size index used in the final model.

The final predictive model uses the best fit linear equation to a plot of the normalized "equilibrium" rate constants and below-ground biomass, seen again in Figure 5.16.

Using this model, the cumulative mass removed can be estimated at any time and below-ground biomass using the equation:

$$NCMR = [K * BGB + B]t \qquad [5.5]$$

where

NCMR=cumulative mass PHC removed with respect to mass of contaminated soil (mg_{PHC}/kg_{soil})

K=slope of the normalized cumulative mass of PHC removed over final time interval, constant at 0.052 mg_{PHC}/kg_{soil}*day

BGB=below-ground biomass (g)

B=intercept, constant at 0.18 mg_{PHC}/kg_{soil}*day

t=time (days)

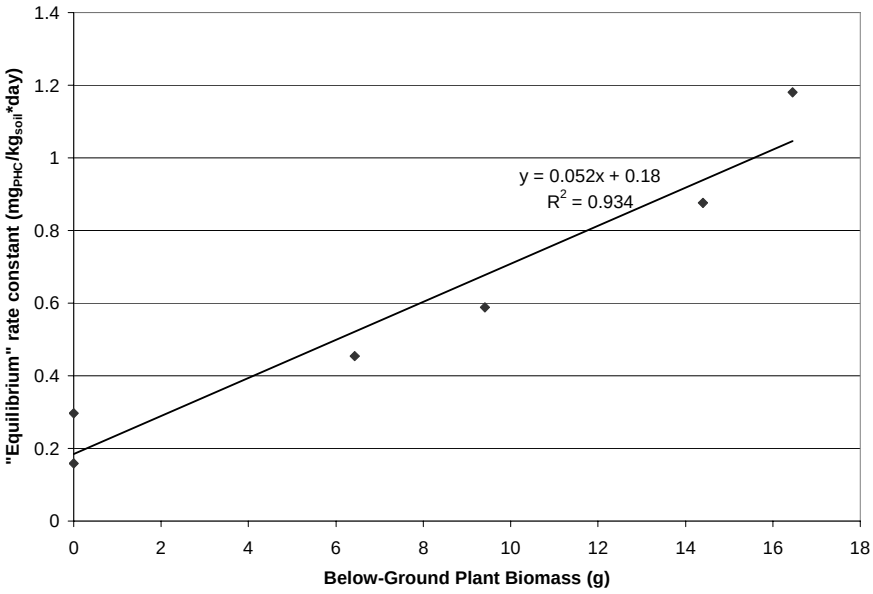

Figure 5.16: Rationally-Based Model for Prediction of Phytoremediation of Diesel-Contaminated Field Soils using Hybrid Poplars

Values of NCMR for the actual and predicted data as well as the R^2 and the RMSE for Figure 5.16 can be seen in Table 5.5.

Table 5.5: Actual and Predicted Values of the Cumulative Mass of PHC Removed over Time Normalized with Respect to the Mass of Contaminated Soil, and values of R^2 and RMSE

$NCMR_{actual}$ (mg_{PHC}/kg_{soil})	$NCMR_{predicted}$ (mg_{PHC}/kg_{soil})	R^2	RMSE
0.59	0.68		
1.18	1.05		
0.88	0.94	0.934	0.089
0.45	0.52		
0.30	0.18		
0.16	0.18		

It must be acknowledged that this model is very preliminary. Due to time constraints the "equilibrium" rate constants may not be at equilibrium, resulting in an over estimation of the mass of contaminant removed from the soil at extrapolated times. However, this model is a staring point to predict phytoremediation in the field and for further research into this area.

Chapter 6: Conclusions and Recommendations

6.1 Overview

To date most phytoremediation research has examined one of two extremes: first, phytoremediation that is well monitored but occurs under artificial conditions, such as in hydroponic growth media, substantially different than expected field conditions; or, second, in-situ phytoremediation that is not well monitored, due to logistical constraints. The purpose of this project was to investigate phytoremediation between these extremes, namely phytoremediation that is well monitored and occurs under controlled laboratory conditions which are reasonably close to field conditions.

Within these constraints, the main objectives of this project were: first, to examine PHC transfer and degradation processes involved in phytoremediation; second, to examine phytoremediation of contaminated field soils compared to natural, intrinsic bioremediation; and, third, using the data collected, to develop a rationally-based model that could be used to predict degradation rates.

To achieve these objectives, a laboratory scale experiment was designed to monitor phytoremediation occurring under simulated field conditions in a closed and controlled laboratory environment.

Experimental test cells were designed to separate the soil and roots from the stem and leaves in order to individually quantify the amount of contaminant degraded microbially, volatilized from soil and phytovolatilized. Each test cell consisted of two chambers, a lower chamber containing the soil and roots and an upper chamber containing the stem and leaves. The lower and upper chambers were sealed from each other at the base of the tree stem and, as each chamber was air tight, they were also sealed from the atmosphere. Lower chambers were attached to a respirometer to measure soil and root respiration and obtain estimated values of the amounts of contaminant degraded microbially. Air sampling tubes were placed downstream of the lower and upper chambers to measure the amount of PHC volatilized from the soil and through the plant.

To simulate field conditions, the experiment modelled pole planting of hybrid poplars into diesel-contaminated field soils. The entire system was placed in an environmental chamber and was exposed to day/night cycles of light and temperature typical of a Canadian summer.

The experiment was initiated on August 12, 2005 and was terminated between March 15 and March 30, 2006. Upon completion of the experiment the test cells were disassembled one at a time and a number of samples were taken and analyzed.

The data obtained over the course of the experiment included: mass of PHC volatilized from the soil, mass of PHC phytovolatilized, O_2 consumption (a surrogate for microbial degradation), initial and final soil conditions (mass of PHC, grain size, moisture content, etc.) and biological measurements.

6.2 Conclusions

Conclusions from this experiment are presented for each of the three main project objectives.

6.2.1 PHC Transfer and Degradation Processes

Monitoring data collected over the duration of the experiment determined the mass of PHC removed for three monitored degradation pathways: volatilization from soil, phytovolatilization and microbial degradation,.

Based on the monitoring data collected, it is concluded microbial degradation had the largest influence on the removal of diesel from the soil when compared to volatilization from soil and phytovolatilization. For cells with trees the percentage of the total mass of contaminant degraded microbially was between 96.3 and 98.7%, the percentage of the total mass of contaminant volatilized from soil was between 0.9 and 2.5% and the percentage of the total mass of contaminant phytovolatilized was between 0.4 and 1.6%.

Although microbial degradation, volatilization from soil and phytovolatilization were monitored, other PHC transformation and degradation processes were not. These processes were: cometabolism of PHC by microbes, degradation of PHC by root exudates, storage and transformation of contaminant within the plant, sorbtion to roots and other organic matter in the soil, conversion to new biomass and humus, and small amounts of PHC degradation by anaerobic bacteria. These processes would have removed PHC from the soil but were not accounted for though any of the pathways being monitored.

Another limitation to monitoring PHC transfer and degradation processes was the lower limit of PHC identification from GC analysis of soils and air sampling tubes. The lower limit of identification was imposed by the desorbing solvent and the lightest identifiable hydrocarbon standard. In this experiment the desorbing solvents used were CS_2 and toluene and the hydrocarbon standards used were nC6, nC10, nC16 and nC34. Chromatograms of hydrocarbon standards in CS_2 show nC6 as a distinct standard peak near the solvent peak and chromatograms of hydrocarbon standards in toluene show nC10 as a distinct standard peak near the solvent peak. Therefore, upon processing the chromatograms, PHC equivalent to or heavier than nC6 were quantified in soils and air sampling tubes extracted with CS_2 and PHC equivalent to or heavier than nC10 were quantified in soils and air sampling tubes extracted with toluene. This lower limit of identification may have resulted in an underestimation of the mass of PHC volatilized from the soil and phytovolatilized as PHC lighter than nC6 would not be quantified in soils and air sampling tubes extracted with CS_2 and PHC lighter than nC10 would not be quantified in soils and air sampling tubes extracted with toluene.

6.2.2 Phytoremediation Compared to Natural Intrinsic Bioremediation

Monitoring data collected over the duration of the experiment showed that a greater mass of contaminant was removed from the soil in the presence of plants compared to the absence of plants. The percent of the total mass removed based on the initial mass of PHC and the monitored mass removed was between 8 and 28% with phytoremediation and 6% (for both test cells without plants) with bioremediation only.

6.2.3 Development of a Rationally-Based Model to Predict Phytoremediation

Monitoring data and biological measurements of the hybrid poplars were used to develop a rationally-based model for prediction of phytoremediation. First, the total mass of PHC removed, normalized with respect to the mass of contaminated soil, was compared to root length, root mass, below-ground plant biomass, above-ground plant biomass, total plant biomass, and total biomass. The Pearson correlation coefficient (r), standard error of the correlation coefficient (S.E. of r), and probability that the Pearson correlation coefficient is equal to 0 [P(r=0)] were determined for the data. In decreasing magnitude of correlation at $P(r=0) \leq 0.05$, were root length, below-ground biomass, root mass, total biomass and total plant biomass were found to correlate significantly. Correlation with above-ground biomass was not significant.

Second, rate constants were determined for each test cell using two different methods. The first fit a number of mathematical models to the normalized cumulative mass of PHC removed over time for each container and identified the rate constant from the best fit model. The second method identified the "equilibrium" normalized rates of removal of PHC for each test cell.

Next, the rate constants obtained using each method were plotted against the three most significant biological measurements: root length, root mass, and below-ground biomass and, based on these plots, the best method of determining rate constants was selected to be used in the final model (Figure 5.15).

There are a couple limitations to the model that must be emphasized. The first, and perhaps most obvious, limitation is the short time period over which the experiment took place. The second limitation, which is related to the first, is the small size of the trees, i.e. low biomass values.

Although it was assumed that each test cell was under equilibrium conditions, this may have not been true. Had the experiment continued, different "equilibrium" conditions may have resulted and the predictive model would be slightly different, most likely with a smaller *K* constant due to decreasing rates of the mass of PHC removed over time.

Low biomass values, also related to the short period of time over which the experiment took place, may have resulted in unexpected variability in the results. During the course of the experiment a number of leaves died and were removed from the experimental containers. As the dry leaf mass makes up between 16 and 37% of above-ground plant biomass, removing leaves may have resulted in biased results.

6.3 Recommendations

A number of recommendations can be made based on the results of this project, both for the application of the rationally-based model in the field and for future work.

In applying the rationally-based model for prediction of phytoremediation of diesel contaminated soils, it is recommended that the model be used to estimate PHC removal rates over time under similar field conditions. Although field monitoring data may be compared to this "expected" behaviour to evaluate the model at full scale and under field

conditions, it must be recognized that the model was a result of a laboratory experiment and that, while the experiment simulated field conditions, many field conditions are inherently variable and, therefore, impossible to simulate.

Recommendations for future work include performing longer-term and larger-scale experiments, using intact soil samples from the field, increasing the number of experimental cells, and using uncontaminated controls of the same soil. While future work is recommended for each of these situations individually, any or all combinations would contribute to phytoremediation research.

Longer-term experiments would address the limitations of the present predictive model, give an indication of degradation rates over a greater percentage of the total life of the tree, and increase the percentage of stem mass contributing to above-ground plant biomass so that small variations in leaf mass would not be as significant. Increasing the duration of the experiment would necessitate increasing the size of the experimental cells to accommodate larger trees.

The use of intact soil samples from the field would more closely replicate field conditions by maintaining the soil structure and reducing soil placement effects resulting from soil homogenization prior to placement.

Increasing the number of experimental cells would add information that may influence the predictive model.

Lastly, the use of uncontaminated controls of the same soil would provide an excellent point of reference to compare phytoremediation and intrinsic bioremediation of contaminated soil with the same properties and from the same location.

References

Agriculture and Agri-food Canada**,** Prairie Farm Rehabilitation Centre (PRFA) website. http://www.agr.gc.ca/pfra/shelterbelt/shbpub7.htm. Accessed July 13, 2006.

Alexander, M., 1995. How toxic are toxic chemicals in soil? Environmental Science and Technology. 29(11): 2713-2717.

Alkorta, I., Garbisu, C., 2001. Phytoremediation of organic contaminants in soils. Bioresource Technology. 79: 273-276.

Allison, L., 1965. Organic Carbon. Methods of Soil Analysis Part 2. American Society of Agronomy. Madison, WI. 1367-1378.

Alvarez-Cohen, L., McCarthy, P., Roberts, P., 1993. Sorbtion of trichloroethylene onto a zeolite accompanied by methanotrophic biotransformation. Environmental Science and Technology. 27: 2141-2148.

American Society for Testing and Materials (ASTM), 2002. ASTM D422-63: Standard test method for particle-size analysis of soils. Annual Book of ASTM Standards 04.08).

Anderson, T.A., Guthrie, E.A., Walton, B.T. 1993. Bioremediation in the rhizosphere. Environmental Science and Technology. 27(13): 2630-2636.

Aronstein, B., Calvillo, Y., Alexander, M., 1991. Effect of surfactants at low concentrations on the desorption and subsequent biodegradation of sorbed aromatic contaminants in soil. 25: 1728-1731.

Bossert, I., Berta., A.S., 1994. 'Hydrocarbons in soil ecosystems', in. Petroleum Microbiology. Atlas, R.M. (editor). MacMillan Pub. 453-474.

Bregnard, T., Höhener, P., Häner, A., Zeyer, J., 1996. Degradation of weathered diesel fuel by microorganisms from a contaminated aquifer in aerobic and anaerobic microcosms. Environmental Toxicology and Chemistry. 15(3): 299-307.

Briggs, G.G., Bromilow, R.H., Evans, A.A., 1982. Relationships between lipophilicity and root uptake and translocation of non-ionized chemicals by barley. Pesticide science, 13: 495-504.

Burken, J., Ross, C., Harrison, L., Marsh, A., Zetterstrom, L., Gibbons, J. 2001. Benzene toxicity and removal in laboratory phytoremediation studies. Practice Periodical of Hazardous, Toxic, and Radioactive Waste Management. 5(3): 161-171.

Burken, J.G., Schnoor, J.L., 1996. Phytoremediation: plant uptake of atrazine and role of root exudates. Journal of Environmental Engineering. 122(11): 958-963.

Burken, J.G., Schnoor, J.L., 1998. Predictive relationships for uptake of organic contaminants by hybrid poplar trees. Environmental Science and Technology 32: 3379-3385.

Canadian Council of Ministers of the Environment, 2001. Reference method for the Canada-wide standard for petroleum hydrocarbons in soil-tier 1. http://www.ccme.ca/assets/pdf/final_phc_method_rvsd_e.pdf. Accessed August 1, 2005.

Chapelle, F.H., 1992. Ground-water microbiology and geochemistry. John Wiley and Sons, Inc. 424 p.

Chiou, C., Sheng, G., Manes, M., 2001. A partition-limited model for the plant uptake of organic contaminants from soil and water. Environmental Science and Technology. 35(7): 1437-1444.

Columbus Instruments, 2002. Micro-Oxymax Respirometer Manual. 99 p.

Cunningham, S.D., Berti, W.R. 1993. Remediation of contaminated soil with green plants: an overview. In Vitro Cellular and Developmental Biology. 29P: 207-212.

Curl, E.A., Truelove, B., 1986. The Rhizosphere. Singer-Verlag. 288 p.

Davis, G., Johnston, C., Patterson, B., Barber, C., Bennett, M., 1998. Estimation of biodegradation rates using respiration tests during in situ bioremediation of weathered diesel NAPL. Ground Water Monitoring and Remediation. 18(2): 123-132.

Delille, D., Coulon, F., Pelletier, E., 2004. Effects of temperature warming during a bioremediation study of natural and nutrient-amended hydrocarbon-contaminated sub-Antarctic soil. Cold Regions Science and Technology. 40: 61-70.

Dibble, J.T., Bartha, R., 1979. Effect of environmental parameters on the biodegradation of oil sludge. Applied Environmental Microbiology. 37: 729-739.

Domenico, P.A., Schwartz, W., 1997. Physical and chemical hydrogeology, 2nd edition. John Wiley and Sons, Inc. 506 p.

Donahue, R., Miller, R, Shickluna, J., 1983. Soils: an introduction to soils and plant growth. Prentice-Hall, Inc. 667 p.

Downey, D., Guest, P., Ratz, J., 1995. Results of a two-year in situ bioventing demonstration. Environmental Progress. 14:.121-125.

Dupont, R., 1993. Fundamentals of bioventing applied to fuel contaminated sites. Environmental Progress. 12(1): 45-53.

Eweis, J.B., Ergas, S.J., Chang, D.P.Y., Schroeder, E.D., 1998. Bioremediation principles. McGraw-Hill, Inc. 296 p.

Fetter, C.W., 1994. Applied Hydrology, 3rd edition. Prentice-Hall, Inc. 691 p.

Farrell, R.E., Frick, C.M., Germida, J.J., 2000. PhytoPet — A Database of Plants that Play a Role in the Phytoremediation of Petroleum Hydrocarbons. http://www.phytopet.usask.ca/mainpg.php. Accessed July 13, 2006

Gibb, A., Chu, A., Wong, R.C.K., Goodman, R.H. 2001. Bioremediation kinetics of crude oil at 5°C. Journal of Environmental Engineering. 127(9): 818-824.

Gillman, G.P., Sumpter, E.A., 1986. Modification to the compulsive exchange method for measuring exchange characteristics of soils. Australian Journal of Soil Research. 24(1):61-66.

Glick, B.R., 2003. Phytoremediation: synergistic use of plants and bacteria to clean up the environment. Biotechnology Advances. 21: 383-393.

Glynn, C., Herms, D.A., Egawa, M., Hansen, R., Mattsen, W.J., 2003. Effects of nutrient availability on biomass allocation as well as constitutive and rapid increased herbivore resistance in poplar. OIKOS. 101:385-397.

Greenburg, A.E., Clesceri, L.S., Eaton, A.D., 1992. Standard Methods for the Examination of Water and Wastewater, 18th Edition. Washington D.C. American Public Health Association.

Gunasekara, A., Xing, B., 2003. Sorption and desorption of naphthalene by soil organic matter: importance of aromatic and aliphatic components. Journal of Environmental Quality. 32: 240-246.

Hanson, P.J., Edwards, N.T., Garten, C.T., Andrews, J.A., 2000. Separating root and soil microbial contributions to soil respiration: A review of methods and observations. Biogeochemistry. 48: 115-146.

Hassett, J.J., Banwart, W.L., Wood, S.G., Means, J.C., 1981. Sorption of α-napthol: Implications concerning the limits of hydrophobic sorption. Soil Science Society of America Journal. 45: 38-42.

Hatzinger, P.B., Alexander, M., 1996. Effect on aging of chemicals in soil on their biodegradability and extractability. Environmental Soil Science. 29: 537-545.

Hinchee, R., Ong, S., 1992. A rapid in-situ respirometer test for measuring aerobic biodegradation rates of hydrocarbons in soil. Journal of Air and Waste Management Association. 42(10): 1305 - 1312.

Hrapovic, L., Rowe, K., 2002. Intrinsic degradation of volatile fatty acids in laboratory-

compacted clayey soil. Journal of Contaminant Hydrogeology. 58: 221-242.

Huang, W., Peng, P., Yu, Z., Fu, J., 2003. Effects of organic matter heterogeneity on sorption and desorption of organic contaminants by soils and sediments. Applied Geochemistry. 18: 955-972.

Joner, E., Hirmann, D., Szolar, O., Todorovic, D., Leyval, C., Loibner, A., 2004. Priming effects on PAH degradation and ecotoxicity during a phytoremediation experiment. Environmental Pollution. 128: 429-435.

Jordahl, J., Foster, L., Schnoor, J., Alvarez, P. 1997. Effect of hybrid poplar trees on microbial populations important to hazardous waste bioremediation. Environmental Toxicology and Chemistry. 16(6): 1318-1321.

Karickhoff, S.W., Brown, D.S., Scott, T.A., 1979. Sorption of hydrophobic pollutants on natural sediments. Water Research. 13(3): 249-254.

Kim, J., Sung, K., Yavuz Corapcioglu, M., Drew, M., 2004. Solute transport and extraction by a single root in unsaturated soils: model development and experiment. Environmental Pollution. 131: 61-70.

Leahy, J.G., Colwell, R.R., 1990. Microbial degradation of hydrocarbons in the environment. Microbiological Reviews. 54(3): 305-315.

Lyman, W.J., Reidy, P.J., Levy, B., 1992. Mobility and degradation of organic contaminants in subsurface environments. C.K. Smoley, Inc. 395 p.

Ma, X., Richter, A.R., Albers, S., Burken, J.G., 2004. Phytoremediation of MTBE with hybrid poplar trees. International Journal of Phytoremediation. 6(2): 157-167.

Margesin, R., 2000. Potential of cold-adapted microorganisms for bioremediation of oil-polluted Alpine soils. International Biodeterioration and Biodegradation. 46: 3-10.

McCarty, P.L., Reinhart, M., Rittmann, B.E., 1981. Trace organics in groundwater. Environmental Science and Technology. 15(1): 40-51.

McKeague, J., Ed., 1976. Manual on Soil Sampling and Methods of Analysis. Subcommittee (of Canada Soil Survey Committee) on Methods of Analysis. Soil Research Institute. 212 p.

Nash, R.G., Woolson, E.A., 1967. Persistence of chlorinated hydrocarbon insecticides in soil. Science. 157(3791): 924-927.

Ogram, A, Jessup, R., Ou, L., Rao, P., 1985. Effects of sorption on biological

degradation rates of (2,4-dichlorophenoxy) acetic acid in soils. Applied and Environmental Microbiology. 49: 582-587.

Orchard, B.J., Doucette, W.J., Chard, J.K., Bugbee, B., 2000. Uptake of trichloroethylene by hybrid poplar trees grown hydroponically in flow through plant growth chambers. Environmental Toxicology and Chemistry. 19(4): 895-903.

Park, J., Kay, D., Zhao, X., Boyd, S., Voice, T., 2001. Kinetic modeling of bioavailability for sorbed-Phase 2,4-dichlorophenoxyacetic acid. Journal of Environmental Quality. 30: 1523-1527.

Pignatello, J.J., Xing, B., 1996. Mechanisms of slow sorption of organic chemicals to natural particles. Environmental Science and Technology. 30(1): 1-11.

Ramaswami, A., Rubin, E., 2001. Measuring phytoremediation parameters for volatile organic compounds: focus on MTBE. Practical Periodical of Hazardous, Toxic and Radioactive Waste Management. 5(3): 123-129.

Rendig, V.V., Taylor, H.M., 1989. Principals of plant-soil interrelationships. McGraw-Hill, Inc. 275 p.

Reid, B.J., Northcott, G.L., Jones, K.C., Semple, K.T., 1998. Evaluation of spiking procedures for the introduction of poorly water soluble contaminants into soil, Environmental Science & Technology. 32(20): 3224-3227.

Riser-Roberts, E. 1998. Remediation of petroleum contaminated soils: biological, physical and chemical processes. Boca Raton, FL. Lewis Publishers. 542 p.

Ross, D.S., Recommended Methods for Determining Soil Cation Exchange Capacity. http://ag.udel.edu/extension/agnr/pdf/soiltesting/CHAP9-95.pdf. Accessed July 15, 2006.

Salt, D.E., Smith, R.D., Raskin, I., 1998. Phytoremediation. Annual Reviews of Plant Physiology and Molecular Biology. 49: 643-648.

Schwab, A., Su, J., Wetzel, S., Pekarek, S., Banks, M., 1999. Extraction of petroleum hydrocarbons from soil by mechanical shaking. Environmental Science and Technology. 33(11): 1940-1945.

Schwarzenbach, R.P., Westall, J., 1981. Transport of nonpolar organic compounds from surface water to groundwater. Laboratory sorption studies. Environmental Science and Technology. 15(11): 1360-1367.

Schnoor, J.L., Licht, L.A., McCutcheon, S.C., Wolfe, N.L., Carreira, L.H. 1995.

Phytoremediation of organic contaminants. Environmental Science and Technology. 29: 318A-323A.

Sharer, M., Park, J., Voice, T, Boyd, S., 2003. Organic compounds in the environment: aging effects on the sorption-desorption characteristics of anthropogenic compounds in soil. Journal of Environmental Quality. 32: 1385-1392.

Siciliano, S.D., Germida, J.J. 1998. Mechanisms of phytoremediation: biochemical and ecological interactions between plants and bacteria. Environmental Review. 6: 65-79.

Swarmy, S.L., Mishra, A., Puri, S., 2006. Comparison of growth, biomass and nutrient distribution in five promising clones of Populus deltoids under a agrisiliviculture system. Bioresource Techology. 97(1): 57-68.

Tan, K.H., 1994. Environmental Soil Science. Marcel Dekker, Inc. 225p.

Tumeo, M.A., Guinn, D.A., 1997. Evaluation of bioremediation in cold regions. Journal of Cold Regions Engineering. 11(3): 221-231.

W. A. Hammond Drierite® Product Catalogue, Indicating Drierite®. www.drierite.com/default.cfm. Accessed July 4, 2006.

Wullscheger, S.D., Yin, T.M., DiFazio, S.P., Tschaplonski, T.J., Gunter, L.E., Davis, M.F., Tuskan, G.A., 2005. Phenotypic variation in growth and biomass distribution for two advanced-generation pedigrees of hybrid poplar. Canadian Journal of Forest Research. 35(8): 1779-1789.

Zynter, R.G., Salb, A., Brook, T.R., Leunissen, M., Stiver, W.H., 2001. Bioremediation of diesel contaminated soil. Canadian Journal of Civil Engineering. 28(1) Supplement: 131-140.

Appendix A: Drawings

This Appendix contains working drawing of the experimental test cells, diagrams of the initial and final soil configurations of the experimental test cells and, in a separate file, the measurements taken to determine the initial and final soil configurations and densities.

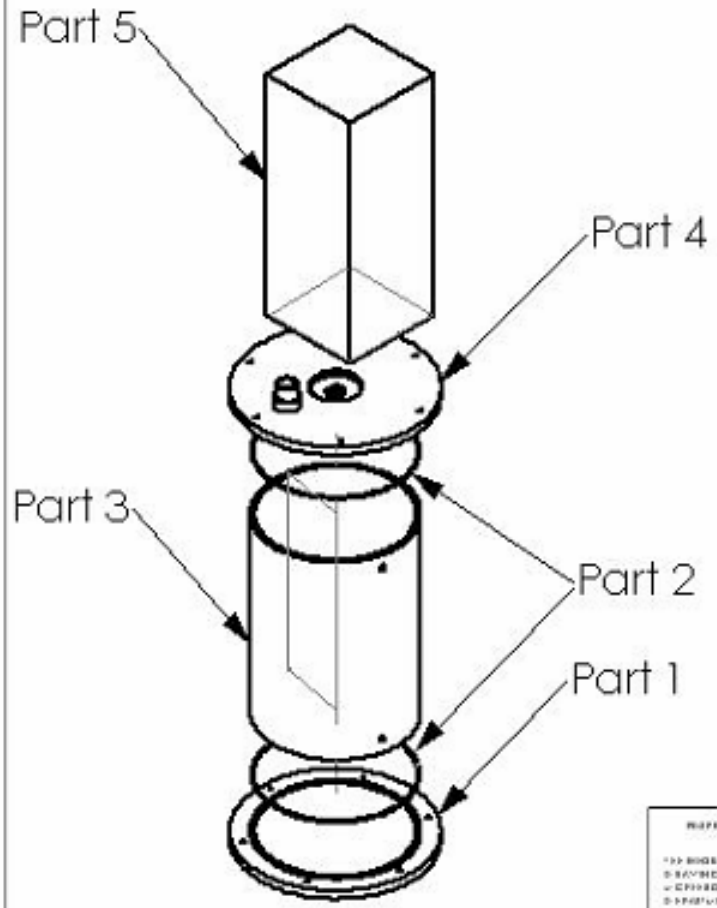

Note: The lower chamber (Parts 1-4) was held together by six steel rods running through six sets of holes from Part 1to Part 4. Each rod had a bolt permanenty attached to one end and was threaded at the other. The bolt was flush to Part 1 and a thumbscrew was tightened flush to Part 4.

		TITLE: Exploded Assembly
	PVC and Acrylic	Alexis McPherson
	--	26/02/07
	SOLIDWORKS DRAWING	SIZE A, DWG. NO. 1-5, REV.

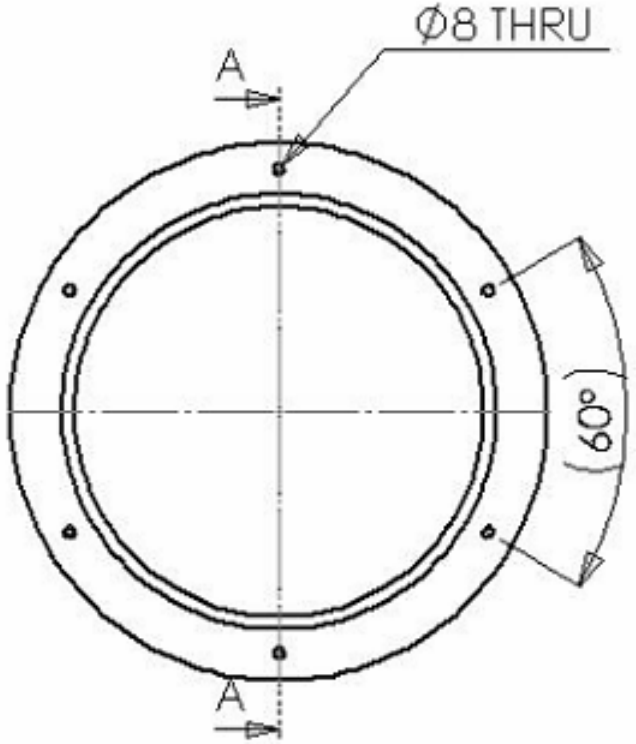

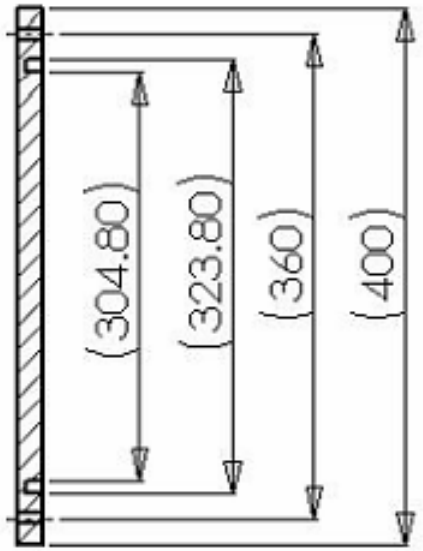

A-A

	TITLE: Lower PVC Plate
PVC	Alexis McPherson
--	26/02/07
	A 1

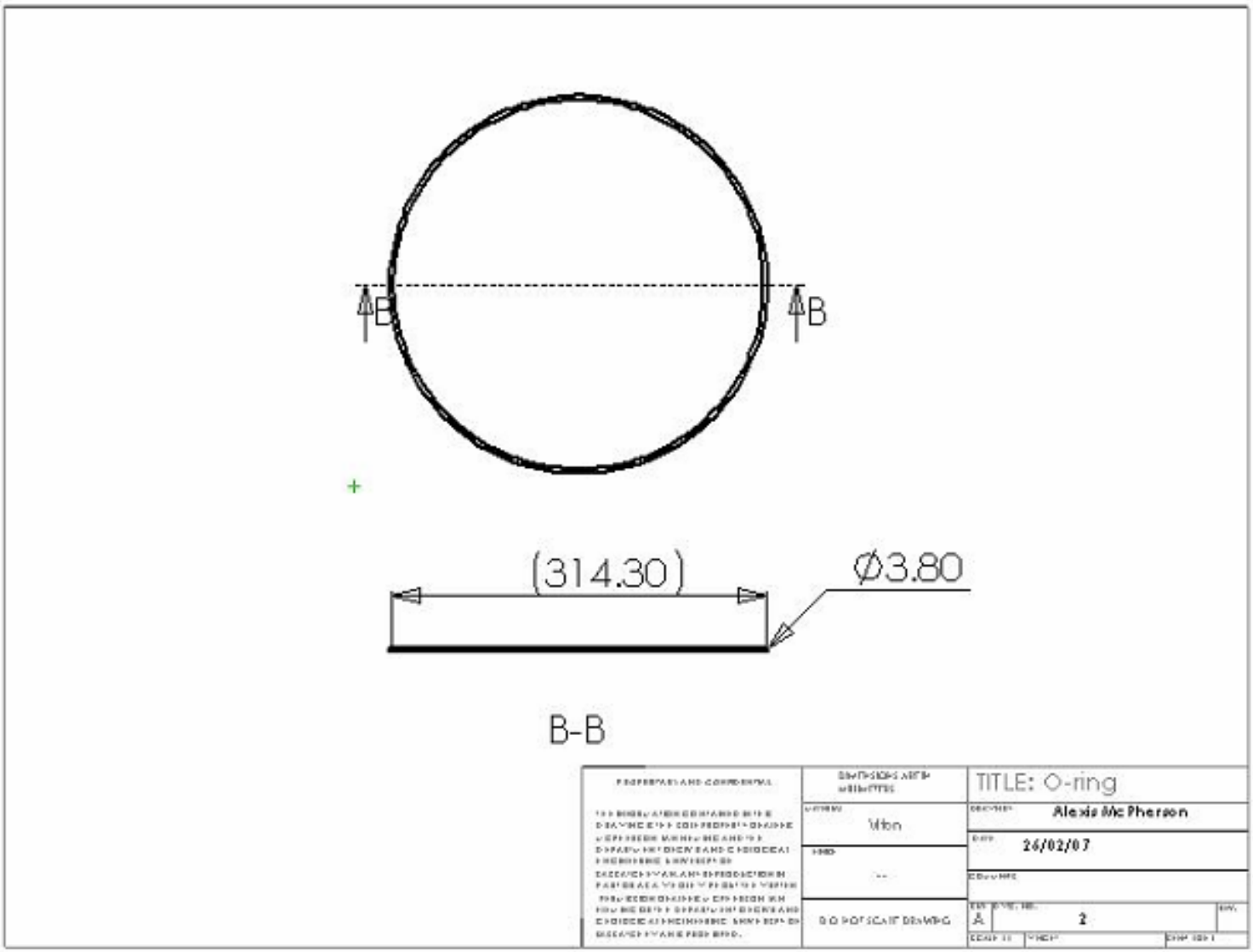
B
B
(314.30)
Ø3.80
B-B
TITLE: O-ring
Alexis Mc Pherson
26/02/07
Viton
--
A
2

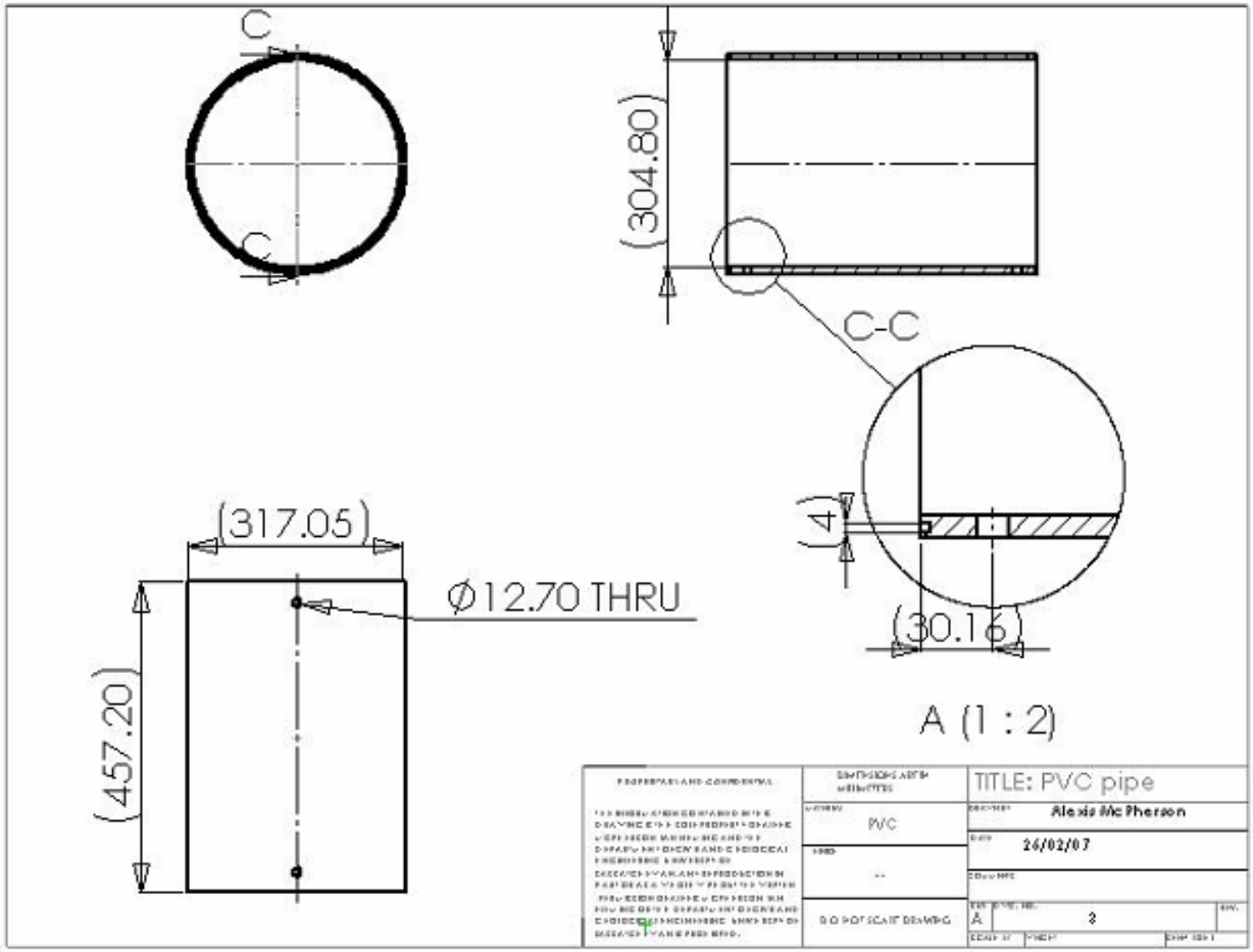
C
C
(304.80)
C-C
4
(30.16)
(317.05)
Ø12.70 THRU
(457.20)
A (1 : 2)
TITLE: PVC pipe
Alexis Mc Pherson
24/02/07
PVC
--
A
3

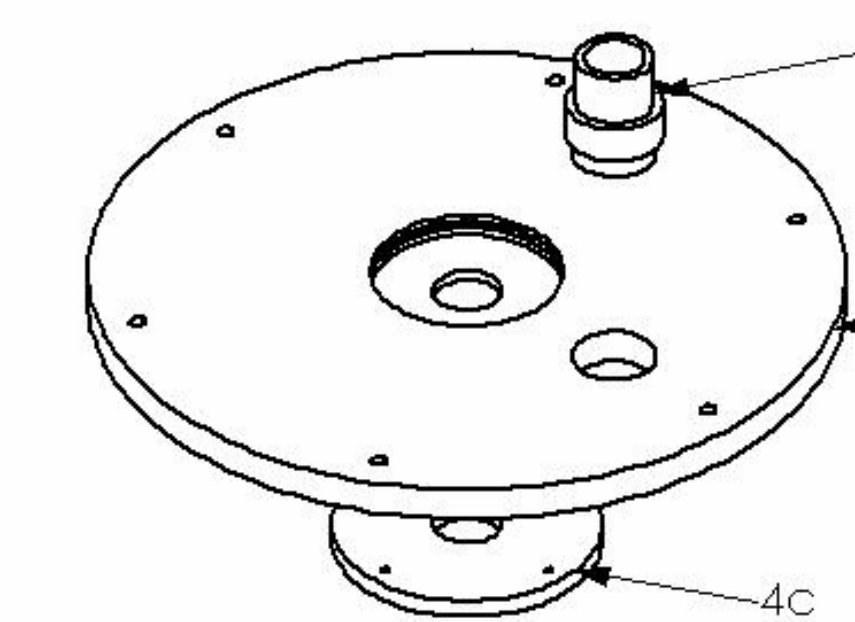

Note: Part 4a was glued to Part 4b. Part 4c was attached to Part 4b with four screws. A plastic fuel spout was placed through the centre holes of Parts 4b and 4c. Part 4d was then attached to Part 4c with three screws to attach and seal the plastic fuel spout.

PROPRIETARY AND CONFIDENTIAL THE INFORMATION CONTAINED IN THIS DRAWING IS THE SOLE PROPERTY OF [illegible]. ANY REPRODUCTION IN PART OR AS A WHOLE WITHOUT THE WRITTEN PERMISSION OF [illegible] IS PROHIBITED.	DO NOT SCALE DRAWING	TITLE: Upper PVC Plate DRAWN: Alexis Mc Pherson DATE: 26/02/07 SIZE: A DWG. NO.: 4 REV:
	MATERIAL: PVC FINISH: --	

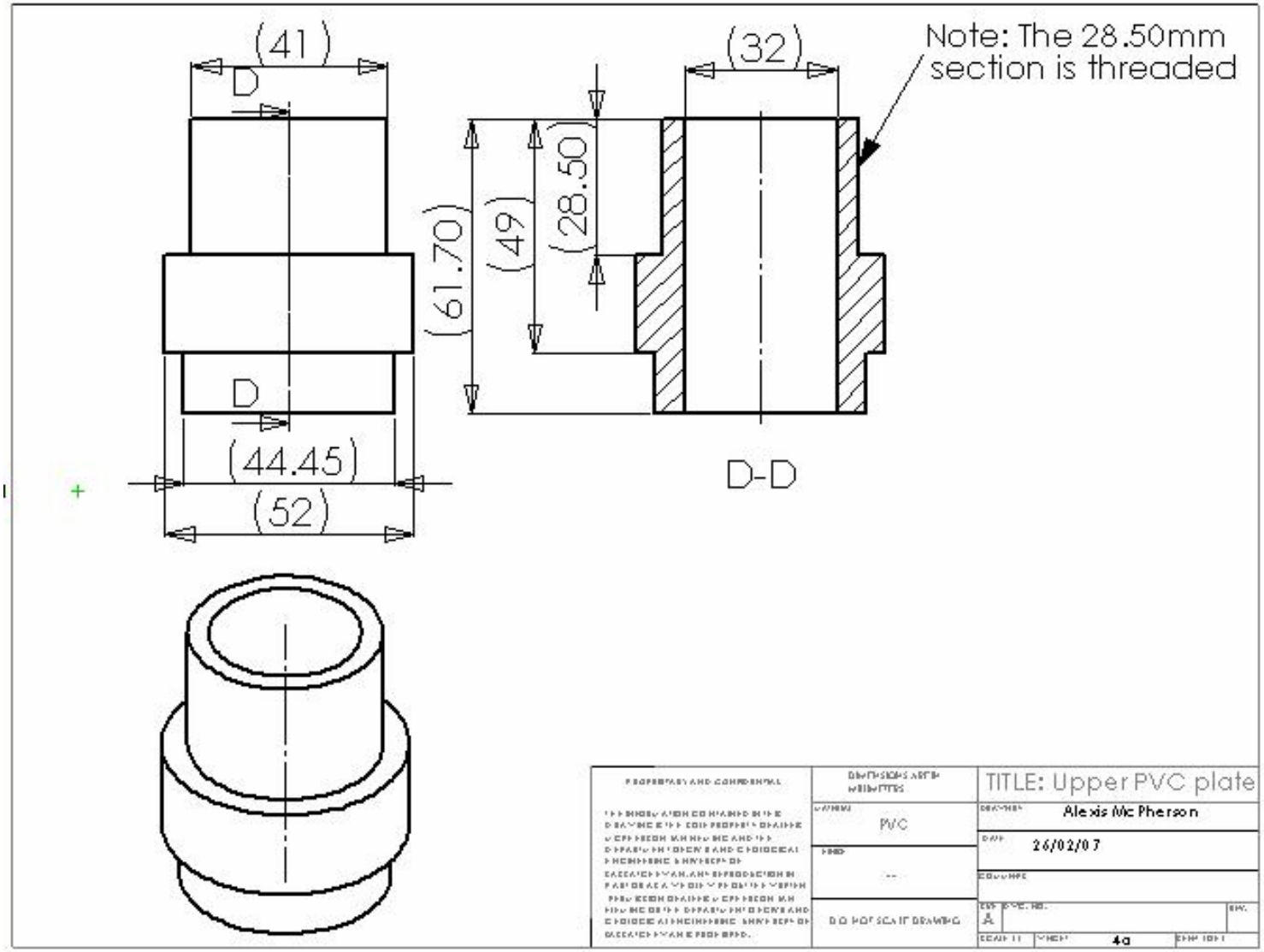
(41)
D
D
(44.45)
(52)
(32)
(61.70)
(49)
(28.50)
Note: The 28.50mm section is threaded
D-D
PROPRIETARY AND CONFIDENTIAL
DIMENSIONS ARE IN MILLIMETERS
PVC
--
DO NOT SCALE DRAWING
TITLE: Upper PVC plate
Alexis Mc Pherson
26/02/07
A
4a

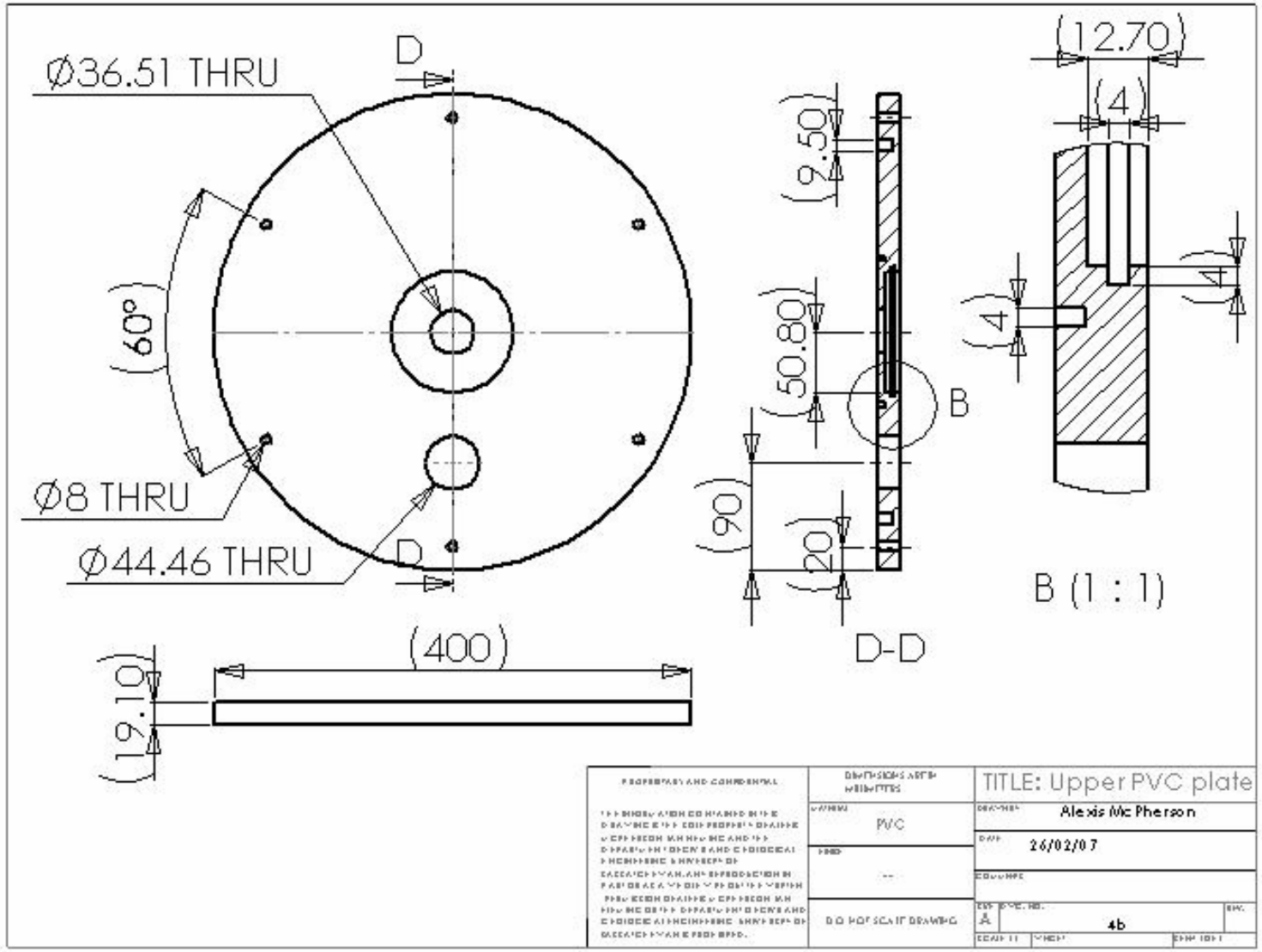
Ø36.51 THRU
D
60°
Ø8 THRU
Ø44.46 THRU
D
(400)
(19.10)
(9.50)
(50.80)
(90)
(20)
B
D-D
(12.70)
(4)
(4)
(4)
B (1 : 1)
DIMENSIONS ARE IN MILLIMETERS
PVC
--
DO NOT SCALE DRAWING
TITLE: Upper PVC plate
Alexis Mc Pherson
26/02/07
A
4b

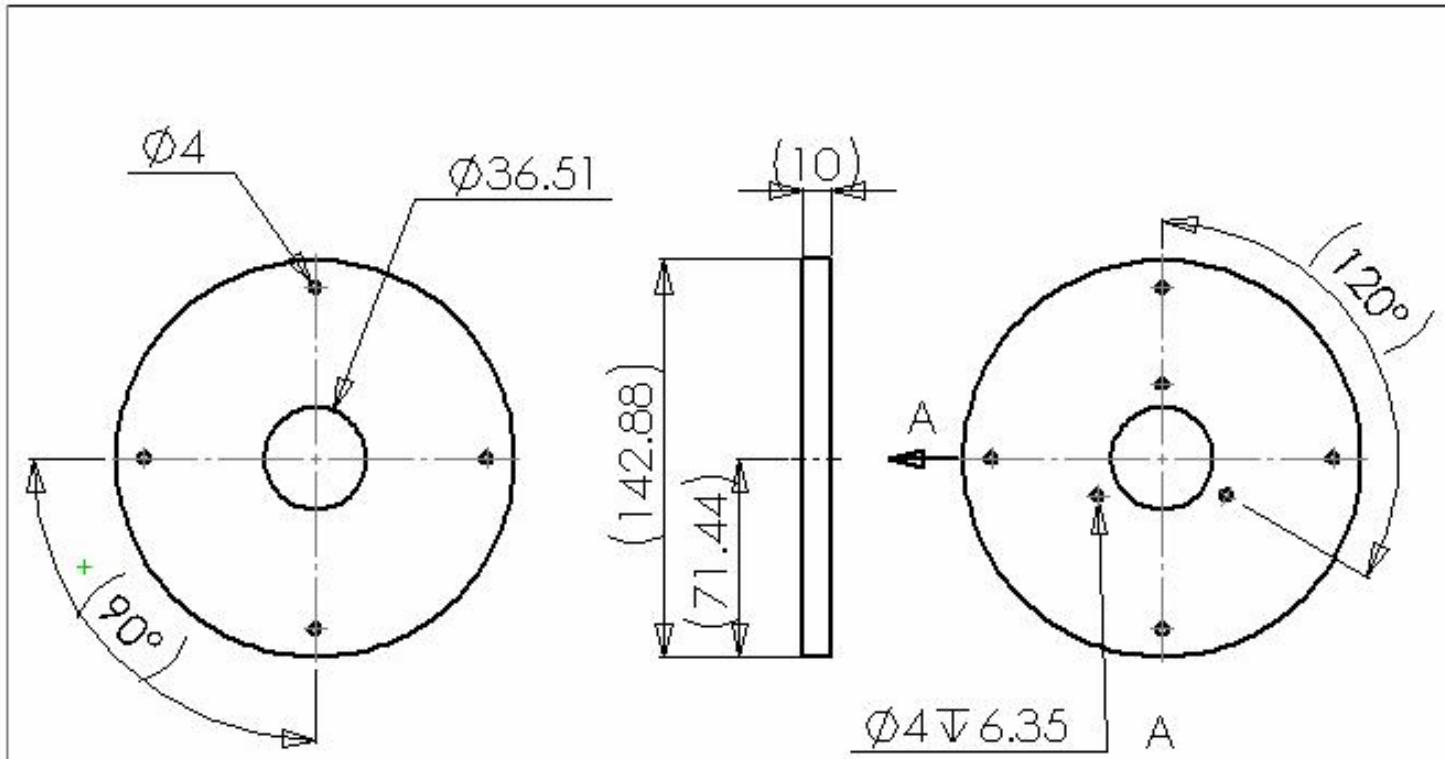

PROPRIETARY AND CONFIDENTIAL	DIMENSIONS ARE IN MILLIMETERS	TITLE: Upper PVC plate
	MATERIAL: PVC	DRAWN: Alexis Mc Pherson
	FINISH: --	DATE: 26/02/07
	DO NOT SCALE DRAWING	COMMENTS:
		DWG. NO.: A — REV.
		SCALE: 1/1 — SHEET: 4c — SIZE: A4

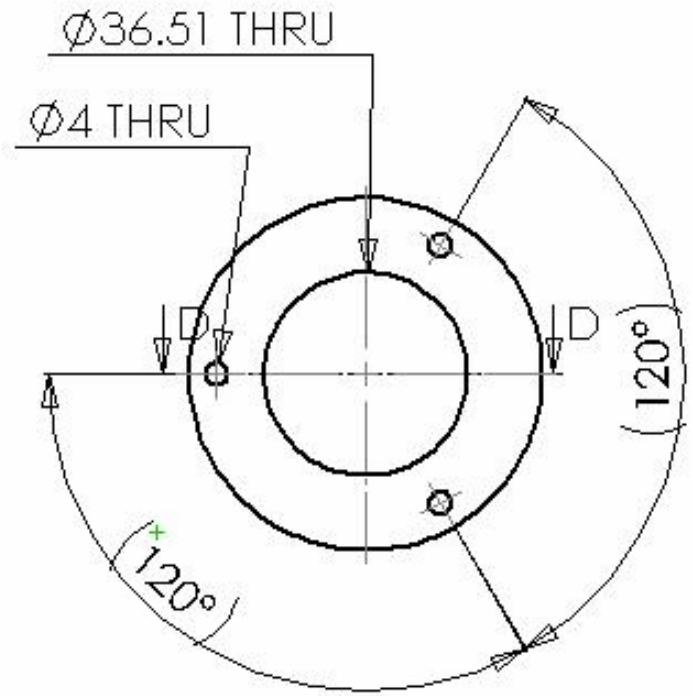

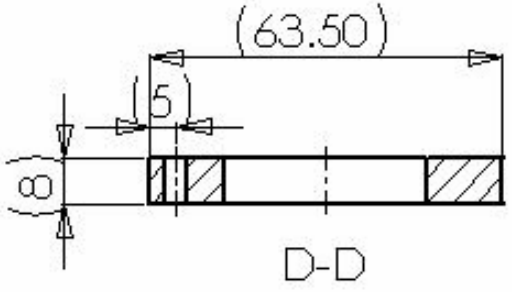

PROPRIETARY AND CONFIDENTIAL	DIMENSIONS ARE IN MILLIMETERS	TITLE: Upper PVC plate
	MATERIAL: PVC	DRAWN: Alexis Mc Pherson
	FINISH: --	DATE: 26/02/07
	DO NOT SCALE DRAWING	SIZE: A, DWG. NO.: 4d, REV.
		SCALE: 1:1, SHEET, DWG NO.

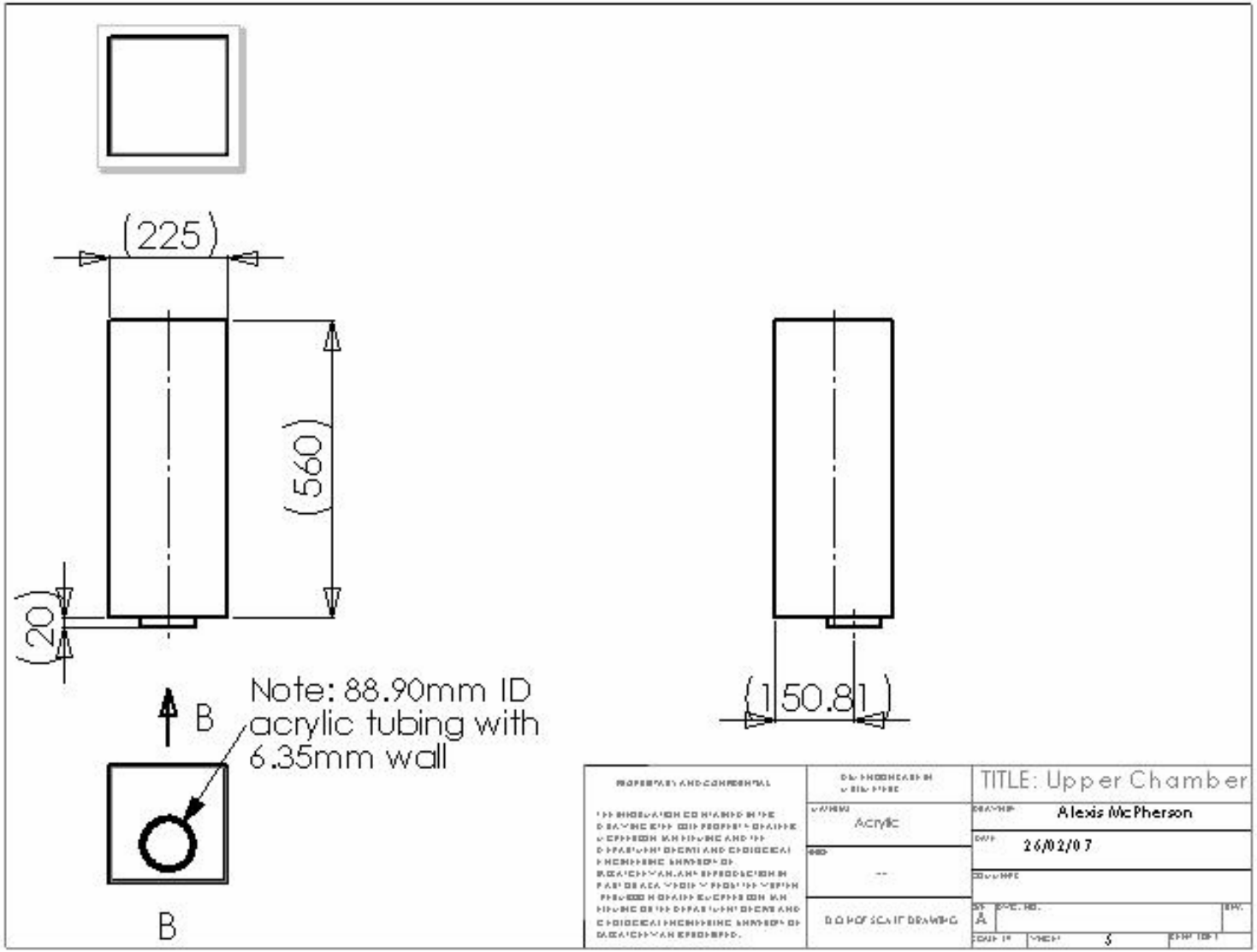
(225)
(560)
(20)
B
B
Note: 88.90mm ID
acrylic tubing with
6.35mm wall
(150.81)
TITLE: Upper Chamber
Alexis McPherson
26/02/07
Acrylic
--
A

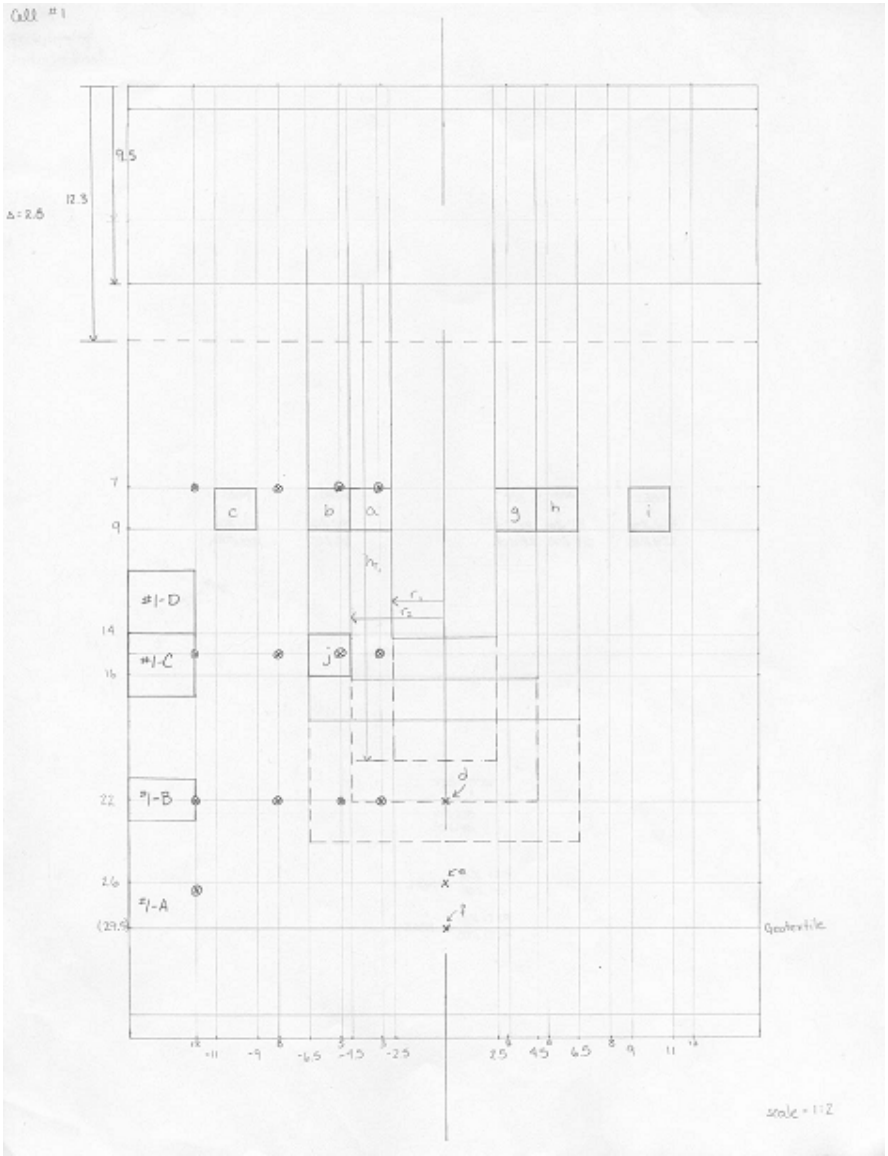
Cell #1
9.5
12.3
Δ = 2.8
7
9
14
16
22
26
(29.9)
c
b
a
g
h
i
j
#1-D
#1-C
#1-B
#1-A
Geotextile
-11
-9
-6.5
-4.5
-2.5
2.5
4.5
6.5
9
11
scale = 1:2

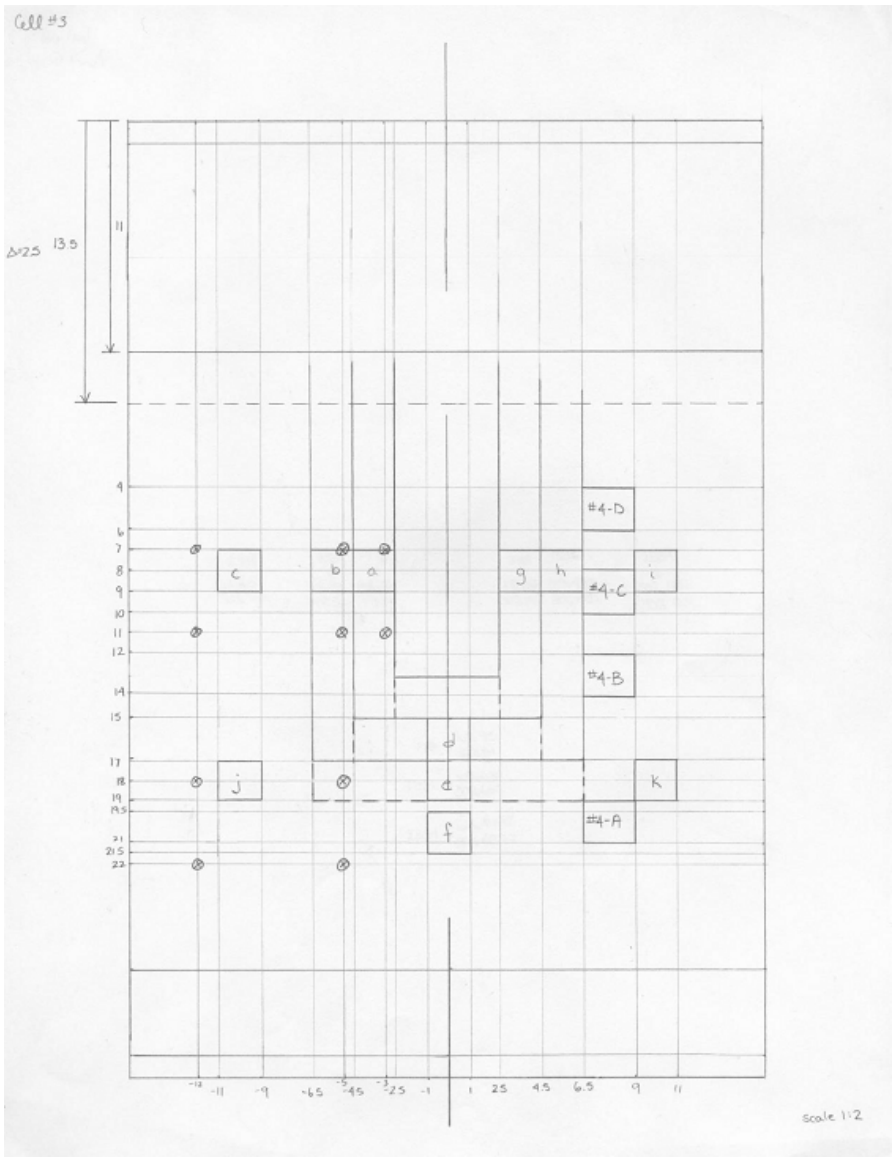
Cell #3
Δ=2.5
13.5
11
4
6
7
8
9
10
11
12
14
15
17
18
19
19.5
21
21.5
22
#4-D
#4-C
#4-B
#4-A
a
b
c
d
e
f
g
h
i
j
K
-12
-11
-9
-6.5
-5
-4.5
-3
-2.5
-1
1
2.5
4.5
6.5
9
11
scale 1:2

Gel #4

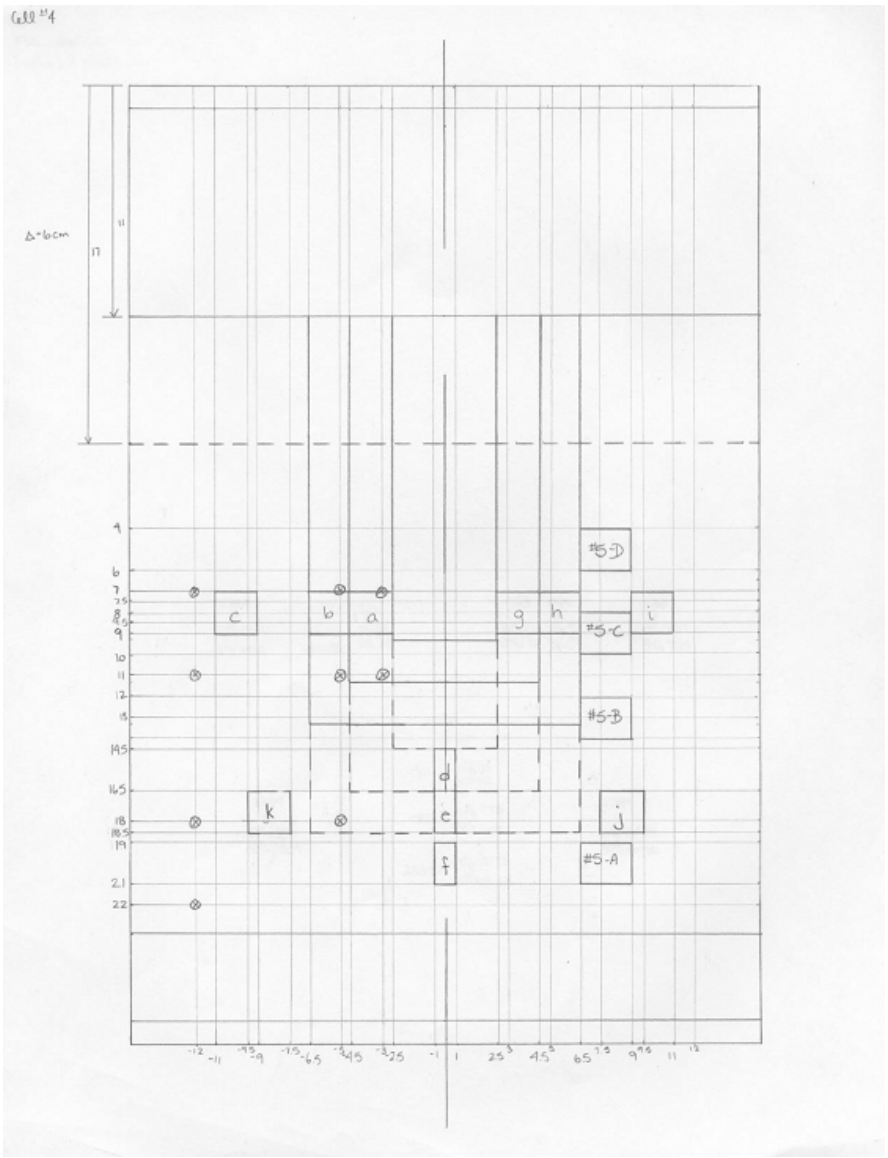
Δ-6cm
11
4
6
7
7.5
8
8.5
9
10
11
12
13
14.5
16.5
18
18.5
19
21
22
a
b
c
d
e
f
g
h
i
j
k
#5-D
#5-C
#5-B
#5-A
-12
-11
-9.5
-9
-7.5
-6.5
-4.5
-3.5
-2.5
-1
1
2.5
3
4.5
5
6.5
7.5
9
9.5
11
12

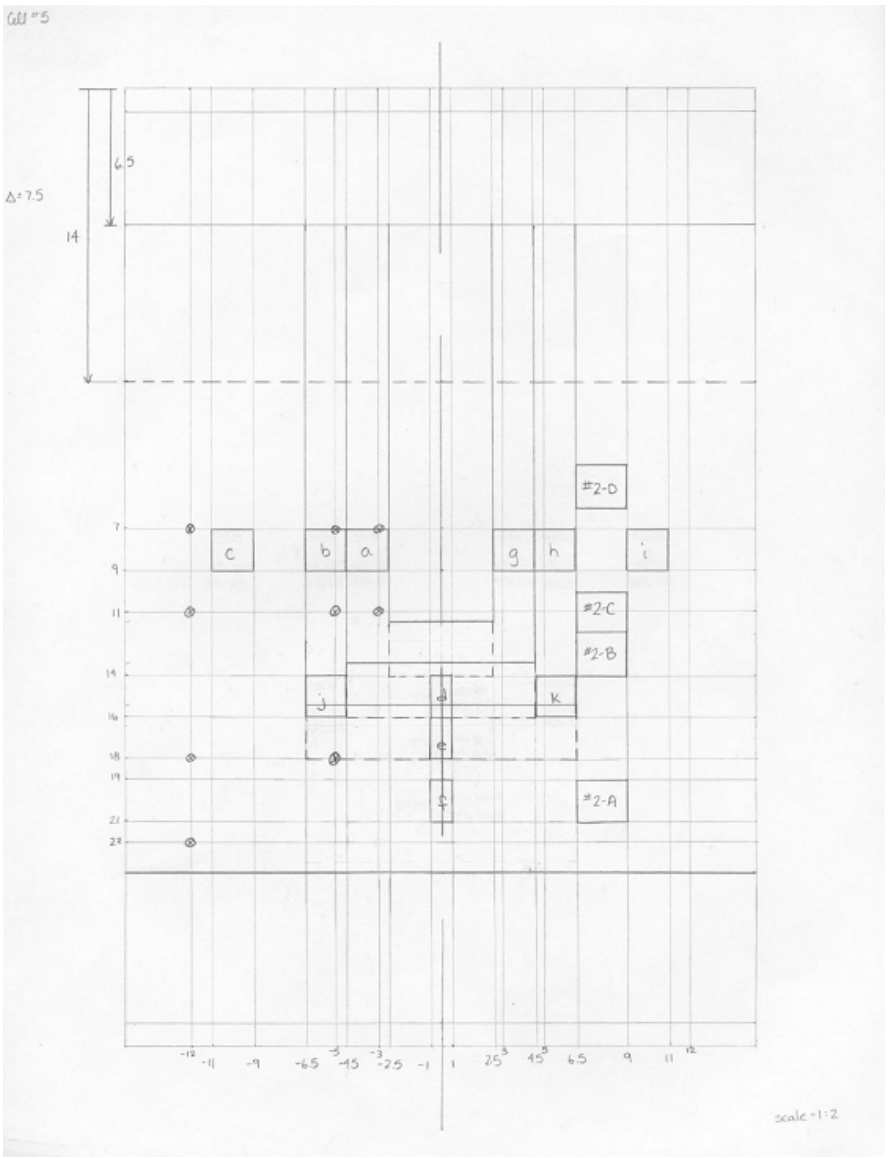
GU = 5
Δ = 7.5
6.5
14
#2-D
#2-C
#2-B
#2-A
c
b
a
g
h
i
j
d
k
e
f
7
9
11
14
16
18
19
21
22
-12
-11
-9
-6.5
-5
-4.5
-3
-2.5
-1
1
2.5
3
4.5
5
6.5
9
11
12
scale = 1:2

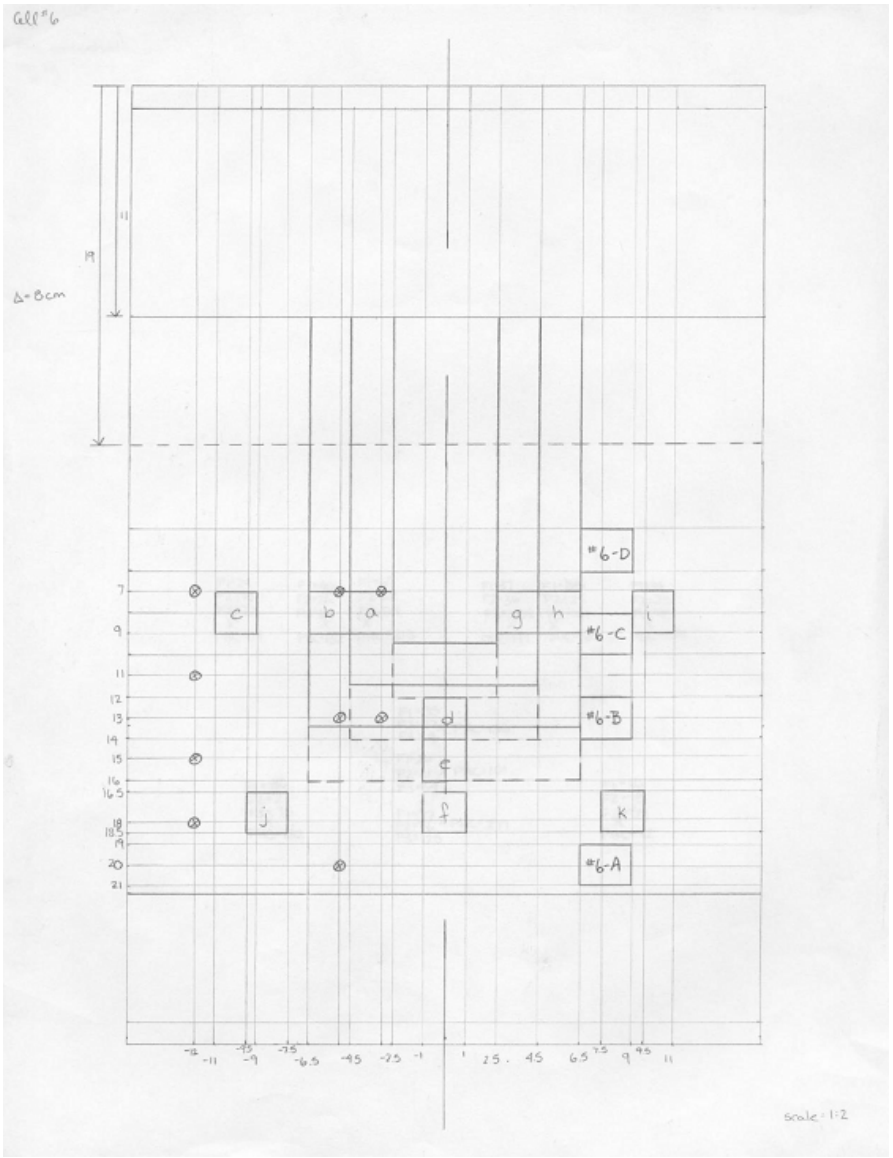
Cell #6
Δ=8cm
19
11
#6-D
#6-C
#6-B
#6-A
a
b
c
d
e
f
g
h
i
j
K
7
9
11
12
13
14
15
16
16.5
18
18.5
19
20
21
-12
-11
-9.5
-9
-7.5
-6.5
-4.5
-2.5
-1
1
2.5
4.5
6.5
7.5
9
9.5
11
scale: 1:2

Appendix B: Micro-Oxymax Respirometer

This appendix presents details regarding the Micro-Oxymax respirometer hardware, software, set-up, system diagnostics, leaks and volume measurement, settings, calibration, initialization and calculations. Many of the details presented are specific to the use of the Micro-Oxymax respirometer in this experiment.

B.1 Overview

The Micro-Oxymax respirometer from Columbus Instruments, Columbus, OH periodically measures headspace gas concentration using a 0-10% or 0-100% carbon dioxide, CO_2, sensor, 0-10% or 0-100% methane, CH_4, sensor and an oxygen, O_2, sensor. In this experiment the 0-10% CO_2 sensor, 0-10% CH_4 sensor and O_2 sensor were used. The CO_2 and CH_4 sensors are single-beam infrared sensors and the O_2 sensor is a paramagnetic oxygen sensor. CH_4 headspace concentrations were monitored to ensure that the microbial degradation taking place was aerobic. The Micro-Oxymax is a closed system respirometer, meaning the air is pumped from the test chamber, through the gas sensors and returned to the test chamber without being exposed to the environment. There is one exception to this however, which is called 'refresh'. Continued production and consumption of gases, in this case CO_2 and O_2, results in changes in gas concentration which may inhibit the respiration being monitored. To resolve this problem the channels are 'refreshed', meaning the headspace gas is replaced with fresh gas at specified measurement intervals or gas concentration changes. The instrument is continually recalibrated using a reference chamber with a reference air supply resulting in measurements that are independent of changes in ambient conditions. The air in the chamber is measured periodically and changes in gas concentrations are used to compute O_2 consumption and CO_2 production. The software automatically normalizes consumption and production information to standard temperature, 0°C, and pressure, 760 mmHg (Columbus Instruments, 2002).

B.2 Components and Set-Up

The instrumentation was assembled according to the manufacturers' instructions (Columbus Instruments, 2002). Tubing was connected from the lower chamber to a condensing air dryer, to a three way valve and then to air sampling tube(s). Downstream of the air sampling tube(s) tubing was connected to PTFE hydrophobic membrane filters and then to the expansion interface. From the expansion interface the tubing was connected to the system sample pump, to each of the gas sensors, back to the system sample pump, back to the expansion interface and into the lower chamber. The expansion interface, system sample pump, and gas were connected to each other and to a microcomputer. The microcomputer, interfaced with a compatible computer with the appropriate Micro-Oxymax software, controlled the instrument and collected, stored and presented the data.

B.2.1 Condensing Air Dryer and Air Sampling Tubes

Tubing ran from each of the lower chambers to 6 of 10 connections at the bottom of the condensing air dryer. The condensing air dryer was cooled to ~-2°C and was used to condense water vapour from the chamber gas and return that water to the chamber.

From the top of the condensing air dryer tubing, corresponding to one of the lower chambers, was connected to a three way valve. The three way valve allowed gas to flow in two possible directions; from the condensing air dryer to the ORBO^{TM}402 (when being used) and ORBO^{TM}32L air sampling tube(s) or from the condensing air dryer to a sealed

piece of tubing. This was done so that when the air sampling tube(s) were replaced the valve could be adjusted so no gas from the container escaped.

From the air sampling tube(s) the tubing was connected to PTFE hydrophobic membrane filters. These filters were used for extra protection against liquid entering the system and to prevent bacteria from entering and contaminating the system. Then, from the PTFE membrane hydrophobic filters, the tubing was connected to the expansion interface.

B.2.2 Expansion Interface and Gas Sensors

The front of the expansion interface has 10 connections going in and 10 connections coming out. As only one lower chamber can be measured at a time (there is only one tube going through the gas sensors and the system sampling pump) the expansion interface, controlled by the microcomputer, controls which headspace gas is being circulated through the gas sensors. One tube leaves the back of the expansion interface and is connected to the system sample pump. From the system sample pump tubing runs to the O_2 sensor, the CO_2 sensor and the CH_4 sensor. The tubing is then connected from the CH_4 sensor back to the system sample pump and then runs from the system sample pump to the expansion interface. Tubing from the expansion interface to the lower chamber then allows the headspace gas to flow back.

The expansion interface also detects liquid entering the system. If liquid is detected the tubing from each of the chambers is sealed at the expansion interface so the sample in

which liquid has been detected cannot continue through the system sampling pump and into the gas sensors.

Before the experiment is started all the gas sensors must be calibrated. Calibration of the gas sensors is discussed in Sections B.5 and B.6.

B.2.3 System Sample Pump

The system sample pump controls the headspace gas flow rate from the lower chamber and the atmospheric air flow rate during a 'refresh' using two flow meters, one for the headspace gas and one for the 'refresh'. The back of the system sample pump has fittings for two drying columns, one to dry the headspace gas from the lower chamber before it goes to the gas sensors and one to dry the air from the atmosphere during a 'refresh'. Each drying column is filled with indicating Drierite® which contains <98% anhydrous calcium sulfate, $CaSO_4$, and >2% cobalt chloride, $CoCl_2$. The $CaSO_4$ is impregnated with the $CoCl_2$. Both of these compounds act as dessicants but the $CoCl_2$ also acts as an indicator, changing the colour of the indicating Drierite® from blue to pink as moisture is absorbed (W. A. Hammond Drierite® Product Catalogue online, accessed 2006). The Drierite® was replaced when exhausted and reused after being dried in an oven.

There is also a calibration/refresh port, a nitrogen port and a gas exhaust port at the back of the system sample pump. Attached to both the calibration/refresh port and the nitrogen port is an air filter and a T air fitting. The air filters prevent debris from entering the system during 'refresh' and calibration and the T air fitting allows for gas overflow

from the calibration bottles. The gas exhaust port is used while the instrument is 'purging' or 'refreshing' so headspace gas can escape into the atmosphere. Lastly, there is also a temperature probe connection at the back of the system sampling pump.

B.2.4 Software

Software for the Micro-Oxymax respirometer was provided by Columbus Instruments. As mentioned previously, the Micro-Oxymax microcomputer is interfaced with a compatible computer with Micro-Oxymax software. In this case the microcomputer was interfaced with an IBM desktop computer. The Micro-Oxymax program can be accessed on the desktop computer by selecting the Micro-Oxymax program from the Start Menu. By selecting the main menus in the Micro-Oxymax window the user can run diagnostics on the system, test for chamber volumes and leaks in the instrument or tubing, access the instrument setup, calibrate the gas sensors and flow meters, and view and run experiments.

B.3 System Diagnostics

After the tubing and cables were properly connected diagnostics tests was run to ensure the temperature, pressure and gas sensors, drying column, gas ports and expansion interface were working properly. First, short pieces of tubing were connected to the in and out ports of each connection on the expansion interface, basically replacing each lower chamber with a short piece of tubing. Next, system diagnostics were run by accessing Diagnostics under the Tools menu. These are three tabs under diagnostics: Basic Operations, Valves and Sensors, and Expansion Unit. The Basic Operations tabs

tests the operation of the temperature and pressure sensors and gives a pass or fail for each test; the Valves and Sensors tab tests the restriction, volume and leakage of the drying column, the calibration and nitrogen ports for high restrictions and the sensors for restrictions; and the Expansion Unit tab tests the restriction, volume and leakage of the connections within the expansion interface and gives a pass or fail for each channel. All three of these diagnostics were run to ensure that every component of the system was given a pass and the results generated were saved.

B.4 Leaks and Volume Measurement

After completing the system diagnostics, the system was checked for leaks and the final volume of the system was determined. The system was checked for leaks and for reasonable and reproducible volume measurements using Volumes Measurement located in the Tools Menu under Utilities. Volume and leak measurements of Drier #1 measure the internal sensor volume, the drier volume, the volume of the tubing connecting the sensors to the sample pump and detects any leaks within these components and tubing connections. Volume and leak measurements of Channels #1 through 10 measure the volume of the lower chambers and the tubing from the lower chambers to the expansion interface and detects any leaks in the lower chambers, the condensing air dryer and the tubing connections.

Starting with the simplest tubing configuration, the same configuration that was used for system diagnostics, the system was checked for leaks and for reasonable and reproducible volume measurements. With this tubing configuration, volume and leak measurements

of Drier #1 and Channels #1 through 10 were made. As there were never any leaks detected in Drier #1, the measured volume of Drier #1 was transferred automatically to Sensor Volume Drier #1 in the Volume Settings tab in System Properties under the File menu. Volume and leak measurements of Channels #1 through 10 were made numerous times to ensure that the volume measurements were fairly consistent, the leak measurements were within an acceptable range (+/- 0.2 ml/min) and the readings were given a pass. Channels #1 through 10 measured the tubing volume connecting the in and out ports on the expansion interface and detected leaks in the tubing connections. Any leaks were fixed by fine-tuning the tubing connections.

When the volume measurements were reasonable and reproducible and the system was free of leaks the complexity of the tubing configuration was increased and leak and volume checks were made. The complexity of the tubing configuration was increased incrementally and leak and volume checks were made after each change until the tubing was in the desired configuration for experimentation

Next, the tubing was connected to the filters and the three way valve and both ends of the tubing were connected to the in and out ports of the expansion interface. With this configuration volume and leak measurements of Channels #1 through 10 were made numerous times to ensure the volume measurements were fairly consistent, the leak measurements were within an acceptable range (+/- 0.2 ml/min) and the readings were given a pass. Again, any leaks were fixed by fine-tuning the tubing connections.

The next step was to include the condensing air dryer and a glass container of known volume. Volume and leak measurements of Channels #1 through 10 were measured numerous times with this configuration to ensure that the volume measurements were fairly consistent, the leak measurements were within an acceptable range (+/- 0.2 ml/min) and the readings were given a pass. Again, any leaks were fixed by fine-tuning the tubing connections. These final volume measurements minus the volume of the glass containers were taken to be the tubing volume up to the expansion interface.

As Volumes Measurement cannot be used for measuring volumes greater than 2 liters (L) and the headspace volume of every lower chamber was greater than 2 L the headspace volumes of the lower chambers were measured manually. The system volume was calculated by adding the headspace volume of each lower chamber with its respective tubing volume. These values were then entered in the Chamber Setup tab in Setup under the Experiment Menu as described in Section B.7.

B.5 Settings

After system diagnostics were run and the volumes of every channel were determined and the channels were free of leaks, a number of settings were specified for the experiment. These settings were: Setpoints/Modes, Volume Settings, Mass Flow Settings, Sensors 1-2, Sensors 3-4 and Sensors 5-6 and were accessed in System Properties under the File menu.

The Setpoints/Modes tab contains four groups of settings including System Timing, Sensors Setpoints, Modes and Calibration Bottle Port Configuration. The System Timing settings control the amount of time the system circulates gases through the sensors. These settings were set by Columbus Instruments and were not changed. The Sensor Setpoints settings control the pressure in the sensors during measurement and the maximum number of channels available. These settings were also set by Columbus Instruments and were not changed. The Modes settings control what type of calibration method is being used to calibrate the sensors. The 'Bottled' method, the preferred method of calibration, was used. With this method gas sensors were calibrated using precisely mixed gas standards. The standards used were 100% nitrogen, 19.9% oxygen with a nitrogen balance and 8.99% CH_4 and 9.01% CO_2 with a nitrogen balance. Each of the gas standards were identified with the Calibration Bottle Port Configuration settings which specify which Bottle Port Connection refers to which calibration standard. Based on this information and the identification of the concentration and type of calibration gas entered in the Sensors tabs when the calibration procedure is initiated (see Section B.6) the instrument will prompt for the attachment of the proper calibration gas standard. Bottle 1 Port Connection was set to Nitrogen, Bottle 2 Port Connection was set to Calibration and Bottle 3 Port Connection was set to Calibration.

The Volume Settings tab contains numerous volume and flow rate settings used by the instrument in its calculations including Sensor Volume Drier #1 and #2, Reference Chamber Volume, Volume Correction Factor, Expansion Unit Shared Volume, Refresh Volumes, Refresh Flow Rate, Calibration Mixing Chamber and Expansion Units

Volumes #1-#8. The Sensor Volume Drier #1 and Drier #2 are settings for the internal volumes of the sensors, tubing and the drier. In this case only Drier #1 was included in the system and this value was measured automatically when the Volumes Measurement, located in the Tools Menu under Utilities, was preformed. The Reference Chamber Volume is the volume of the reference gas chamber located inside the system sample pump. This value was set by Columbus Instruments and was not changed. The Volume Correction Factor is associated with the internal sampling pump. This value was also set by Columbus Instruments and was not changed. The Expansion Unit Shared Volume is the volume of the expansion manifold connection which connects the expansion interfaces to the sample pump. This value was set at zero by Columbus Instruments because the instrument has only has one expansion interface. Upon addition of expansion interfaces an expansion manifold would be purchased and the value for the Expansion Unit Shared Volume would change accordingly. The Refresh Volumes setting controls the number of volumes of air that moves through the chamber upon refresh. This volume was set to 4 by Columbus Instruments and was not changed. The Refresh Flow Rate is the flow rate to the 'refresh' air. Columbus Instruments specifies that this value should be set between 3 and 4 liters per minute (lpm). It was set to 3 lpm by Columbus Instruments and was not changed. The Calibration Mixing Chamber was set to zero by Columbus Instruments and was not changed. The Expansion Unit Volumes #1-8 are the internal volumes of each of the expansion units. Since only one expansion unit was used only expansion unit #1 was activated. The value was set by Columbus Instruments and does not need to be changed unless the tubing inside the expansion interface is replaced.

The Mass Flow Settings tab was not used and all settings were disabled. This tab is only for use with the Open Flow High Metabolic option that is not available with this instrument configuration.

The sensor tabs are used to calibrate the sensors for the specific gases being used. Sensor 1 was the paramagnetic oxygen sensor, Sensor 2 was the CO_2 sensor and Sensor 3 was the CH_4 sensor. The remaining sensors were not activated. The Offset Gas Concentration was set to zero for all the sensors and the Offset Gas Source/Bottle was set to Bottle 1. Bottle 1 contained 100% nitrogen. Under Sensor 1, the oxygen sensor, the Span Gas Concentration was set to 19.9% and the Gas/Source Bottle was set to Bottle 2. Bottle 2 contained 19.9% oxygen with a nitrogen balance. Under Sensor 2, the CO_2 sensor, the Span Gas Concentration was set to 9.01% and the Gas/Source Bottle was set to Bottle 3 and under Sensor 3, the CH_4 sensor, the Span Gas Concentration was set to 8.99% and the Gas/Source Bottle was set to Bottle 3. Bottle 3 contained 8.99% CH_4 and 9.01% CO_2 with a nitrogen balance.

B.6 Calibration

Calibration of the gas sensors was initiated by accessing Calibration under the Tools menu in the main window and following detailed instructions provided by the software upon calibration. All adjustments of the gas concentrations were made as instructed by the calibration procedure by adjusting the offset gas and span gas dials on the front of the appropriate sensors. After the dials were adjusted they were locked to prevent accidental movement.

B.7 Initialization

After the respirometer components were setup and connected together properly, diagnostics were run and passed, volume measurements were taken and leaks were in an acceptable range and the gas sensors were calibrated the respirometer was ready to be initialized. The respirometer was initialized by accessing Setup under the Experiment menu. There are five tabs in the Setup window; Setup, Chamber Setup, Comments, Data and Graphing.

The Setup tab contains four groups of settings including Channels, Timing, Refresh, Data Units and Misc. Setup. The Channels setting control which channels are being measured throughout the experiment. The Start Chamber was set to 1 and the end chamber was set to 6. Channels 1 through 4 measured the soil and root respiration of contaminated soil planted with trees and channels 5 and 6 measured the soil respiration of contaminated soil without trees. The Timing settings control the sampling interval and the duration of the experiment. The Sampling Interval was set to 'Auto' meaning the instrument automatically calculates the minimum time required to measure the channels at the beginning of the experiment and uses that time throughout the experiment. The Experiment Duration was set to 'N.A' meaning the length of the experiment was not specified and would continue until the experiment was manually terminated. The Refresh settings control when each of the channels are refreshed and how long the channels are refreshed for. There are two options for specifying timing of the refresh; a threshold value specifying the increase or decrease of a gas concentration by percentage

before a refresh will be preformed or an interval value measuring the number of measurement intervals before a refresh will be preformed. The Refresh Threshold was used and was set to 1% for the entire experiment with the exception of four days during the experiment when Channel 2 was leaking. The Refresh interval was disabled. The Refresh Window controls how long the channels are refreshed for. This was calculated to be 520 seconds, s, using Equation B1 below from Columbus Instruments (Columbus Instruments, 2002).

$$RW = \left(\frac{60 * D * Vol}{F} \right) + E$$

Equation B1 (Columbus Instruments, 2002)

Where RW is the Refresh Window in seconds, D is the refresh duration volumes, which was set at 4, Vol is the maximum bottom container headspace volume, F is the fresh pump flow, which is 4500 mL/minute, and E is the pressure equalize time, which is 10 seconds. Using the maximum container headspace volume of 9417 ml the RW was 512 seconds which was rounded up to 520 seconds. This value was used throughout the entire experiment. The Data Units settings gives the option of selecting the units that the data in displayed in. The data units were set as microliters, μL, and minutes, min. The Misc. Setup settings include Auto Volume Measurement, Purge Sensors, Switch Driers, O_2 Consumption Positive, Enable Open Flow Mode and Aux. Temp. Start Channel. The Auto Volume Measurement setting gives the option of automatically measuring the headspace volume and using that volume for calculations at this point in the experimental setup. This setting was disabled as the headspace volumes were calculated manually.

The Purge Sensors setting gives the option of purging the sensors between each measurement. This setting was activated to eliminate the possibility of residual gases in the sensors influencing measurements for other headspaces. The Switch Driers setting gives the option of switching between Drier #1 and Drier #2 for each sampling interval. This setting was disabled. The O_2 Consumption Positive setting gives the option of displaying the O_2 consumption as a positive value in the Data and Graphing tabs discussed later in this section. This setting was disabled. The Enable Open Flow Mode setting was disabled as this setting is only used with the Open Flow High Metabolic option that is not available with this instrument configuration. The Aux. Temp. Start Channel may be used when two groups of samples are being monitored at different temperatures, one temperature is detected with the temperature probe and another temperature with the auxiliary temperature probe. This setting was not used.

The Chamber Setup tab contains setup options for the channels being used including Volume, Normalized Units, Restriction, Leakage and Channel Label for each activated channel. The Volume column was where the container headspace volumes were entered. The Normalized Units is used if the O_2 consumption and CO_2 production is to be normalized by the sample size. This was not used so the Normalized Units were all set to 1. The Restriction and Leakage columns are used to identify excess pressures and leaks at this point in the experimental setup. This was not used at this point. The final column, Channel Label, allows comments or sample descriptions to be entered about specific channels and saved with the data file.

The Comments tab allows comments to be entered and saved with the data file.

The Data tab displays the experimental data while the experiment is running and after the experiment has been terminated. In columns from left to right the data displayed is; the interval, channel, time, channel temperature, respiration quotient, percent O_2, O_2 consumption rate, cumulative O_2 consumed, percent CO_2, CO_2 production rate, cumulative O_2 produced, percent CH_4, CH_4 consumption rate, cumulative CH_4 consumed, pressure and the refresh and/or error status.

The final tab in this window is the Graphing tab. This window displays a graph of the data while it is being collected or the data that has been collected from a previous experiment. The data can display all the channels in use simultaneously with the option of placing a number of different measured values on the y-axis and the interval number on the x-axis. The graphing options for the y-axis include the percent of each gas being measured, the cumulative amount of each gas being measured, the pressure and the temperature.

Also, while the experiment is running the Experiment Status Window is available for consultation. This window indicates the file name, start time, sampling interval, experiment duration, current time, sample interval number, time until the next data point, which drier is active and measurement status.

B.8 Calculations

Numerous calculations were preformed to transform the raw respirometer data to an inferred mass of PHC degraded. Firstly the raw data files were converted into Microsoft Excel format. Next two more columns were added to change the cumulative amount of O_2 produced, which was a negative value, to the cumulative amount of O_2 consumed, a positive value, and to determine the amount of O_2 consumed over each time interval. Next three more columns were added to change units of the amount of O_2 consumed over each time interval from μL to moles, to calculate the cumulative amount of O_2 consumed in moles and to normalize the amount of O_2 with the mass of soil. To change the units of the amount of O_2 consumed over each time interval the gas law was used as seen below in Equation B2.

$$PV = nRT$$

Equation B2

In this equation P is pressure, V is volume, n is the number of moles, R is the universal gas constant with a value of 8.3145 J/mole*K and T is the temperature. To determine the number of moles produced over each time interval Equation B2 above was solved for n. As the measurements are normalized to standard pressure and temperature the pressure value used was 760 mmHg which equals 101325 Pa and the temperature value used was 0 ^{O}C which equals 273.15 K. The volume used was the volume of O_2 consumed over the interval converted from μL to meters cubed, m^3. Next another column was added to determine the amount of CO_2 produced over each time interval. Next three more columns were added to change units of the amount of CO_2 produced over each time

interval from μL to moles, to calculate the cumulative amount of CO_2 produced in moles and to normalize the amount of CO_2 with the mass of soil. To change the units of the amount of CO_2 produced over each time interval the gas law the same way it was used to change the amount of O_2 consumed.

After the cumulative number of moles of O_2/CO_2 consumed/produced during the experiment was determined those values were converted to mg of PHC using three equations for the stoichiometry of diesel found in literature. The stoichiometric equations used were as follows:

1. $C_{16}H_{34}+24.5O_2 \rightarrow 17H_2O+16CO_2$

(after Zynter et al.)

2. $C_{14.4}H_{49.9+}27O_2 \rightarrow 9.4H_2O+14.5CO_2$

(after Mittal and Sharma)

3. $C_{10.8}H_{18.7}+15.5O_2 \rightarrow 9.4H_2O+10.8CO_2$

(after Huang et al.)

The final inferred amount of diesel degraded microbially was determined from using the O_2 readings and the average amount of diesel degraded from the three stoichiometric equations above. The O_2 reading were used because the paramagnetic oxygen sensor is more sensitive than the single beam infra-red CO_2 sensor.

During the course of the experiment there were numerous instances when the respirometer program was restarted due to replanting a few trees, the termination of measurement of certain channels (initially the respiration was also measured form the top portion of the containers) and to the bottom containers and tubing developing leaks over the course of the experiment. In the situation where the containers and tubing were leaking attempts were made to fix the leaks while the instrument was running but it was often necessary for the experiment to be restarted. Both restarting the respirometer program and fixing leaks without restarting the respirometer program resulted in erroneous readings of cumulative O_2 consumption and CO_2 production. To solve this problem the cumulative O_2 consumption and CO_2 production was extrapolated using a number of values from the previous data set and, when leaks were fixed without restarting the respirometer program, previous to any detected leaks.

Appendix C: Index and Characteristic Soil Tests

This appendix presents the procedures used for the index and characteristic soil tests.

C.1 CEC Determination by the $BaCl_2$ Compulsive Exchange Method

Donald S. Ross after Gillman and Sumpter, 1986

Equipment:

1. Centrifuge and 30 mL centrifuge tubes.
2. Reciprocating shaker.
3. Scale capable of weighing to nearest mg.
4. Conductivity and pH meters.

Reagents:

1. 0.1 M $BaCl_2.2H_2O$ extracting solution: Dissolve 24.428 g of barium chloride ($BaCl_2.2H_2O$) in a 1 L volumetric flask containing ~800 mL of distilled water. Dilute to volume with distilled water and mix. [Caution: Barium is toxic if ingested].
2. 2 mM $BaCl_2$.2H2O equilibrating solution: Dilute 20 mL of the 0.1 M $BaCl_2$ solution to 1 L with distilled water.
3. 0.1 M $MgSO_4.7H_2O$: Dissolve 24.648 g of magnesium sulfate ($MgSO_4.7H_2O$) in a 1 L volumetric flask that contains about 800 mL of distilled water. Dilute to volume with distilled water and mix.
4. 1.5 mM and 5 mM $MgSO_4.7H_2O$: Dilute 15 and 50 mL of the 0.1 M $MgSO_4$ solution, respectively, each to 1 L with distilled water and mix well.

5. 0.05 M sulfuric acid: Add 2.8 mL of concentrated H_2SO_4 to a 1 L volumetric flask almost filled with distilled water, make to volume, and mix thoroughly.

Procedure:

1. Weigh each 30 mL centrifuge tube to the nearest mg.
2. Add 2.00 g of soil, 20 mL of 0.1 M $BaCl_2.2H_2O$, cap, and shake for 2 hours.
3. Centrifuge at about 10,000 rpm and decant carefully.

   Note: A good direct measure for CECe can be obtained at this point by measuring Ca, Mg, K, and Al in this extract by ICP or AA (Hendershot and Duquette, 1986). If results are in mg/L: CEC =[Ca20 + Mg12 + K39 + Al9] For a safer method, substitute 1 M NH_4Cl for $BaCl_2$ and then determine the cations in the NH_4Cl extract. Ammonium chloride cannot be substituted for $BaCl_2$ in the full CEC procedure.
4. Add 20 mL of 2 mM $BaCl_2.2H_2O$, cap and shake for 1 hour. If needed, shake vigorously at first to disperse soil pellet.
5. Centrifuge and discard supernatant.
6. Repeat steps 4 and 5 twice. Before the third centrifugation, obtain slurry pH.
7. After the third decantation of 2 mM $BaCl_2.2H_2O$, add 10.00 mL of 5 mM $MgSO_4$ and shake gently for one hour.
8. Determine conductivity of the 1.5 mM $MgSO_4$ solution (it should be ~300 S or mhos). If conductivity of the sample solution is not 1.5x this value, add 0.100 mL increments of 0.1 M $MgSO_4$ until it is (keep track of amount added).

9. Determine the pH of the solution. If it is not within 0.1 units of the previous measure, add 0.05 M H_2SO_4 dropwise until pH is in appropriate range.
10. Add distilled water, with mixing, until the solution conductivity is that of the 1.5 mM $MgSO_4$. Adjust solution pH and conductivity alternately until the endpoints are reached.
11. Wipe outside of the tube dry and weigh.

Calculations for CEC:

1. Total solution (mLs) [assumes 1 mL weighs 1 g] = final tube weight (g) - tube tare weight (g) - 2 g [weight of soil used]
2. Mg in solution, not on CEC (meq)= total solution (mLs) x 0.003 (meq/mL) [1.5 mM MgSO4 has 0.003 meq/mL]
3. Total Mg added (meq) = 0.1 meq [meq in 10 mLs of 5 mM MgSO4] +meq added in 0.1 M MgSO4 [mLs of 0.1 M MgSO4 x 0.2 meq/mL (0.1 M MgSO4 has 0.2 meq/mL)]
4. CEC (meq/100g) = (c - b) x 50 [Total Mg added - Mg in final solution; 50 is to convert from 2 g of soil to 100 g]

Example:

Tube tare: 19.858 g; final wt.: 49.743 g; added 0.1 M MgSO4: 0.3 mL.

1. Total solution (mLs) = 49.743 [final tube wt.]- 19.858 [tare wt.]- 2.00 [soil wt.]= 27.885

2. Mg in solution (meq) = 27.885 mLs x 0.003 meq/mL [1.5 mM $MgSO_4$] = 0.0837 meq
3. Total Mg added (meq) = 0.1 meq [10 mLs of 5 mM $MgSO_4$] + (0.3 mLs x 0.2 meq/mL) [0.1 M $MgSO_4$] = 0.16 meq
4. CEC (meq/100g) = (0.16 meq [added]- 0.0837 meq [final]) x (50) = 3.8 meq/100 g

C.2 Organic Carbon by Modified Walkley-Black Wet Oxidation Method

The University of Western Ontario

Faculty of Engineering Centre

Geotechnical Research Centre

Equipment:

1. Fume hood.
2. #140 sieve.
3. 400 mL beakers.
4. Graduated cylinder.
5. Scale capable of weighing to nearest mg.

Reagents:

1. M/6 potassium dichromate ($K_2Cr_2O_7$), 49.04 g/L

   Dry the potassium dichromate for 1 hr at 150°C
2. Concentrated sulphuric acid (H_2SO_4, not less than 96%)
3. Concentrated o-phosphoric acid (H_3PO_4, 85%)
4. Ammonium ferrous sulphate solution, 0.5 M,

   196 g ammonium ferrous sulphate + 40 mL concentrated H_2SO_4 in 1 L of distilled water.

   Standardize daily by titrating against 10 mL M/6 $K_2Cr_2O_7$.

Procedure:

1. Grind the oven dried soil to pass a #140 (0.106 mm) sieve having first taken care to remove all the large roots.
2. Weigh a sample of 0.100 to 2.00 g (depending on organic matter content), and transfer to a 400 mL beaker.
3. Add 10 mL of potassium dichromate solution using an automatic pipette and gently swirl the flask to mix the reagent with the soil.

Steps 4-7 should be performed in a fume hood

4. Rapidly add 20 mL. of concentrated sulfuric acid from a measuring (graduated) cylinder and again swirl the flask for about 30 seconds.
5. Allow the flask to stand on an asbestos pad for 30 minutes. As the degree of oxidation depends on the heat generated all samples must be allowed to cool uniformly.

   N.B. If the solution has a green colour, add more $K_2Cr_2O_7$ and H_2SO_4. Keep the sample proportions as before, i.e. 1:2.

   (Add to standards also).
6. After cooling add approximately 200 mL of distilled water to the conents of the flask.
7. Add 10 mL concentrated H_3PO_4.
8. Titrate the excess dichromate with ammonium ferrous sulphate solution.

   N.B. In some samples the endpoint can be sharpened by the addition of 10 mL concentrated phosphoric acid after dilution of the sample with 200 mL of

distilled water above. The H_3PO_4 eliminates interference by ferric iron (Schollenberger, 1931).

NOTE: If the endpoint cannot be obtained then all the dichromate has been reduced. In such cases the experiment should be repeated using more dichromate solution or a smaller sample size. For soils containing high amounts of organic carbon it is preferable to use correspondingly more dichromate rather that reduce the amount of soil analyzed (Hesse, 1971, 214).

9. Make a blank determination following the above procedure but without soil. This serves to standardize the ferrous solution. At least three replicates should be titrated, and an average value obtained. [Average value 22.7 (841122)]

Calculations and Expression of Results:

The results can be expressed simply as percent, oxidizable organic carbon, OOC. It is more usual, however, to present the results either as percent total organic carbon (OC), or as percent organic matter (OM).

1. % oxidizable organic carbon (OOC):

$$x = \frac{(blank - actual) * 0.3^{*} * M}{weight_{soil}}$$

where M is the concentration of ferrous solution (0.5 M)

2. % total organic carbon (OC):

x*1.33

N.B. This assumes an apparent percentage recovery for the technique of 75%

3. % organic matter (OM):

x*2.29

N.B. This constant is a product of the above 1.33 and the Van Bemmelen constant (1.724)

*This value represents the equivalence value for organic carbon:

1 g equivalent of OC=12.01/4=3 g

1 mL 1M ferrous solution=3/1000=0.003 g

$$x = \frac{(blank - actual) * 0.003 * M * 100}{weight_{soil}}$$

$$x = \frac{(blank - actual) * 0.3 * M}{weight_{soil}}$$

C.3 ATP Assay

Modified from a procedure developed by Celsis (formerly Lumac, Landgraaf, the Netherlands) and obtained from Dr. Leila Hrapovic at Queen's University in Kingston, Ontario, Canada (Hrapovic and Rowe, 2002.

Equipment:

6. Luminometer (a Lumat LB 9507 luminometer from Berthold Technologies, Bad Wildbad, Germany was used in this experiment)

Reagents:

1. ATP releasing reagent

   the releasing reagent used
2. rLuciferase/Luciferin reagent
3. ATP standard

   the rLuciferase/Luciferin reagent and the ATP standard used were purchased from Promega Corperation, Madison, Wisconson, USA as part of the EnLiten® ATP Assay System
4. Sterile double DI water
5. Sterile pipette tips for a 1-10 mL auto-pipette and a 0-50 μL auto-pipette
6. Clean, sterile 100 mL beakers
7. Clean, sterile glass stirring rods
8. Sterile 12 mm*75 mm, 5 mL glass test tubes
9. Tris-EDTA buffer (100x concentration)

Procedure:

1. Determine the moisture content of the soils on which the ATP assay is being performed.
2. Create a measurement protocol on the luminometer with the following specifications:
    - raw data protocol
    - 110 µL from injector 1
    - 100 µL from injector 2
    - injection 1 follows injection 2
    - 10 s delay between the injections
    - 2 s delay between the last injection and measurement
    - 10 s measurement time
    - background measurement enabled
    - automatic background reading subtract disabled
    - background measured for 0.5 s
    - maximum tolerance for the background reading, 150 RLU/s
3. Prepare the instrument for measurement by rinsing the injectors with sterilized double DI water, attaching the releasing reagent and the rLuciferase/Luciferine reagent to the injectors and priming the injectors so only the reagents and not the rinsing water are injected into the samples.
4. Prepare internal standards by diluting the ATP standard with sterilized, double DI water. The standard provided had a concentration of $1*10^{-7}$ M and the standards prepared had concentrations of $5*10^{-8}$ M, $2.5*10^{-8}$ M and $1.25*10^{-8}$ M.

5. Weigh approximately 1 g dry mass of soil and place in a clean, sterilized 100 mL beaker. Record the actual mass of soil placed in the beaker and calculate the dry mass of soil in the beaker. Add 49 mL of sterilized, double DI water and 0.49 mL of Tris-EDTA buffer to the beaker and mix for 1 minute using a clean, sterile glass stirring rod.
6. Immediately after stirring the sample place three 50 µL aliquots in three 12 mm*75 mm, 5 mL test tubes.
7. Place one of the test tubes into the luminometer and start the measurement protocol. Record the results.
8. Place 20 µL of two different internal standards in the two remaining test tubes. The standards should be chosen so that the measured RLUs are between 2x and 5x that of the sample without an internal standard added. In turn, place each of the test tubes in the luminometer and start the measurement protocol. Record the results.
9. Repeat steps 4-7 for each ATP assay.
10. Upon completion of the ATP assays, clean the injectors with double DI water and shut down the luminometer.

Calculations:

1. Using this equation:

$$\Delta RLU = RLU_2 - RLU_1$$

where RLU_1 is the RLU measurement of the aliquot without the internal standard and RLU_2 is the RLU measurement of the aliquots with the internal standards determine ΔRLU for both internal standards.

2. Using this equation:

$$c_{ATP} = \frac{\left(\frac{RLU_1}{\left(\frac{\Delta RLU}{ATP_{standard}} \right)} \right)}{v_a} * \frac{v_s}{m_s}$$

where $ATP_{standard}$ is the amount of ATP in the standard in nanograms (ng), v_a is the volume of the sample aliquot in mL (0.05 mL), v_s is the volume of the sample liquid in mL (49.49 mL) and m_s is the dry mass of the soil sample, determine c_{ATP}, the concentration of ATP in ng of ATP per g of soil, for both internal standards.

3. Calculate the average concentration of ATP.

Appendix D: PHC Analysis

This appendix presents the instrumentation and procedures used for analyzing soils and air sampling tubes for PHC and processing the chromatograms generated. This includes: instrument specifications of the GC-MS and GC-FID, extraction methods for air sampling tubes, Matlab® scripts used process the raw data, analysis of external standards to determine response factors (RF),and analysis of internal standards to determine extraction efficiencies (E_E).

D.1 GC-MS and GC-FID Specifications

All gas chromatography was performed at the National Hydrology Research Institute, a division of Environment Canada, at Innovation Place adjacent to the University of Saskatchewan Campus by Mr. Kerry Peru.

The GC-MS specifications are as follows:

System: Thermo Trace gas chromatograph with a Thermo Polaris Q mass spectrometer.

Column: 30 m long DB5 with a 0.25 mm I.D. and a 25 μm film

Injection: splitless injection

Injection Volume: 1.0 μL

Injector Temperature: 275^{o}C

Purge Time: 1.20 minute

Source Temperature: 250^{o}C

Transfer Line Temperature: 300^{o}C

Scan Range: 50-450 m/z.

Column Temperature Program: 35^{o}C for 2.0 minutes, then to 160^{o}C at 8^{o}C/minute, then to 295^{o}C at 15^{o}C/minute and held at 295^{o}C for 30 minutes

The GC-FID specifications are as follows:

System: Hewlett Packard model 5890

Column: 30 m long DB5 with a 0.25 mm I.D. and a 25 μm film

Injection: splitless injection

Injection Volume: 1.0 μL

Injector Temperature: 275^{o}C

Purge Time: 1.20 minute

FID temperature: 295^{o}C

Column Temperature Program: 35^{o}C for 2.0 minutes, then to 160^{o}C at 8^{o}C/minute, then to 295^{o}C at 15^{o}C/minute and held at 295^{o}C for 30 minutes

D.2 Extraction Method for Air Sampling Tubes

The extraction method for air sampling tubes was based on the U.S. Department of Labor Occupational Safely and Health Administration (OSHA) Method 07. This method can be seen below and modifications to this method are discussed in Section 3.3.2b.

Organic Vapors
(See section 4)

Method no.:	07
Matrix:	Air
OSHA PELs:	Section 4
Procedure:	Collection on charcoal, extraction with an organic solvent, and analysis by gas chromatography with flame ionization detector.
Recommended air volume and sample rate:	Section 4
Status of method:	This method has been used extensively in the OSHA Salt Lake Technical Center. With slight modification, this method is a generalized version of validated NIOSH methodology.
Date: May 1979 Last Update: May 2000	By: Organic Methods Evaluation Branch By: Methods Development Team

Methods Development Team
Industrial Hygiene Chemistry Division
OSHA Salt Lake Technical Center
Salt Lake City, UT 84115-1802

1. General Discussion

1.1 Background

Background information on the analytes may be obtained from a number of sources such as NIOSH Criteria Documents, chemical dictionaries and industrial hygiene manuals. Solvents are used for degreasing, for dry cleaning, and in the manufacture of many materials ranging from paints, varnishes, shellacs, and lacquers to rubber and synthetic resins. When not being used as solvents, they may function as fuels or act as chemical intermediates with or without regard to their ability to put materials into solution. Toxic effects of the analytes vary with many acting as irritants or causing narcosis, and some having more hazardous effects.

1.2 Statistical parameters

1.2.1 Each analyte included in this general procedure has a validated NIOSH method, (Ref. 5.1) and/or a validated OSHA method. One of the NIOSH validation requirements is that the results obtained be within ±25% of the true values at the 95% confidence level at the air concentration equal to the OSHA standard. Although the OSHA evaluation procedure differs from that of NIOSH, the same validation requirements are used.

1.2.2 Refer to the validated NIOSH methods, (Ref. 5.1) for detailed information on individual analytes.

1.3 Advantages

1.3.1 The sampling device is small, portable, and involves no liquids.

1.3.2 The analysis is by a quick instrumental method.

1.3.3 Interferences can be eliminated by altering chromatographic conditions in most cases.

1.3.4 The method allows simultaneous analysis of two or more analytes.

1.4 Disadvantages

1.4.1 The air volume sampled is limited by the capacity of the charcoal tubes. Exceeding the capacity of the charcoal tube results in loss of sample. The adsorptive capacity is decreased by high humidity.

1.4.2 The method is limited by the reproducibility of the pressure drop across the tubes. The pressure drop affects the flow rate causing the air volume to be imprecise.

1.4.3 The analyst must work with toxic solvents.

1.4.4 When many components are present, elimination of interferences becomes difficult.

2. Sampling Procedure

2.1 Apparatus

2.1.1 A calibrated personal sampling pump whose flow can be determined within ±5% at the recommended flow rate with the sampling device attached.

2.1.2 Charcoal tubes: Glass tubes with both ends flame sealed, 7 cm long with a 6-

mm o.d. and 4-mm i.d., containing two sections of 20/40 mesh activated charcoal separated by a 2-mm portion of urethane foam. The activated charcoal is prepared from coconut shells and is fired at 600°C prior to packing. The adsorbing section contains 100 mg of charcoal, the backup section 50 mg. A3-mm portion of urethane foam is placed between the outlet end of the tube and the backup section. A plug of silylated glass wool is placed in front of the absorbing section. The pressure drop across the tube must be less than 1 in. of mercury at a flow rate of 1 L/min.

2.1.3 Certain analytes require petroleum base charcoal instead of coconut base charcoal. This requirement is specified in Section 4.

2.2 Reagents

None required in sampling procedure.

2.3 Technique

2.3.1 Immediately before sampling, break the ends of the tube to provide an opening at least one-half the internal diameter of the tube (2 mm).

2.3.2 The smaller section of charcoal is used as a backup and should be positioned nearest the sampling pump.

2.3.3 The charcoal tube should be placed vertically during sampling to minimize channeling.

2.3.4 Air being sampled should not be passed through any hose or tubing before entering the charcoal tube.

2.3.5 Do not exceed the recommended air volume.

2.3.6 The charcoal tubes should be capped with the supplied plastic caps immediately after sampling. Under no circumstances should rubber caps be used.

2.3.7 One tube should be handled in the same manner as the sample tube (break, seal and transport) except that no air is sampled through this tube. This tube should be labeled as a blank.

2.3.8 Capped charcoal tubes should be wrapped end to end with official OSHA seals. They should be packed tightly and padded before they are shipped to minimize tube breakage during shipping.

2.3.9 For certain analytes where migration on the charcoal is a significant problem, it may be requested that two charcoal tubes be used in series in order that breakthrough may be distinguished from migration. These tubes must be separated and individually capped and sealed before shipping.

2.4 Breakthrough

Breakthrough data is presented on each analyte in its respective validated NIOSH method (Ref. 5.1).

2.5 Extraction efficiency

2.5.1 The back end of a charcoal tube is opened and the backup portion of activated charcoal is removed, leaving the front 100-mg portion of activated charcoal intact in the tube. The activated charcoal must be of the same lot as that in the tubes used to collect the samples. A known amount of analyte is injected directly into the activated charcoal with a microliter syringe and the tube is capped.

2.5.2 Six tubes at each of three concentration levels (0.5, 1, and 2 times the standard) are prepared by adding an amount of analyte equivalent to that present in a recommended air sample at the selected level. The tubes are allowed to stand at least overnight to assure complete adsorption of the analyte onto the charcoal. These tubes are referred to as the samples. A parallel blank tube should be treated in the same manner except that no analyte is added to it. The sample and blank tubes are extracted and analyzed in exactly the same manner as the sampling tube described in Section 3.

2.5.3 The extraction efficiency (EE) equals the average weight in milligrams recovered from the tube divided by the weight in milligrams added to the tube, or

$$E_E = M_R / M_S$$

where: E_E is extraction efficiency
M_R is mass recovered
M_S is mass spiked

of a gas chromatograph autosampler is acceptable.

3.5.3 Bracket the samples with analytical standards if detected concentrations are above the PEL.

3.5.4 When the identity of a suspected analyte peak is in question, it should be confirmed by GC/MS, GC/IR retention time on at least two GC columns containing different packing material. The identity of the analyte s be considered suspect when detected concentrations are above the PEL.

3.6 Interferences

Interferences to the analytical method will in most cases appear as poor resolution of the analyte peak from o components. This may be overcome by prudent selection of a more suitable chromatographic condition or co

3.7 Calculations

3.7.1 An equivalent air concentration for analytical standards is used to calibrate the data processor 2.5.4 If there is a significant change in extraction efficiency over the range of loadings studied, a plotted curve of EE versus mass recovered must be used to correct for adsorption losses.

2.5.5 If there is no significant change in EE over the range studied, reconfirmations

need only be carried out at one loading in the middle of the range.
2.6 Recommended air volume and sample rate

See Section 4. for recommended air volume and sampling rate.

2.7 Interferences
2.7.1 It is important to be aware of other components in the atmosphere which may interfere with the collection of the analyte.

2.7.2 High relative humidity may significantly affect the collection of some analytes.
2.8 Safety precautions
2.8.1 Care must be taken when opening the sealed ends of charcoal tubes to avoid cuts to the hands.

2.8.2 Safety glasses should be worn when opening the sealed ends of charcoal tubes to avoid injury to the eyes from glass splinters.
3. Analytical procedure
3.1 Apparatus
3.1.1 Gas chromatograph equipped with flame ionization detector.

3.1.2 Columns. A variety of columns are suitable. Two good selections are a 60-m × 0.32 mm DB-1 capillary column with 1m df or a 60-m × 0.32 mm DB-Wax capillary column with 1 μm df. Similar columns from other manufactures are acceptable.

3.1.3 A suitable method of measuring peak areas, such as an electronic integrator or data system.

3.1.4 Two-milliliter vials with either screw-on or crimp-on caps which contain PTFE-lined septa.

3.1.5 Microliter syringes; one-microliter for GC injections and 10-μL for standard preparation, or other suitable sizes.

3.1.6 Pipets for dispensing extracting solvent (ES). A Glenco 1-mL reagent dispenser is adequate and convenient.

3.1.7 Volumetric Flasks. Five-milliliter and other convenient sizes.

3.1.8 Glass tubing cutter.
3.2 Reagents
3.2.1 Chromatographic quality extracting solvent (ES). Although carbon disulfide is commonly used as the ES, certain analytes can be more effectively extracted with the use of alternate solvents or solvent solutions. These alternate ESs are listed in Chemical Sampling Information located at http://www.osha.gov and are normally used when the single analyte is requested or when the requested analytes are known to be effectively extracted with that ES. When analysis for a number of analytes

requiring different extracting solutions is requested, the preferred ES will usually be carbon disulfide.

3.2.2 Analyte standard, reagent grade.

3.2.3 Internal standard, (optional) reagent grade. p-Cymene and n-hexylbenzene are suitable internal standards for many solvents.

3.2.4 Chromatographic quality helium, nitrogen, hydrogen, and air.
3.3 Standard preparation
3.3.1 Prepare analyte standard at a concentration of 1 µL of analyte per milliliter of ES by adding 5 µL of analyte to a 5-mL volumetric flask partially filled with ES. Fill the volumetric flask to the mark and invert 3 or 4 times for proper mixing. Other size volumetric flasks may also be used to prepare the 1 µL/mL analyte standards. At least two standards at 1 µL/mL are prepared. Standards must be used the day they are prepared. In some cases, analyte standards in concentrations other than 1 µL/mL may be more suitable, especially with analytes that have extremely high or low OSHA standards.

3.3.2 Injection of standards is accomplished with a 1-µL or other suitable syringe. The syringe is rinsed thoroughly in carbon disulfide between standards. Injector septa should be checked for wear daily.

3.3.3 Injection sizes other than 1-µL and injection by means of a gas chromatograph autosampler are acceptable in most cases.
3.4 Preparation of samples
3.4.1 The status of the seals on each charcoal tube is noted and recorded as intact, broken, or none.

3.4.2 The field identification number, the laboratory identification number and signature of the industrial hygienist on each sample seal are checked with those on the sample identification sheets.

3.4.3 The seal is removed and the charcoal tube is opened with a glass tubing cutter at the end containing the larger portion of charcoal. The front and back sections of charcoal are transferred to separate 2-mL capped vials. The glass wool plug and the small wad of urethane foam separating the two sections of charcoal are discarded.

3.4.4 The charcoal lot number is noted in order that the proper extraction efficiency is used in later calculations.

3.4.5 Gas chromatography parameters are set as recommended in the instruments manual. Oven temperature and column are varied until an optimum chromatogram is produced by the analyte standard.

3.4.6 Once the internal standard has been verified as not interfering with other peaks

in the chromatogram, the samples are extracted. One milliliter of ES is dispensed into each sample vial. The vial is immediately sealed. Each vial is swirled periodically to increase the rate of extraction. Twenty to thirty minutes is typical for the extraction process.

3.5 Analysis

3.5.1 The data processor can be calibrated to provide results directly in units of mass. With a few of the analytes an additional similar correction may be necessary due to extraction efficiencies that change with concentration. The linear nature of the flame ionization detector allows the use of a point calibration, but the bracketing of samples with analytical standards is a good practice. The calculation of the equivalent air concentration for an analytical standard is detailed in Section 3.7.1.

3.5.2 Sample injection is accomplished with a 1-µL or other suitable syringe. The syringe is rinsed thoroughly in carbon disulfide between samples. Injector septa should be checked for wear periodically. Injection by means such that analytical results are obtained directly in mass, mg.

$$W=V_S*d$$

where: W is weight of analyte in µg
V_S is volume of analyte in µL
d is density of analyte in µg/µL

$$C_V=(V_M*W)/(M_r*V*E_E)$$

where: C_V is air concentration reported to IH
V_M is molar volume at 25°C and 760 mmHg, 24.46 L/mol
W is weight of analyte
M_r is molecular weight of the analyte
V is air volume sampled
E_E is extraction efficiency

3.7.2 The following example is the calculation for toluene:

$$W=867\ \mu g=1\ \mu L*867\ \mu g/\ \mu L$$

$$C_v=23.73\ ppm=[(24.46\ L/mol)(867\ \mu g)]/[(92.15\ g/mol)(10\ L)(0.97)$$

The calculations should be considered an example only, and various parameters confirmed before used in actual analysis.

3.8 Safety precautions

3.8.1 Care must be taken when opening charcoal tubes to avoid cuts to the hands.

3.8.2 Safety glasses must be worn throughout the analytical procedure.

3.8.3 Work involving solvents open to the atmosphere must be performed in a hood.
3.9 Reporting results
3.9.1 When results uncorrected for air volume are greater than 10 ppm, three significant digits will be reported. For results below 10 ppm, the chemist will use his judgment, but in no cases report more than three significant digits.

3.9.2 The estimated detection limit based on the lowest mass per sample injected as a standard.

3.9.3 All concentration levels down to the detection limit are reported.

3.9.4 If the concentration of analyte found on the back section of the charcoal tube is equal to or greater than 25% of the concentration found on the front section, the charcoal tube is considered to be saturated and reported as such on the analyst worksheet.

3.9.5 The presence of significant peaks caused by unrequested components in the sample is noted on the analyst worksheet and they are identified and quantitated if possible.

3.9.6 All data processor print-outs and chart recorder chromatograms are filed in a central file according to laboratory sample identification number.

3.9.7 Analytical data and results are checked by a fellow chemist before the completed analyst worksheets are given to the team leader.
4. Analytes

The following table contains those analytes which can be analyzed by this procedure. Standard size charcoal tubes containing coconut base charcoal are used unless specified otherwise in the table. Listed PELs are 8-h time weighted averages unless denoted as a ceiling concentration with a "(C)", before the PEL value. Before taking samples, the OSHA Chemical Sampling Information at http://www.osha.gov should be consulted for additional and more detailed information.

Table 4.
Recommended Sampling Parameters for Analytes Covered by This Procedure.

ANALYTE	PEL (ppm)	air vol (L)	max rate (L/min)	NIOSH Method
Allyl alcohol	2	10	0.2	1402

Allyl chloride	1	48	0.2	1000
n-Amyl acetate	100	10	0.2	1450
sec-Amyl acetate	125	10	0.2	1450
Benzyl chloride	1	10	0.2	1003
Bromoform	0.5	10	0.2	1003
Butyl acetate	150	10	0.2	1450
sec-Butyl acetate	200	10	0.2	1450
tert-Butyl acetate	200	10	0.2	1450
Butyl alcohol	100	10	0.2	1401
sec-Butyl alcohol	150	10	0.2	1401
tert-Butyl alcohol	100	10	0.2	1400
n-Butyl glycidyl ether (BGE)	50	10	0.2	1616
p-tert-Butyltoluene	10	24	0.2	1501
Camphor	2 mg/m^3	24	0.2	1301
Carbon tetrachloride	10	15	0.2	1003
Chlorobenzene (monochlorobenzene)	75	10	0.2	1003
Chlorobromomethane	200	5	0.2	1003
Cumene	50	10	0.2	1501
Cyclohexane	300	5	0.2	1500
Cyclohexanol	50	10	0.2	1402
Cyclohexene	300	5	0.2	1500
Diacetone alcohol (4-hydroxy-4-methyl-2-pentanone)	50	10	0.2	1402
o-Dichlorobenzene	(C)50	3	0.2	1003
p-Dichlorobenzene	75		0.05	1003
1,1-Dichloroethane	100	10	0.2	
1,2-Dichloroethylene	200	3	0.2	1003
Dichloroethyl ether	(C)15	15	1.0	1004
1,1-Dichloro-1-nitroethane**	(C)10	15	1.0	1601
Difluorodibromomethane(F-12-B2)*	100	10	0.2	1012
Diisobutyl ketone	50	10	0.2	1300
Dioxane (diethylene dioxide)	100	10	0.2	1602

Epichlorohydrin	5	20	0.2	1010
Ethyl acetate	400	6	0.2	1457
Ethyl sec-amyl ketone (5-methyl-3-heptanone)	25	25	0.2	1301
Ethyl bromide	200	4	0.2	1011
Ethyl butyl ketone (3-heptanone)	50	25	0.2	1301
Ethylene chlorohydrin**	5	35	0.2	2513
Ethyl ether	400	3	0.2	1610
Ethyl formate	100	10	0.2	1452
Glycidol (2,3-epoxy-1-propanol)	50	50	1.0	1608
n-Heptane	500	4	0.2	1500
Hexachloroethane	1	10	0.2	1003
n-Hexane	500	4	0.2	1500
2-Hexanone (MBK)	100	10	0.2	1300
sec-Hexyl acetate	50	10	0.2	1450
Isoamyl acetate	100	10	0.2	1450
Isoamyl alcohol	100	10	0.2	1402
Isobutyl acetate	150	10	0.2	1450
Isobutyl alcohol	100	10	0.2	1401
Isophorone**	25	12	0.2	2508
Isopropyl acetate	250	8	0.2	1454
Isopropyl ether	500	3	0.05	1618
Isopropyl glycidyl ether	50	10	0.2	1620
Mesityl oxide	25	25	0.2	1301
Methyl acetate	200	7	0.2	1458
Methylal (dimethoxymethane)	1000	2	0.2	1611
Methyl-(n-amyl)ketone	100	25	0.2	1301
Methylcyclohexane	500	4	0.2	1500
Methyl isobutyl carbinol	25	10	0.2	1402
a-Methyl styrene	(C)100	3	0.2	1501
Octane	500	4	0.1	1500
Pentane	1000	2	0.05	1500
2-Pentanone	200	10	0.05	1300

Phenyl glycidyl ether	10	50	0.1	1619
n-Propyl acetate	200	10	0.2	1450
Propyl alcohol	200	10	0.2	1401
Propylene dichloride	75	10	0.2	1013
n-Propyl nitrate**	25	70	0.1	S227
1,1,1,2-Tetrachloro-2, 2-difluoroethane	500	2	0.035	1016
1,1,2, 2-Tetrachloro-1, 2-difluoroethane	500	2	0.035	1016
1,1,2,2-Tetrachloroethane**	5	10	0.2	1019
Tetrahydrofuran	200	5	0.2	1609
Tetramethyl succinonitrile	0.5	48	0.2	S155
1,2,3-Trichloropropane	50	10	0.2	1003
Vinyl toluene	100	24	0.2	1501

*Use two charcoal tubes in series for sampling.
**Use petroleum base charcoal for sampling.

5. References

5.1 "NIOSH Manual of Analytical Methods", ed. 4 Vol. 1-3 National Institute of Occupational Safety and Health, U.S. Government Printing Office, Washington, D.C. (1998)

D.3 Matlab® Scripts

Matlab® Script used to analyze soil and air sampling tube extracted with CS_2:

```
plot(filename(:,1), filename(:,2), filename(:,1), filename(2401,2))
data=filename(:,2);
samplerate=0.00083333333;
t1=C6 start time;
t2=C10 peak time;
t3=C16 peak time;
t4=C34 peak time;
index1=t2-t1;
index2=t3-t2;
index3=t4-t3;
for i=1:index1
store1(i)=samplerate*(data(t1-1+i)+data(t1+i))/2;
end
for i=1:index2
store2(i)=samplerate*(data(t2-1+i)+data(t2+i))/2;
end
for i=1:index3
store3(i)=samplerate*(data(t3-1+i)+data(t3+i))/2;
end
```

```
two_min=data(2401);
takeoff1=two_min*(t2-t1)*samplerate;
takeoff2=two_min*(t3-t2)*samplerate;
takeoff3=two_min*(t4-t3)*samplerate;
integration(1)=sum(store1)-takeoff1;
integration(2)=sum(store2)-takeoff2;
integration(3)=sum(store3)-takeoff3;
clear data;
clear store1;
clear store2;
clear store3;
clear index1;
clear index2;
clear index3;
clear two_min;
clear takeoff1;
clear takeoff2;
clear takeoff3;
```

Matlab® Script used to analyze soil and air sampling tube extracted with toluene:

```
plot(filename(:,1),filename(:,2), filename(:,1), filename(2401,2))
data= filename(:,2);
samplerate=0.00083333333;
t2=C10 peak time;
t3=C16 peak time;
t4=C34 peak time;
index2=t3-t2;
index3=t4-t3;
for i=1:index2
store2(i)=samplerate*(data(t2-1+i)+data(t2+i))/2;
end
for i=1:index3
store3(i)=samplerate*(data(t3-1+i)+data(t3+i))/2;
end
two_min=data(2401);
takeoff2=two_min*(t3-t2)*samplerate;
takeoff3=two_min*(t4-t3)*samplerate;
integration(2)=sum(store2)-takeoff2;
integration(3)=sum(store3)-takeoff3;
clear data;
clear store2;
```

```
clear store3;

clear index2;

clear index3;

clear two_min;

clear takeoff2;

clear takeoff3;
```

Appendix E: Soil Configuration and Sampling Locations

This appendix presents details regarding the initial and final soil configuration, the soil sampling locations and the calculations used to determine the mass of soil corresponding to each sampling location. The information in this appendix is available only on the disk provided with the hard copy of this thesis.